Phenomenological Studies of B mesons

Anupama Bhol

A Thesis Submitted to

Indian Institute of Technology Hyderabad

In Partial Fulfillment of the Requirements for

The Degree of Doctor of Philosophy

भारतीय प्रौद्योगिकी संस्थान हैदराबाद
Indian Institute of Technology Hyderabad

Department of Physics

May 2014

Declaration

I declare that this written submission represents my ideas in my own words, and where ideas or words of others have been included, I have adequately cited and referenced the original sources. I also declare that I have adhered to all principles of academic honesty and integrity and have not misrepresented or fabricated or falsified any idea/data/fact/source in my submission. I understand that any violation of the above will be a cause for disciplinary action by the Institute and can also evoke penal action from the sources that have thus not been properly cited, or from whom proper permission has not been taken when needed.

_____

(Signature)

(*Anupama Bhol*)

ph10p004
(Roll No.)

Certificate

I hereby certify that the matter embodied in this thesis entitled "**Phenomenological studies of B mesons**" has been carried out by **Anupama Bhol** at the Department of Physics, Indian Institute of Technology Hyderabad, India under my supervision and that it has not been submitted elsewhere for the award of any degree or diploma.

(Signature)

(*Anupama Bhol*)
ph10p004
(Roll No.)

(Signature)

(Dr. Anjan Kumar Giri)
Advisor

Approval Sheet

This Thesis entitled "Phenomenological Studies of B mesons" by *Anupama Bhol* is approved for the degree of Doctor of Philosophy from IIT Hyderabad

Prof. R. Sinha
IMSc Chennai
Examiner

Prof. S. Uma Sankar
IIT Bombay
Examiner

Dr. N. Sahu
IIT Hyderabad
Examiner

Dr. A. K. Giri
IIT Hyderabad
Advisor

18/03/2014.

Dr. B. Mallik
IIT Hyderabad
Chairman

Acknowledgements

Firstly I would like to express my utmost gratitude to my supervisor Dr. Anjan Kumar Giri for his invaluable guidance, continual patience and constructive suggestions regarding this research work, without which, I would have been lost. His constant support and supervision led me towards the completion of this thesis. I sincerely thank him.

I would like to thank my doctoral committee members -Dr. V. Kanchana and Dr. Raja Banerjee for their comments, valuable suggestions and encouragement.

I would also like to thank especially Dr. Rupak Dutta, with whom I had the pleasure to work with during my Ph.D. I sincerely thank to the members of Physics lab for their help and co-operation. I wish to acknowledge all the non-academic staffs for their work. I thank the institute and its academic and administrative members for providing excellent academic atmosphere and facilities for research work.

My special thanks to Prof. U B Desai (director, IIT Hyderabad) for providing such a nice environment to work during my PhD program.

I am thankful to my hostel-mates, Vandana, Sweta, Deepika. They have made my stay happy and comfortable. I will surely miss them when I will be away from IIT Hyderabad.

I thank to my parents, sisters for their love, support and constant encouragement which was necessary for all this to have happened.

Dedicated to my parents

Abstract

The Standard Model (SM) is the most successful theoretical framework of particle physics ever formulated till today which says that matter ultimately consists of two types particles namely leptons and quarks, and it unifies the electromagnetic and weak forces, and also it describes the interaction between fundamental particles in terms of exchange of the fundamental force particles i.e. gauge bosons. The latest monumental discovery of a Higgs like particle by CMS and ATLAS further confirms the validity of the SM for which Peter Higgs and Francois Englert were awarded the Nobel Prize for the year 2013 in Physics.

B mesons provide a strong ground for studying flavour physics and CP Violation. The B mesons containing one b(bottom) quark and one d(down) or u(up) quark or s(strange) quark or c(charm) quark can decay to other mesons containing the lighter quark that provides us to test the SM predictions and also to check for various physical observables which can be determined from the experiment. From experimental observables (decay rates, asymmetry parameters etc.) we can perform indirect searches for New Physics via any measured deviation from the SM expectation and also we can constrain the New Physics parameters. Studying B physics phenomenology allows the possibility for the measurement of CKM matrix elements and the sides and the angles of the unitarity triangle. Therefore, the main motivation in studying various B decays is to verify the SM predictions and to look for signals of New Physics.

Recent measurements of exclusive $B^- \to \tau^- \nu$ and $B^0 \to \pi^+ l^- \bar{\nu}_l$ decays via $b \to u\, l\, \nu$ transition process differ from the Standard Model expectation and if persist in future B experiments, will be definite hint of the Physics beyond the Standard Model. Similar hints of New Physics have been observed in $b \to c$ semileptonic transition processes as well. BaBar measures the ratio of branching fractions of $B \to (D,\, D^*)\, \tau\, \nu$ to the corresponding $B \to (D,\, D^*)\, l\nu$, where l represents either an electron or a muon, and finds 3.4σ discrepancy with the SM expectation. In this context, we consider a most general effective Lagrangian for the $b \to u\, l\, \nu$ and $b \to c\, l\, \nu$ transition processes in the presence of New Physics and perform a combined analysis of all the $b \to u$ and $b \to c$ semi-(leptonic) data to explore various New Physics operators and their couplings. We consider various New Physics scenarios and give prediction for the $B_c \to \tau\nu$ and $B \to \pi\tau\nu$ decay branching fractions. We also study the effect of these New Physics parameters on the ratio of the branching ratios of $B \to \pi\tau\nu$ to the corresponding $B \to \pi\, l\, \nu$ decays.

Flavour changing neutral current decays of B meson mediated via $b \to s\, l\, \bar{l}$ transition process, where l represents an electron, a muon, or a tau lepton, provide promising probes for physics beyond the Standard Model. In this context, we use the most general effective Hamiltonian for $b \to s\, l\, \bar{l}$ process and study the branching ratio and various asymmetries of $B^- \to \Lambda\, \bar{p}\, \mu^+\, \mu^-$ four body baryonic decays of B meson. We also see the effect of various New Physics couplings in this decay mode. Within the Standard Model, the branching ratio of $B^- \to \Lambda\, \bar{p}\, \mu^+\, \mu^-$ decay mode is found to be 1.08×10^{-7} and hence can be tested in the forthcoming or future B factories.

We study the $B_s \to {D_s}^{(*)}\, l\, \bar{\nu}_l$ semileptonic decays involving quark level transition $b \to c\, l\, \nu$, in the framework of standard model (SM). We calculate the branching ratios and we define observables such as ratio of branching fractions R_{D_s, D_s^*} for different leptonic modes and $R_{\tau,\, l}$ where $l = e^-$, μ^- for same leptonic mode and we estimate their numerical values. We also study observables such as differential branching ratio and forward-backward asymmetry and their implications.

Contents

List of Figures

List of Tables

Chapter 1

Introduction

The main objective of the study of particle physics is to understand the mystery behind the nature of fundamental particles and their interactions and to find out the solutions to the fundamental problems observed in nature. There are still many problems and questions that are not answered or understood within our current understanding. Questions like why we have so many fundamental constituents of matter with differing properties, the observed dissimilar masses and mixing pattern of quarks and leptons, what makes them to form as bound states the way they are showing the behavior of confinement and asymptotic freedom, the difference in fundamental forces and their interactions, are these forces unified at some higher energy scale and if so why, observed matter-antimatter asymmetry of Universe, the dark matter problem, creation of universe itself which is found to be expanding and its evolution since the beginning are some of the interesting issues which motivate the research in particle physics.

The Standard Model (SM) of particle physics is a simple formalism which can explain the beauty and complexity of nature observed, at least up to the energy we have explored so far. The SM is based upon quantum field theory, gauge principles and it combines the electromagnetic, weak and strong interactions into one single theory. The Standard Model is the most successful theoretical framework of particle physics ever formulated which has passed almost all experimental tests in the last few decades. The matter content in this framework essentially consists of two types fundamental entities, namely, leptons and quarks, and can successfully explain the interactions between fundamental particles in terms of exchange of the mediating particles, called gauge bosons, which are actually the carriers of various forces involved.

The SM has been very successful in explaining almost all the existing data. One of the remarkable success is the recent discovery of Higgs like particle by ATLAS and CMS in 2012 for which Peter Higgs and Francois Englert were awarded the Nobel Prize in physics for the year 2013. In 1964 the Higgs particle had been conceived [1, 2] which is believed to be responsible for giving the masses to other particles through Higgs mechanism. But unfortunately, the SM does not correctly explain observed disappearance of antimatter, it ignores gravity, does not unify/explain all the interactions, it does not say why there are so many (and may be only three) generations of fundamental constituents and why their weak interaction involves a peculiar way of mixing pattern and why there is mass hierarchy etc. The phenomenon of neutrino oscillation and the evidence of dark matter cannot be understood

within the framework of the SM. Again on top of all these questions, the problem of including General Relativity with the Standard Model still remains and we do not yet have a quantized theory of gravity. Combining gravity and quantum mechanics produces a non-renormalizable quantum field theory. All these indicate that there are many unresolved issues with our current understanding and the SM is incomplete. Moreover, based on the understanding so far it has been speculated that there exists some New Physics at some higher energy, whose form is not known, but at the same time SM is thought to be a some kind of a low energy effective theory of that.

Many ideas have been suggested in the form of various beyond the Standard Model scenarios to address these problems. The most popular ones being supersymmetry, extra dimensions, fourth quark generation, extra Z boson model etc, which could in principle be the possible New Physics scenario beyond that of the simplest and perfect model, namely, the Standard Model. Interestingly, there seems to be indications for the existence of New Physics, if not convincing at this point of time, from the observed experimental results, and if found true in the future, could provide the existence of Physics beyond the SM. In the last one decade or so we have seen some discrepancies between the theoretical predictions and experimental results in case of some observable, none of them have been significant enough to claim as the New Physics signal. Needless to mention that the significant deviations from the SM expectations have gone away with time and/or more refined measurements and accumulation of more statistics, approaching that of the Standard Model predictions. But if we can reduce the theoretical uncertainties then we can have precise SM predictions and that will be very much essential to decipher the New Physics. So precision measurements and minimum theoretical errors will be the key to find the nature of NP in the coming years.

In this thesis we have worked on various observables within the Standard Model framework. Before claiming for the existence of New Physics we must be absolutely sure that our the Standard Model predictions are most accurate where the theoretical errors are minimal and as precise the experimental results and vice-versa. We need inputs from all possible sources, all possible decay processes to arrive at a decisive conclusion. Therefore working towards that goal in this thesis we have undertaken some of the phenomenological studies of the weak decays of B-mesons in the framework of the SM and tried to see the effects of possible New Physics, if any. It should be noted here that we have not found any concrete evidence of any New Physics model till date. Since there is no indication regarding the nature of the physics beyond the Standard Model, we have considered the model independent way of introducing the New Physics and studied the effect of the same with respect to various observables.

The beauty of B meson lies on its rich phenomenological ground for studying flavour physics and CP Violation. Flavour physics in the past has contributed in a significant way in building the modern particle physics. In order to accommodate CP violation into the theory Kobayashi and Maskawa (KM) advocated that there must be at least three generation of quarks. In fact later on the third generation of quarks were discovered. It was thereafter realized that B meson system can exhibit large CP violation unlike the Kaons. And one brilliant idea by Pier Oddone led to the construction of so-called asymmetric B-factories at SLAC and KEK. These B-factories provided us huge data set in the bottom sector of the Standard Model in addition to other data. Large CP violation in B system was observed and KM mechanism was verified for which Kobayashi

and Maskawa got the Nobel Prize in Physics in 2008. Apart from verifying the Standard Model predictions and establishing the KM mechanism one of the other goals of the B-factory was to look for signals of New Physics. Interestingly, we do not have clear understanding of the transition of quark level to hadron level physics or in other words the quark-hadron dynamics.

In the recent years we have found some indications of bound state structures beyond that of the meson (quark-anti-quark) and baryon (three quarks) states in the form of tetra-quark, penta-quark and molecular states etc. Whether these states will be confirmed in the future experiments or not will be clear in the coming year but at least these indications have forced us to look beyond the quark model. In this context, it is very important now to corroborate the finding from all possible sources. For example, the transition containing baryon-anti-baryon pair, multi-particle final states etc. in addition to the two body and leptonic B decays. Needless to mention here that in the Belle II regime we will get an opportunity to study a lot of multi-particle states. The understanding of the quark-hadron dynamics will play a major role in interpreting these results within the framework of the SM and guide us to the world of physics beyond the SM. The B meson which contain one b (bottom) quark and one d (down) or u (up) quark or s (strange) quark or c (charm) quark can decay to other mesons containing the lighter quark that provides us to test for the SM predictions and also to check for various physical observables which can be determined from the experiment. From experimental observables (decay rates, CP asymmetry parameters etc.) we can perform indirect searches for New Physics via any measured deviation from the Standard Model expectation and also we can constrain the New Physics parameters. Studying B physics phenomenology allows the possibility for the measurement of CKM matrix elements and the sides and the angles of the unitarity triangle.

The Standard Model (SM) is defined by the gauge symmetry $SU(3)_C \times SU(2)_L \times U(1)_Y$. Due to the vaccum expectation value (VEV) of scalar field, ϕ, the gauge group is spontaneously broken and the gauge symmetry is reformed to $SU(3)_C \times U(1)_{EM}$ and the W and Z bosons acquire their mass through the mechanism of spontaneous symmetry breaking. The Standard Model Lagrangian $\mathcal{L}_{SM}$ consists of the following 3 parts [3], Kinetic, Higgs and Yukawa parts . The Yukawa part of Lagrangian is CP violating and the CP violation is due to the complex Yukawa couplings. These complex Yukawa couplings to all 3 generations of quarks give rise to mixing matrix called Cabibbo-Kobayashi-Maskawa (CKM) matrix [4].

1.1 CKM Matrix

The down-type quark weak eigenstates (d', s', b') can be expressed as the mixing of the corresponding mass eigenstates (d, s, b). Both weak eigen states (d', s', b') and mass eigenstates (d, s, b) are related to each other through the CKM matrix, V_{CKM}.

$$\begin{pmatrix} d' \\ s' \\ b' \end{pmatrix} = V_{CKM} \begin{pmatrix} d \\ s \\ b \end{pmatrix} = \begin{pmatrix} V_{ud} & V_{us} & V_{ub} \\ V_{cd} & V_{cs} & V_{cb} \\ V_{td} & V_{ts} & V_{tb} \end{pmatrix} \begin{pmatrix} d \\ s \\ b \end{pmatrix} \tag{1.1}$$

Now we want to find out the number of independent parameters required to parametrise the CKM matrix. In general, for N generations, i.e., with $2N$ quarks, the $N \times N$ CKM matrix require $2N^2$ number of real parameters to be specified. But there are N^2 constraints coming from unitarity condition of the CKM matrix as $V^\dagger V = V^\dagger V = 1$, and $(2N-1)$ number of phases can be absorbed by quark field redefinitions. Thus the number of independent parameters is $2N^2 - N^2 - (2N-1) = (N-1)^2$. Among these $(N-1)^2$ parameters $N(N-1)/2$ are rotation angles called the quark mixing angles and the remaining $(N-1)(N-2)/2$ are the complex phases that cause CP violation.

For the case $N = 2$, there is only one independent parameter which is a mixing angle between the two generations of quarks. This was the first proposed quark mixing matrix when two generations were known and the mixing angle is called Cabibbo angle (θ_c) after its inventor Nicola Cabibbo [5]. For the Standard Model, $N = 3$, therefore there are 4 independent parameters out of which 3 parameters are the mixing angles and one parameter is the complex phase which cause CP violation. The CKM matrix is unitary which assures the absence of elementary Flavour Changing Neutral Current (FCNC) vertices and therefore the FCNC processes are suppressed in the SM.

1.1.1 Parametrizations of CKM matrix

There are different parametrizations for the CKM matrix that have been suggested in the literature. Here we will discuss about the two most popular parametrizations of CKM matrix, the standard parametrization [6] and the Wolfenstein parametrization [7].

The standard parametrization was proposed by Chau and Keung. Now introducing the notations, $c_{ij} = \cos\theta_{ij}$ and $s_{ij} = \sin\theta_{ij}$ with i and j being generation labels $(i, j = 1, 2, 3)$ and θ_{ij} are the rotation angles. The standard parametrization is given as:

$$V = \begin{pmatrix} c_{12}c_{13} & s_{12}c_{13} & s_{13}e^{-i\delta} \\ -s_{12}c_{23} - c_{12}s_{23}s_{13}e^{i\delta} & c_{12}c_{23} - s_{12}s_{23}s_{13}e^{i\delta} & s_{23}c_{13} \\ s_{12}s_{23} - c_{12}c_{23}s_{13}e^{i\delta} & -s_{23}c_{12} - s_{12}c_{23}s_{13}e^{i\delta} & c_{23}c_{13} \end{pmatrix}$$

where c_{ij} and s_{ij} can all be chosen to be positive and δ is the phase necessary for CP violation and the value of δ may vary in the range $0 \leq \delta \leq 2\pi$.

It has been proved that s_{13} and s_{23} are small numbers: $\mathcal{O}(10^{-3})$ and $\mathcal{O}(10^{-2})$, from the extensive phenomenology of the last years. The value of c_{13} and c_{23} can be approximated to 1 and the four independent parameters are as follows:

$$s_{12} = |V_{us}|, \qquad s_{13} = |V_{ub}|, \qquad s_{23} = |V_{cb}|, \qquad \delta \tag{1.2}$$

Here δ is the phase sensitive for CP violation in various processes involving CKM matrix element $|V_{ub}|$.

In Wolfenstein parametrization the CKM matrix elements are expressed in an expanded form power series of the small parameter $\lambda = |V_{us}| = 0.22$.

$$V = \begin{pmatrix} 1 - \frac{\lambda^2}{2} & \lambda & A\lambda^3(\rho - i\eta) \\ -\lambda & 1 - \frac{\lambda^2}{2} & A\lambda^2 \\ A\lambda^3(1 - \rho - i\eta) & -A\lambda^2 & 1 \end{pmatrix} + \mathcal{O}(\lambda^4)$$

Here the four independent parameters are λ, A, ρ, η. This parametrization is very useful in the phenomenology of flavour physics. It provides us the unitarity triangle which has a very transparent geometrical representation of the stucture of the CKM matrix and also it enables us to find out several analytic results. The Wolfenstein parametrization is characterised by several nice features.

* The matrix has not only the unitarity property but also the experimental information: $|V_{us}| \ll 1$, $V_{cb} \sim |V_{us}|^2$, $|V_{ub}| \ll |V_{cb}|$.

* The matrix is approximately unitary and exact unitarity can be achieved by a series expansion.

* The matrix is almost diagonal and symmetric and again its element become smaller as we move away from the diagonal.

* The six unitarity triangles can be characterised through the dependence of λ.

The standard parametrization and Wolfenstein parametrization can be related as follows [8]:

$$s_{12} = \lambda, \qquad s_{23} = A\lambda^2, \qquad s_{13}e^{-i\delta} = A\lambda^3(\rho - i\eta) \tag{1.3}$$

There can be a CP violating quantity which is independent of different parametrizations of CKM matrix. Jarlskog parameter [9] is the possible parameter which can measure the strength of CP violation in the SM and is defined by,

$$J_{CP} = |\mathcal{I}m(V_{i\alpha}V_{j\beta}V_{i\beta}V_{j\alpha})|, \qquad (i \neq j, \alpha \neq \beta) \tag{1.4}$$

The Jarlskog parameter explicitly can be written as,

$$J_{CP} = c_{12}c_{23}c_{13}^2 s_{12}s_{23}s_{13}\sin\delta \simeq \lambda^6 A^2 \eta \tag{1.5}$$

1.1.2 The Unitarity Triangle (UT) of the CKM Matrix

The CKM matrix is unitary ($V^\dagger V = 1 = VV^\dagger$). This leads to 12 equations consisting of 6 normalization and 6 orthogonality relations. Thus the six orthogonality relations can be shown through 6 different triangles in the complex plane known as unitarity triangles [10]. The area of any triangle can be expressed in terms of Jarlskog parameter [11].

$$2A = J_{CP} \tag{1.6}$$

The six orthogonality relations are written as following.

$$V_{ud}V_{us}^* + V_{cd}V_{cs}^* + V_{td}V_{ts}^* = 0 \tag{1.7}$$
$$V_{us}V_{ub}^* + V_{cs}V_{cb}^* + V_{ts}V_{tb}^* = 0 \tag{1.8}$$
$$V_{ud}V_{ub}^* + V_{cd}V_{cb}^* + V_{td}V_{tb}^* = 0 \tag{1.9}$$
$$V_{ud}V_{cd}^* + V_{us}V_{cs}^* + V_{ub}V_{cb}^* = 0 \tag{1.10}$$
$$V_{cd}V_{td}^* + V_{cs}V_{ts}^* + V_{cb}V_{tb}^* = 0 \tag{1.11}$$
$$V_{ud}V_{td}^* + V_{us}V_{ts}^* + V_{ub}V_{tb}^* = 0 \tag{1.12}$$

Conventionally we consider Eq. 1.9 as the unitarity triangle with all the three sides of $\mathcal{O}(\lambda^3)$. The unitarity triangle (UT) derived from the Eq. 1.9 again can be modified further by choosing the

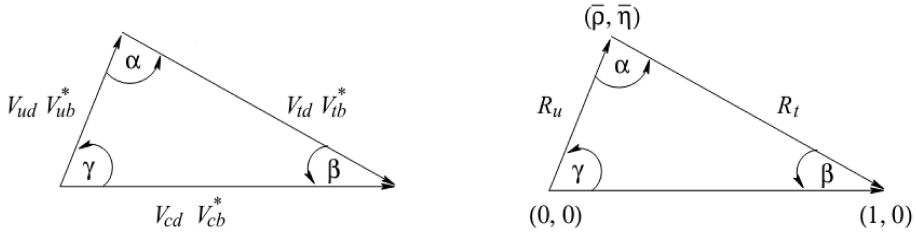

Figure 1.1: Unitarity Triangle from the Eq.(1.10) and rescaled Unitarity triangle

phase convention such that $V_{cd}V_{cb}^*$ is real, and then after dividing the lengths of all sides by $|V_{cd}V_{cb}^*|$. Therefore this new phase convention helps to align one side of the triangle on the real axis, while the division of all lengths by $|V_{cd}V_{cb}^*|$ converts the length of this side to be 1, which is shown in the figure, but the form of the triangle remains unchanged. Two vertices of the rescaled triangle are thus fixed at $(0, 0)$ and $(1, 0)$. We denote the three angles of the unitarity triangle as α, β and γ All the six parameters of the unitarity triangle, three angles and three sides, are very significant from the flavour physics point of view. These parameters are defined by the unitarity relation and can also be measured. Moreover the area of the unitarity triangle gives the measurement of the CP violation.

1.2 The significance of discrete symmetries

We know in physics symmetries lead to conservation laws [12]. In principle the laws of physics should also be invariant under discrete symmetries. A discrete symmetry is a symmetry which is not continuous in a system. Here we will mainly discuss CP symmetry and CPT symmetry.

CP symmetry is the multiplication or product of two symmetries: charge conjugation (C) and parity (P). The CP symmetry means that all physical laws remain invariant under the combined operation of a charge conjugation transformation and a parity transformation. In 1964, CP violation was observed for the first time by James W. Cronin and Val L. Fitch in neutral Kaon decays. If CP is conserved, the short-lived of K meson would always decay into two π mesons, whereas the long-lived of K meson would always decay into three π mesons. But they found that the long-lived neutral K meson does decay into two π mesons [13]. Later in 2001, it was also confirmed experimentally in B mesons by the BaBar [14] and the Belle [15] Collaborations. Thus, the CP violation is observed in weak interactions but not in the strong and electromagnetic interactions.

The phenomenon of CP violation is very significant from physics point of view. The universe consists of mainly of matter, rather than consisting of equal parts of matter and antimatter. Equal amounts of matter and antimatter should have been produced during Big Bang and if CP is conserved, then there should have been total cancellation of both matter and antimatter which would have resulted in a sea of radiation in the universe with no matter. Since CP symmetry is violated which implies, physical laws must have acted in a different manner for both matter and antimatter after the Big Bang.

There are three sources of CP violation in the Standard Model. The first of these, is the complex phase of Cabibbo-Kobayashi-Maskawa (CKM) matrix [4] in the quark sector. But the CP violation is tiny and can only account for a small portion of the CP violation required to explain the matter-antimatter asymmetry. There can be CP violation in the strong interaction as well, but the failure to observe the electric dipole moment of the neutron in experiments suggests that any CP violation in the strong sector is also very small to account for the necessary CP violation in the early universe. The third source of CP violation is in the lepton sector and it described by the Pontecorvo-Maki-Nakagawa-Sakata (PMNS) matrix. It is expected that in the future new sources of CP violation will be found to resolve the whole matter-antimatter asymmetry.

CPT symmetry is associated with the simultaneous transformations of charge conjugation (C), parity transformation (P), and time reversal (T). CPT symmetry is found to be an exact symmetry of nature at the fundamental level. According to the CPT theorem the CPT symmetry holds for all physical phenomena, or more precisely, that any Lorentz invariant local quantum field theory with a Hermitian Hamiltonian must have CPT symmetry.

1.3 Flavour Changing Neutral Currents

Flavour Changing Neutral Current (FCNC) decays provide the promising probes of New Physics. Because they are highly suppressed since they are forbidden in the SM at tree level. They are mediated through either loop diagrams such as penguin or box diagrams. New Physics (NP) particles, in principle, can enter through these loop processes and compete with the SM processes. Thus these loop processes are very sensitive to NP as couplings and masses of new particles, which can contribute virtually, can have a sizeable influence on observables. Ultimately this can lead to modifications of branching fractions or angular distributions of the particles in these decay modes.

The radiative (or electroweak) loops in the Feynman diagrams for the decays of b quarks consist of a W and an intermediate quark (u, c or t) with a radiative γ (or Z). The main contribution comes from the top quark, t, due to its high mass. The box diagrams contain two W bosons (W^+ and W). In theory new particles can just replace any of the intermediate quarks inside these loops and boxes and therefore influence observables indirectly.

1.4 Motivation for studying B Decays

The study of B mesons is a rich phenomenological ground for flavour physics and CP Violation. The B meson decays provide us to test for the SM predictions and to search for possible New Physics. The study of semi-leptonic decays of B mesons allows us the determination of the CKM matrix elements. The determination of $|V_{ub}|$ and $|V_{cb}|$ are free from the effect of any non-standard model physics since it involve W boson exchange. In some New Physics models where charged Higgs coupling is present, though it will not affect the decays involving e^- and μ^-, due to their small mass, but it will affect the decays involving the heavy τ^- lepton, hence sensitive for NP. In the Standard Model (SM), the Flavour Changing Neutral Current decays are suppressed and mediated via electroweak box and penguin type diagrams. Tree level diagrams do not contribute to these

decay processes. Hence these FCNC decays are very sensitive for New Physics. The sides and the angles of the Unitarity triangle can be determined from the study of B-decays. Theory is used to convert experimental data into contours in the $\rho - \eta$ plane, where semileptonic $b \to u l \nu_l$, $c l \nu_l$ decays and $B_{d,s}$-$B_{d,s}$ mixing allow us to determine the UT sides $R_u \equiv \left|\frac{V_{ud}V_{ub}}{V_{cd}V_{cb}}\right|$ and $R_t \equiv \left|\frac{V_{td}V_{tb}}{V_{cd}V_{cb}}\right|$. The two groups CKM-fitter [16] and UT-fit [17] have worked on global analysis to convert the experimental data into contours in the $\bar{\rho} - \bar{\eta}$ plane.

1.5 Basic Formalism of the CP Phenomenology in the B meson decays

We discuss a basic formalism for CP violation in the decays of a pseudoscalar meson B, which in principle could be charged or a neutral [3, 18]. For the validity of field theory we always require Lorentz invariance, Hermiticity of Lagrangian and CPT invariance. In many theories CP and T are separately invariant. It had been believed for a long time that CP is conserved before the discovery of CP violation in the experiment. After the discovery of CP violation, people started investigating the origin of CP violation and also tried to formulate a proper theory for it. CP non-conservation implies that the two processes that are CP-conjugate to each other behave differently. The phase of each partial amplitude may be changed at will and is meaningless, but the relative phase of two partial amplitude is rephasing invariant and in general has observable consequences.

Let us define the decay amplitude of pseudoscalar meson P (which could be charged or neutral) and its CP conjugate $\bar{P}$ to a multi-particle final state f and its CP conjugate $\bar{f}$ as:

$$A_f = \langle f|H|P\rangle, \qquad \bar{A}_f = \langle f|H|\bar{P}\rangle, \qquad A_{\bar{f}} = \langle \bar{f}|H|P\rangle, \qquad \bar{A}_{\bar{f}} = \langle \bar{f}|H|\bar{P}\rangle. \tag{1.13}$$

1.5.1 Neutral Meson Mixing

The mesons P^0 and $\bar{P}^0$ do mix because of weak interaction i.e. they oscillate between themselves before decay. Here P^0 refer to any mesons like B^0, B_s^0, K^0, D^0. Let us consider an initial state which is a superposition of P^0 and $\bar{P}^0$, say

$$|\psi(0)\rangle = a(0)\,|P^0\rangle \,+\, b(0)\,|\bar{P}^0\rangle \tag{1.14}$$

Since it is a mixed state, the effective Hamiltonian can be determined by 2×2 matrix. The Hamiltonian is not hermitian, since otherwise the mesons would only oscillate and not decay. Any complex matrix can be written in terms of hermitian matrices M and Γ as

$$H = M \,-\, \frac{i}{2}\,\Gamma \tag{1.15}$$

M and Γ are connected with $(P^0 - \bar{P}^0) \leftrightarrow (P^0 - \bar{P}^0)$ transtions via off-shell (dispersive) and on-shell (absorptive) intermediate states respectively. The diagonal elements of M and Γ represent the flavour-conserving transitions $P^0 \to P^0$ and $\bar{P}^0 \to \bar{P}^0$ while off-diagonal elements represent the flavour-changing transitions, $P^0 \to \bar{P}^0$.

Explicitly the Hamiltonian in matrix form can be written as:

$$H = \begin{pmatrix} M_{11} - \frac{i}{2}\Gamma_{11} & M_{12} - \frac{i}{2}\Gamma_{12} \\ M_{12}^* - \frac{i}{2}\Gamma_{12}^* & M_{22} - \frac{i}{2}\Gamma_{22} \end{pmatrix}$$

Under Wigner Weisskopf formalism [19, 20], the time evolution of the state vector can be expressed as,

$$|\psi(t)\rangle = a(t)\,|P^0\rangle \,+\, b(t)\,|\bar{P^0}\rangle \tag{1.16}$$

and the effective Schrödinger equation as

$$i\frac{\partial}{\partial t}\,|\psi(t)\rangle = \,H\,|\psi(t)\rangle \tag{1.17}$$

We concentrate on the study of B meson. So instead of P^0 we write B^0. Assuming CPT invariance, the eigen vector of H, by introducing complex parameters p and q, may be written as:

$$\begin{aligned} |B_L\rangle &= p|B^0\rangle \,+\, q|\bar{B^0}\rangle \\ |B_H\rangle &= p|B^0\rangle \,-\, q|\bar{B^0}\rangle \end{aligned} \tag{1.18}$$

where H and L stand for heavy and light mass eigen state respectively, $|B^0\rangle$ and $|\bar{B^0}\rangle$ are flavor eigenstates and with the normalization $|p|^2 + |q|^2 = 1$. Now solving the eigenvalue equation for H one gets,

$$\left(\frac{q}{p}\right)^2 = \frac{M_{12}^* \,-\, \frac{i}{2}\,\Gamma_{12}^*}{M_{12} \,-\, \frac{i}{2}\,\Gamma_{12}} \tag{1.19}$$

1.5.2 CP violating observables

When a meson decays to a final state the decay amplitude and the CP violating observables can be expressed in terms of phase-convention-independent combinations of $A_f, \bar{A}_f, A_{\bar{f}}, \bar{A}_{\bar{f}}$. For charged meson decays the CP violating observables depend on the combinations of $|\bar{A}_{\bar{f}}/A_f|$ but in neutral meson decays, it become problematic because of mixing or $P^0 \leftrightarrow \bar{P^0}$ oscillations and CP violation depends on q/p and also a new quantity λ_f which can be defined as following,

$$\lambda_f \equiv \frac{q}{p}\,\frac{A_{\bar{f}}}{A_f}. \tag{1.20}$$

Since the decay rates of the two mass eigenstates are quite different from each other, one can study their decays independently. But this is not the case for neutral D, B, B_s mesons as $\frac{\Delta\Gamma}{\Gamma}$ are relatively small and so both mass eigenstates must be considered in their evolution.

1.5.3 CP Violation in B meson system

There are three types of CP violation.

• CP violation in the decay and also known as direct CP violation. It occurs both in neutral and charged decays, when amplitude of a decay and its CP conjugate process differ in their magnitude,

i.e. $|\bar{A}_f| \neq |A_f|$.

• CP violation in the mixing or indirect CP violation that occur when two neutral mass eigen-state admixtures can not be chosen as CP eigen-state, i.e. $|q/p| \neq 1$.

• CP violation in the interference of the decays with or without mixing, which is due to decays into flavor-blind final states that are common to both the states, i.e. $\mathcal{I}m\,\lambda_f \neq 0$.

1.6 Effective Hamiltonian of B decays

The B mesons containing heavy b quark and another d, or u, or c, or s quark can decay to other lighter bound state particles. The effective Hamiltonian of B decays has the following generic structure.

$$\mathcal{H}_{eff} = \frac{G_F}{\sqrt{2}}\, V_{CKM} \sum_{i=1}^{10} \mathcal{C}_i(\mu)\, \mathcal{O}_i(\mu) \tag{1.21}$$

where, G_F is the Fermi constant, V_{CKM} is CKM matrix element, $\mathcal{O}_i$ are the local operators governing the decay in the question, $\mathcal{C}_i$ are the Wilson coefficients that describe the strength with which an operator enters into the Hamiltonian.

• Current-Current:

$$O_1 = (\bar{c}b)_{8,V-A}(\bar{s}c)_{8,V-A}, \qquad O_2 = (\bar{c}b)_{1,V-A}\,(\bar{s}c)_{1,V-A}. \tag{1.22}$$

Only a typical combination $(\bar{s}c)$ is given; there may be other combinations.

• QCD Penguins:

$$\begin{aligned} O_{3(4)} &= (\bar{s}b)_{1(8),V-A} \sum_q (\bar{q}q)_{1(8),V-A}\,, \\ O_{5(6)} &= (\bar{s}b)_{1(8),V-A} \sum_q (\bar{q}q)_{1(8),V+A}. \end{aligned} \tag{1.23}$$

• Electroweak Penguins:

$$\begin{aligned} O_{7(8)} &= \frac{3}{2}(\bar{s}b)_{1(8),V-A} \sum_q e_q(\bar{q}q)_{1(8),V+A}, \\ O_{9(10)} &= \frac{3}{2}(\bar{s}b)_{1(8),V-A} \sum_q e_q(\bar{q}q)_{1(8),V-A}. \end{aligned} \tag{1.24}$$

• Magnetic Penguins:

$$\begin{aligned} O_{7\gamma} &= \frac{e}{8\pi^2}\, m_b \bar{s}\sigma^{\mu\nu}(1+\gamma_5)bF_{\mu\nu} \\ O_{8G} &= \frac{g}{8\pi^2} m_b \bar{s}_\alpha \sigma^{\mu\nu}(1+\gamma_5)bT^a_{\alpha\beta}b_\beta G^a_{\mu\nu}. \end{aligned} \tag{1.25}$$

α, β are colour indices and T^a are $SU(3)$ generators.

• Semileptonic Operators:

$$\begin{aligned} O_{9V} &= (\bar{d}b)_{1,V-A}\,(\bar{e}e)_V, \\ O_{10A} &= (\bar{d}b)_{1,V-A}\,(\bar{e}e)_A, \end{aligned} \tag{1.26}$$

The subscripts 1 and 8 denote the singlet-singlet and octet-octet combination respectively. The B decays can be catagorized according to the final state particles of decays.

• Leptonic Decays:

Leptonic decays involve with leptons as final state particles. $B^+ \to l^+\nu_l$ and $B^0(B_s) \to l^+l$ are the examples.

• Semileptonic Decays:

The decays $B \to X_{s,d}l^+\nu$ and $B \to X_{s,d}l^+l$ come under this category.

• Radiative Decays:

They include the decay channel $B \to X_{s,d}\gamma$.

• Nonleptonic Decays or Hadronic Decays:

Some notable examples are $B \to \pi\pi$, $K\pi$, $B \to \eta K$, etc. The complications arise in the weak decays due to QCD effect.

As mentioned before the Standard Model has been very successful to explain the observed phenomena and the existing data to a very good extent but still there are various problems to which the SM does not provide an answer and there are also a few questions in the theory itself. This in turn indicates the fact that the SM is incomplete and we must find another theory which can explain them all including that of the SM.

To establish the existence of New Physics is an important and an enormous task for the Particle Physics community. There is very little evidence for the existence of New Physics, so it is a real challenge to establish NP. But on the other hand the neutrino oscillation, which points that neutrinos having masses, and dark matter problem etc., all these indicate there exist New Physics beyond the Standard Model. Moreover, we also need additional sources of CP violation to explain the observed baryon asymmetry of the universe (BAU) since the amount of CP violation in the SM is unable to explain the baryon asymmetry completely.

There are many New Physics models that have been proposed to solve these problems but we have not followed any of these NP models, rather we have adopted a model independent approach to obtain the information of the nature of New Physics. In this context we have considered the most effective Lagrangian in presence of various New Physics coupling. We have found the allowed NP parameter space using the recent data from the experiment and we have also shown that how these NP couplings affect the various observables which is discussed in Chapter-2.

To investigate the nature of Flavour Changing Neutral Currents is one of the motivations for studying B meson decays. In this direction, we have considered baryonic B semileptonic decay, namely, $B^- \to \Lambda\bar{p}\,\mu^+\,\mu^-$, mediated via $b \to s\,l\bar{l}$ transition. It should be noted that the exploration in the study of baryonic decays is significantly less in comparison to other decays containing meson in the final state and moreover, there are several indications of NP for decays with $b \to s\,l\bar{l}$ transition. These results, if persist in future precision experiments, would be a definite hint of physics beyond the SM and, in principle, will affect any FCNC decays mediated via $b \to s\,l\,\bar{l}$ transition process. In this context, we have used the most general effective Hamiltonian in the presence of NP and have investigated the effect of each NP coupling on various observables in a model independent way. We

have predicted the branching ratio of $B^- \to \Lambda \bar{p}\, \mu^+\, \mu^-$ decay mode, obtained asymmetries in angular distributions and triple product correlations in the SM and in the presence of NP in Chapter-3.

In the past few years, semileptonic $B \to D^{(*)}\, l\, \nu$ decays have been extensively studied following BaBar measurement of R_{D_s} and $R_{D_s^*}$ rather than $B_s \to D_s^{(*)}\, l\, \nu$ semileptonic decays. However, both of these semileptonic decays are related to each other by $SU(3)_F$ flavor symmetry. Both the decays involve the same quark level transition $b \to c\, l\, \nu$ but the only difference is in the spectator quark. For $B \to D^{(*)}\, l\, \nu$ decays, the spectator quark is u or d while for $B_s \to D_s^{(*)}\, l\, \nu$ decays, the spectator quark is s. From experimental side there is no information for the numerical values of branching ratios of $B_s \to D_s^{(*)}\, l\, \nu$ decays. We have studied the $B_s \to {D_s}^{(*)}\, l\, \bar{\nu}_l$ semileptonic decays within the framework of the Standard Model. We have estimated the numerical values of branching ratios, defined new observables such as R_{D_s, D_s^*} and $R_{\tau,\, l}$ which could be measurable in the up-coming Super-B experiments. We have studied the observables such as differential branching ratio and forward-backward asymmetry and their implications in the Chapter-4. In chapter-5 we summarized the work done in the thesis with some concluding remarks.

Chapter 2

New physics in $b \to u$ and $b \to c$ leptonic and semileptonic decays

2.1 Introduction

Although, the Standard Model (SM) of particle physics can explain almost all the existing data to a very good precision, there are some unknowns which are beyond the scope of the SM. The latest discovery of a Higgs like particle by CMS [21] and ATLAS [22,23] further confirm the validity of the SM as a low energy effective theory. There are two ways to look for evidence of New Physics (NP): direct detection and indirect detection. The Large Hadron Collider (LHC), which is running successfully at CERN, in principle, has the ability to detect new particles that are not within the SM, while, on the other hand the LHCb experiment has the ability to perform indirect searches of New Physics (NP) effects, and since any NP will affect the SM observables, any discrepancy between measurements and the SM expectation will be an indirect evidence of NP beyond the SM.

Recent measurements of $b \to u\,\tau\,\nu$ and $b \to c\,\tau\,\nu$ leptonic and semi-leptonic B decays differ from SM expectation. The measured branching ratio of $(11.4 \pm 2.2) \times 10^{-5}$ [24–26] for the leptonic $B^- \to \tau^-\,\nu$ decay mode is larger than the SM expectation [27–29]. However, the measured branching ratio of $(14.6 \pm 0.7) \times 10^{-5}$ [30–32] for the exclusive semileptonic $B^0 \to \pi^+\,l\,\nu$ decays is consistent with the SM prediction. The SM calculation, however, depends on the hadronic quantities such as B meson decay constant and $B \to \pi$ transition form factors and the CKM element $|V_{ub}|$. The ratio of branching fractions defined by

$$R_\pi^l = \frac{\tau_{B^0}}{\tau_{B^-}} \frac{\mathcal{B}(B^- \to \tau^-\,\nu)}{\mathcal{B}(B^0 \to \pi^+\,l^-\,\nu)} \tag{2.1}$$

is independent of the CKM matrix elements and is measured to be (0.73 ± 0.15) [33] and there is still more than 2σ discrepancy with the SM expectation. More recently, BaBar [34] measures the ratio of branching fractions of $B \to (D,\, D^*)\,\tau\,\nu$ to the corresponding $B \to (D,\, D^*)\,l\nu$ and finds 3.4σ

discrepancy with the SM expectation [35]. The measured ratios are

$$R_D = \frac{\mathcal{B}(\bar{B} \to D\tau^-\bar{\nu}_\tau)}{\mathcal{B}(\bar{B} \to D\, l^-\bar{\nu}_l)} = 0.440 \pm 0.058 \pm 0.042\,,$$
$$R_{D^*} = \frac{\mathcal{B}(\bar{B} \to D^*\tau^-\bar{\nu}_\tau)}{\mathcal{B}(\bar{B} \to D^*\, l^-\bar{\nu}_l)} = 0.332 \pm 0.024 \pm 0.018\,, \tag{2.2}$$

where the first error is statistical and the second one is systematic. For definiteness, we consider $B^- \to l^-\,\bar{\nu}_l$, $\bar{B}^0 \to \pi^+\, l^-\,\bar{\nu}_l$, $B^- \to D^0\, l^-\,\bar{\nu}_l$, and $B^- \to D^{*\,0}\, l^-\,\bar{\nu}_l$ throughout this chapter. However, for brevity, we denote all these decay modes as $B \to l\,\nu$, $B \to \pi\, l\,\nu$, $B \to D\, l\,\nu$, and $B \to D^*\, l\,\nu$, respectively.

Due to the large mass of the tau lepton, decay processes with a tau lepton in the final state are more sensitive to some New Physics effects than processes with first two generation leptons. These NP, in principle, can enhance the decay rate for these helicity suppressed decay modes quite significantly from the SM prediction. In Ref. [35], a thorough investigation of the lowest dimensional effective operators that leads to modifications in the $B \to D^*\tau\nu$ decay amplitudes has been done. Possible NP effects on various observables have been explored. Among all the leptonic and semileptonic decays, decays with a tau lepton in the final state can be an excellent probe of New Physics as these are sensitive to non-SM contribution arising from the violation of lepton flavor universality (LFU). A model independent analysis to identify the New Physics models has been explored in Ref. [33]. They also look at the possibility of a scalar leptoquark or a vector leptoquark which can contribute to these decay processes at the tree level and obtain a bound of $m \geq 280\,\text{GeV}$ on the mass of the scalar electroweak triplet leptoquark. Model with composite quarks and leptons also modify these $b \to u$ and $b \to c$ semileptonic measurements [33]. The enhanced production of tau lepton in leptonic and semileptonic decays can be explained by NP contribution with different models among which the minimal supersymmetric standard model (MSSM) is well motivated and charming candidate of NP whose Higgs sector contains the two Higgs doublet model (2HDMs). There are four types of 2HDMs such as type-I, type-II, lepton specific, and flipped [36]. New particles such as charged Higgs bosons whose coupling is proportional to the masses of particles in the interaction can have significant effect on decay processes having a tau lepton in the final state. In Ref. [37–40], the author uses the 2HDM model of type-II for purely leptonic B decays that are sensitive to charged Higgs boson at the tree level. This model, however, can not explain all the $b \to c$ semileptonic measurements simultaneously [34]. A lot of studies have been done using the 2HDM of type II and type III models [41–48]. However, none of the above 2HDMs can accomodate all the existing data on $b \to u$ and $b \to c$ semi-(leptonic) decays. Recently, a detail study of a 2HDM of type III with MSSM-like Higgs potential and flavor-violation in the up sector in Ref. [49] has demonstated that this model can explain the deviation from the SM in R_π^l, R_D, and R_{D^*} simultaneously and predict enhancement in the $B \to \tau\nu$, $B \to D\tau\nu$, and the $B \to D^*\,\tau\nu$ decay branching ratios. Also, in Ref. [50, 51], the authors have used a model independent way to analyse the $B \to D\tau\nu$ and $B \to D^*\tau\nu$ data by considering an effective theory for the $b \to c\,\tau\,\nu$ processes in the presence of NP and obtain bounds on each NP parameter. They consider two different NP scenarios and see the effect of various NP couplings on different observables. This analysis, however, does not include the $B \to \tau\nu$ data. Similar analysis has been performed in Ref. [52] considering a tensor operator in

the effective weak Hamiltonian. Also, in Ref. [53], the author investigates the effects of an effective right handed charged currents on the determination of V_{ub} and V_{cb} from inclusive and exclusive B decays. Moreover, the Aligned Two Higgs Doublet Model (A2HDM) [54] and more recently a non-universal left-right model [55] have been explored in order to explain the discrepancies between the measurements and the SM prediction.

The recent measurements suggest the possibility of having New Physics in the third generation leptons only. However, more experimental studies are needed to confirm the presence of NP. A thorough investigation of these decays will enable us to have significant constraints on NP scenarios. In this chapter, we use the most general effective Lagrangian for the $b \to q$ semi-(leptonic) transition decays and do a combined analysis of $b \to u$ and $b \to c$ semi-(leptonic) decay processes where we use constraints from all the existing data related to these decays. It differs considerably from earlier treatment. Firstly, we have introduced the right handed neutrinos and their interactions for our analysis. Secondly, we have performed a combined analysis of all the $b \to u$ and $b \to c$ data. We illustrate four different scenarios of the New Physics and the effects of each NP coupling on various observables are shown. We predict the branching ratio of $B_c \to \tau\nu$ and $B \to \pi\tau\nu$ decay processes in all four different scenarios. We also consider the ratio of branching ratio R_π of $B \to \pi\tau\nu$ to the corresponding $B \to \pi\, l\, \nu$ decay mode for our anaysis.

The chapter is organised as follows. In section 2.2, we start with a brief description of the effective Lagrangian for the $b \to (u,\, c)\, l\, \nu$ processes and then present all the relevant formulae of the decay rates for various decay modes in the presence of various NP couplings. We then define several observables in $B \to \pi\tau\nu$, $B \to D\tau\nu$, and $B \to D^*\tau\nu$ decays. The numerical prediction for various NP couplings and the effects of each NP coupling on various observables are presented in section 2.3. We also discuss the effects of these NP couplings on $\mathcal{B}(B_c \to \tau\nu)$, $\mathcal{B}(B \to \pi\tau\nu)$, and the ratio R_π for various NP scenarios in this section. We conclude with a summary of our results in section 2.4.

2.2 Effective Lagrangian and decay amplitude

The most general effective Lagrangian for $b \to q'\, l\, \nu$ in presence of NP, where $q' = u,\, c$, can be written as [56, 57]

$$\begin{aligned}
\mathcal{L}_{\rm eff} \;=\; & -\frac{g^2}{2\,M_W^2}\,V_{q'b}\,\Big\{(1+V_L)\,\bar{l}_L\,\gamma_\mu\,\nu_L\,\bar{q'}_L\,\gamma^\mu\,b_L + V_R\,\bar{l}_L\,\gamma_\mu\,\nu_L\,\bar{q'}_R\,\gamma^\mu\,b_R \\
& + \widetilde{V}_L\,\bar{l}_R\,\gamma_\mu\,\nu_R\,\bar{q'}_L\,\gamma^\mu\,b_L + \widetilde{V}_R\,\bar{l}_R\,\gamma_\mu\,\nu_R\,\bar{q'}_R\,\gamma^\mu\,b_R \\
& + S_L\,\bar{l}_R\,\nu_L\,\bar{q'}_R\,b_L + S_R\,\bar{l}_R\,\nu_L\,\bar{q'}_L\,b_R \\
& + \widetilde{S}_L\,\bar{l}_L\,\nu_R\,\bar{q'}_R\,b_L + \widetilde{S}_R\,\bar{l}_L\,\nu_R\,\bar{q'}_L\,b_R \\
& + T_L\,\bar{l}_R\,\sigma_{\mu\nu}\,\nu_L\,\bar{q'}_R\,\sigma^{\mu\nu}\,b_L + \widetilde{T}_L\,\bar{l}_L\,\sigma_{\mu\nu}\,\nu_R\,\bar{q'}_L\,\sigma^{\mu\nu}\,b_R\Big\} + \text{h.c.}\,,
\end{aligned} \tag{2.3}$$

where g is the weak coupling constant which can be related to the Fermi constant by the relation $g^2/\,8\,M_W^2 = G_F/\sqrt{2}$ and $V_{q'b}$ is the Cabibbo-Kobayashi-Maskawa (CKM) Matrix elements. The New Physics couplings denoted by $V_{L,R}$, $S_{L,R}$, and T_L involve left handed neutrinos, whereas, the

NP couplings denoted by $\widetilde{V}_{L,R}$, $\widetilde{S}_{L,R}$, and $\widetilde{T}_L$ involve right handed neutrinos. We assume the NP couplings to be real for our analysis. Again, the projection operators are $P_L = (1-\gamma_5)/2$ and $P_R = (1+\gamma_5)/2$. We neglect the New Physics effects coming from the tensor couplings T_L and $\widetilde{T}_L$ for our analysis. With this simplification, we obtain

$$\begin{aligned}
\mathcal{L}_{\rm eff} &= -\frac{G_F}{\sqrt{2}}\, V_{q'b} \Big\{ G_V\, \bar{l}\,\gamma_\mu\,(1-\gamma_5)\,\nu_l\,\bar{q'}\,\gamma^\mu\,b - G_A\,\bar{l}\,\gamma_\mu\,(1-\gamma_5)\,\nu_l\,\bar{q'}\,\gamma^\mu\,\gamma_5\,b \\
&\quad + G_S\,\bar{l}\,(1-\gamma_5)\,\nu_l\,\bar{q'}\,b - G_P\,\bar{l}\,(1-\gamma_5)\,\nu_l\,\bar{q'}\,\gamma_5\,b \\
&\quad + \widetilde{G}_V\,\bar{l}\,\gamma_\mu\,(1+\gamma_5)\,\nu_l\,\bar{q'}\,\gamma^\mu\,b - \widetilde{G}_A\,\bar{l}\,\gamma_\mu\,(1+\gamma_5)\,\nu_l\,\bar{q'}\,\gamma^\mu\,\gamma_5\,b \\
&\quad + \widetilde{G}_S\,\bar{l}\,(1+\gamma_5)\,\nu_l\,\bar{q'}\,b - \widetilde{G}_P\,\bar{l}\,(1+\gamma_5)\,\nu_l\,\bar{q'}\,\gamma_5\,b \Big\} + \text{h.c.}\,, \qquad (2.4)
\end{aligned}$$

where

$$\begin{aligned}
&G_V = 1 + V_L + V_R\,, && G_A = 1 + V_L - V_R\,, \\
&G_S = S_L + S_R\,, && G_P = S_L - S_R\,, \\
&\widetilde{G}_V = \widetilde{V}_L + \widetilde{V}_R\,, && \widetilde{G}_A = \widetilde{V}_L - \widetilde{V}_R\,, \\
&\widetilde{G}_S = \widetilde{S}_L + \widetilde{S}_R\,, && \widetilde{G}_P = \widetilde{S}_L - \widetilde{S}_R\,. \qquad (2.5)
\end{aligned}$$

In the SM, $G_V = G_A = 1$ and all other NP couplings are zero.

The expressions for $B \to l\nu$, $B \to P\,l\nu$, and $B \to V\,l\,\nu$ decay amplitude depends on non-perturbative hadronic matrix elements that can be expressed in terms of B_q meson decay constants and $B \to (P,\,V)$ transition form factors, where P denotes a pseudoscalar meson and V denotes a vector meson, respectively. The B meson decay constant and $B \to (P,\,V)$ transition form factors are defined as

$$\begin{aligned}
\langle 0|\bar{q'}\,\gamma_\mu\,\gamma_5\,b|B(p)\rangle &= -i\,f_{B_{q'}}\,p_\mu \\
\langle P(p')|\bar{q'}\,\gamma_\mu\,b|B(p)\rangle &= F_+(q^2)\left[(p+p')_\mu - \frac{m_B^2 - m_P^2}{q^2}\,q_\mu\right] + F_0(q^2)\,\frac{m_B^2 - m_P^2}{q^2}\,q_\mu \\
\langle V(p',\epsilon^*)|\bar{q'}\,\gamma_\mu\,b|B(p)\rangle &= \frac{2\,i\,V(q^2)}{m_B + m_V}\,\varepsilon_{\mu\nu\rho\sigma}\,\epsilon^{*\nu}\,p'^{\rho}\,p^\sigma\,, \\
\langle V(p',\epsilon^*)|\bar{q'}\,\gamma_\mu\,\gamma_5\,b|B(p)\rangle &= 2\,m_V\,A_0(q^2)\,\frac{\epsilon^*.\,q}{q^2}\,q_\mu \;+\; (m_B + m_V)\,A_1(q^2)\left[\epsilon^*_\mu \;-\; \frac{\epsilon^*.\,q}{q^2}\,q_\mu\right] \\
&\quad - A_2(q^2)\,\frac{\epsilon^*.\,q}{(m_B \,+\, m_V)}\left[(p+p')_\mu \;-\; \frac{m_B^2 \,-\, m_V^2}{q^2}\,q_\mu\right], \qquad (2.6)
\end{aligned}$$

where $q = p - p'$ is the momentum transfer. Again, from Lorentz invariance and parity, we obtain

$$\begin{aligned}
&\langle 0|\bar{q'}\,\gamma_\mu\,b|B(p)\rangle = 0\,, \\
&\langle P(p')|\bar{q'}\,\gamma_\mu\,\gamma_5\,b|B(p)\rangle = 0\,, \\
&\langle V(p',\epsilon^*)|\bar{q'}\,b|B(p)\rangle = 0\,. \qquad (2.7)
\end{aligned}$$

We use the equation of motion to find the scalar and pseudoscalar matrix elements. That is

$$\begin{aligned}
\langle 0|\bar{q'}\,\gamma_5\,b|B(p)\rangle &= i\,\frac{m_B^2}{m_b(\mu)+m_{q'}(\mu)}\,f_{B_{q'}}\,,\\
\langle P(p')|\bar{q'}\,b|B(p)\rangle &= \frac{m_B^2-m_P^2}{m_b(\mu)-m_{q'}(\mu)}\,F_0(q^2)\,,\\
\langle V(p',\epsilon^*)|\bar{q'}\,\gamma_5\,b|B(p)\rangle &= -\,\frac{2\,m_V\,A_0(q^2)}{m_b(\mu)+m_{q'}(\mu)}\epsilon^*.\,q\,,
\end{aligned} \tag{2.8}$$

where, for the $B\to\pi$ form factors, we use the formulae and the input values reported in Ref. [58]. Similarly, we follow Refs. [59–62] and employ heavy quark effective theory (HQET) to estimate the $B\to D$ and $B\to D^*$ form factors.

Using the effective Lagrangian of Eq. (2.4) in the presence of NP, the partial decay width of $B\to l\nu$ can be expressed as

$$\begin{aligned}
\Gamma(B\to l\nu) \;=\; & \frac{G_F^2\,|V_{ub}|^2}{8\,\pi}\,f_B^2\,m_l^2\,m_B\left(1-\frac{m_l^2}{m_B^2}\right)^2\Bigg\{\Big[G_A-\frac{m_B^2}{m_l\,(m_b(\mu)+m_u(\mu))}\,G_P\Big]^2\\
&+\Big[\widetilde{G}_A-\frac{m_B^2}{m_l\,(m_b(\mu)+m_u(\mu))}\,\widetilde{G}_P\Big]^2\Bigg\}\,,
\end{aligned} \tag{2.9}$$

where, in the SM, we have $G_A=1$ and $G_P=\widetilde{G}_A=\widetilde{G}_P=0$, so that

$$\Gamma(B\to l\nu)_{\rm SM} \;=\; \frac{G_F^2\,|V_{ub}|^2}{8\,\pi}\,f_B^2\,m_l^2\,m_B\left(1-\frac{m_l^2}{m_B^2}\right)^2. \tag{2.10}$$

It is important to note that the right handed neutrino couplings denoted by $\widetilde{V}_{L,R}$ and $\widetilde{S}_{L,R}$ appear in the decay width quadratically, whereas, the left handed neutrino couplings denoted by $V_{L,R}$ and $S_{L,R}$ appear linearly in the decay rates. The linear dependence, arises due to the interference between the SM couplings and the NP couplings, is suppressed for the right handed neutrino couplings as it is proportional to a small factor m_ν and hence is neglected. We now proceed to discuss the $B\to P\,l\,\nu$ and $B\to V\,l\,\nu$ decays. First, we discuss about the form factors of $B\to P\,l\,\nu$ and $B\to V\,l\,\nu$ decays then we discuss about the helicity methods of Ref. [63, 64] for the $B\to P\,l\,\nu$ and $B\to V\,l\,\nu$ semileptonic decays using which we have calculated the differential decay rates.

2.2.1 B to π Form Factors

For the $B\to\pi$ transition form factors, there are two non-perturbative methods for calculating the $B\to\pi$ form factors: light cone sum rules (LCSR) and lattice QCD (LQCD). QCD light-cone sum rules with pion distribution amplitudes allow one to calculate the $B\to\pi$ form factors at small and intermediate momentum transfers $0\le q^2\le q^2_{\rm max}$, where $q^2_{\rm max}$ varies from 12 to 16 GeV^2 [65–69]. The most recent lattice QCD computations with three dynamical flavours predict these form factors at $q^2\ge 16\,{\rm GeV}^2$, in the upper part of the semileptonic region $0\le q^2\le (m_B-m_\pi)^2$, with an accuracy reaching 10%. There are also recent results available in the quenched approximation on a fine lattice [70–72]. Very recently, in Ref. [58], the author uses the sum rule results for the form factors as an input for a z-series parameterization that yield the q^2 shape in the whole semileptonic region of $B\to\pi\,l\,\nu$. The relevant formulae for $F_+(q^2)$ and $F_0(q^2)$ pertinent for our discussion, taken

from Ref. [58], are

$$F_+(q^2) = \frac{F_+(0)}{\left(1-\frac{q^2}{m_B^2}\right)}\left\{1+\sum_{k=1}^{N-1} b_k\left(z(q^2,t_0)^k - z(0,t_0)^k - (-1)^{N-k}\,\frac{k}{N}\left[z(q^2,t_0)^N - z(0,t_0)^N\right]\right)\right\}$$
$$F_0(q^2) = F_0(0)\left\{1+\sum_{k=1}^{N} b_k^0\left(z(q^2,t_0)^k - z(0,t_0)^k\right)\right\} \tag{2.11}$$

where by default $F_+(0) = F_0(0)$ and

$$z(q^2,t_0) = \frac{\sqrt{(m_B+m_\pi)^2-q^2}-\sqrt{(m_B+m_\pi)^2-t_0}}{\sqrt{(m_B+m_\pi)^2-q^2}+\sqrt{(m_B+m_\pi)^2-t_0}} \tag{2.12}$$

where the auxiliary parameter t_0 is defined as $t_0 = (m_B+m_\pi)^2 - 2\sqrt{m_B\,m_\pi}\,\sqrt{(m_B+m_\pi)^2-q^2_{\rm min}}$. The central values of $F_+(0) = F_0(0)$ and the slope parameters b_1 and b_1^0 are

$$\begin{aligned} F_0(0) = F_+(0) &= 0.281 \pm 0.028\,,\\ b_1 &= -1.62 \pm 0.70\,,\\ b_1^0 &= -3.98 \pm 0.97\,. \end{aligned} \tag{2.13}$$

For the uncertainties, we add the various errors reported in Ref. [58] in quadrature.

2.2.2 $B \to D$, D^* form Factors using HQET

In the heavy quark effective theory one can write the hadronic matrix elements of current between two hadrons in inverse powers of heavy quark mass and the hadronic form factor in a reduced single universal form which is function of the kinematic variable $v_B.v_{P(V)}$ where v_B and $v_{P(V)}$ are the four velocity of the B meson and the pseudoscalar (vector) meson, respectively. The weak vector and axial vector currents are parametrized as [59, 60]

$$\begin{aligned} \langle\, D(v')|\bar c\,\gamma_\mu\, b|B(v)\rangle &= \sqrt{m_B\,m_D}\left[h_+(\omega)(v+v')_\mu + h_-(\omega)(v-v')_\mu\right],\\ \langle D^*(v',\epsilon')|\bar c\,\gamma_\mu\, b|B(v)\rangle &= i\sqrt{m_B\,m_D}\,h_V(\omega)\,\varepsilon_{\mu\nu\alpha\beta}\,\epsilon'^{*\nu}\,v'^{\alpha}v^{\beta}\,,\\ \langle D^*(v',\epsilon')|\bar c\,\gamma_\mu\,\gamma_5\, b|B(v)\rangle &= \sqrt{m_B\,m_D}\,\Big[\,h_{A_1}(\omega)\,(\omega+1)\,\epsilon'^*_\mu - h_{A_2}(\omega)\epsilon'^*\cdot v\,v_\mu\\ &\quad -h_{A_3}(\omega)\,\epsilon'^*.v\,v'_\mu\,\Big]\,, \end{aligned} \tag{2.14}$$

where the kinemetic variable $\omega = v_B.v_{(D,\,D^*)} = (m_B^2 + m^2_{(D,\,D^*)} - q^2)/\,2\,m_B\,m_{(D,\,D^*)}$. Now, for the $B \to D$ form factors $F_+(q^2)$ and $F_0(q^2)$, we obtain

$$\begin{aligned} F_+(q^2) &= \frac{V_1(\omega)}{r_D}\,,\\ F_0(q^2) &= \frac{(1+\omega)\,r_D}{2}\,S_1(\omega)\,, \end{aligned} \tag{2.15}$$

where $V_1(\omega)$ and $S_1(\omega)$, taken from Ref. [61], are

$$V_1(\omega) = \Big[\, h_+(\omega) - \frac{(1-r)}{(1+r)}\, h_-(\omega) \Big]\,,$$
$$S_1(\omega) = \Big[\, h_+(\omega) - \frac{(1+r)(\omega-1)}{(1-r)(\omega+1)}\, h_-(\omega) \Big]\,, \tag{2.16}$$

and

$$r_D = \frac{2\sqrt{m_B\, m_D}}{(m_B + m_D)}\,, \qquad\qquad r = \frac{m_D}{m_B}. \tag{2.17}$$

We follow Ref. [62] and parametrised $V_1(\omega)$ in terms of ρ_1 and z parameters as

$$V_1(\omega) = V_1(1)\left[1 - 8\,\rho_1^2\, z + (51\,\rho_1^2 - 10)\, z^2 - (252\,\rho_1^2 - 84)\, z^3\right], \tag{2.18}$$

where $z = (\sqrt{\omega+1} - \sqrt{2})/(\sqrt{\omega+1} + \sqrt{2})$. The numerical values of $V_1(1)$ and ρ_1^2 are [78]

$$V_1(1)|V_{cb}| = (43.0 \pm 1.9 \pm 1.4) \times 10^{-3},$$
$$\rho_1^2 = 1.20 \pm 0.09 \pm 0.04. \tag{2.19}$$

The form factor $S_1(\omega)$ has the following parametrisation [62].

$$S_1(\omega) = 1.0036[1 - 0.0068(\omega-1) + 0.0017(\omega-1)^2 - 0.0013(\omega-1)^3]V_1(\omega). \tag{2.20}$$

We now concentrate on the $B \to V$ i.e. $B \to D^*$ form factor in the HQET [35] by defining the universal form factor h_{A_1} which can be related to $A_0(q^2)$, $A_1(q^2)$, $A_2(q^2)$, and $V(q^2)$ as

$$A_1(q^2) = r_{D^*}\frac{\omega+1}{2} h_{A_1}(\omega)\,,$$
$$A_0(q^2) = \frac{R_0(\omega)}{r_{D^*}} h_{A_1}(\omega)\,,$$
$$A_2(q^2) = \frac{R_2(\omega)}{r_{D^*}} h_{A_1}(\omega)\,,$$
$$V_0(q^2) = \frac{R_1(\omega)}{r_{D^*}} h_{A_1}(\omega)\,. \tag{2.21}$$

where $r_{D^*} = 2\sqrt{m_B\, m_{D^*}}/(m_B + m_{D^*})$. The ω dependence of the form factors in the limit of heavy quark can be written as [35, 61]

$$h_{A_1}(\omega) = h_{A_1}(1)[1 - 8\,\rho^2 z + (53\rho^2 - 15)z^2 - (231\rho^2 - 91)z^3]\,,$$
$$R_1(\omega) = R_1(1) - 0.12(\omega-1) + 0.05(\omega-1)^2\,,$$
$$R_2(\omega) = R_2(1) + 0.11(\omega-1) - 0.06(\omega-1)^2\,,$$
$$R_0(\omega) = R_0(1) - 0.11(\omega-1) + 0.01(\omega-1)^2\,, \tag{2.22}$$

where, we use the following numerical values of the free parameters from Refs. [35, 79] for our

numerical analysis. That is

$$
\begin{aligned}
&h_{A_1}(1)\,|V_{cb}| = (34.6 \pm 0.2 \pm 1.0) \times 10^{-3}\,,\\
&\rho_1^2 = 1.214 \pm 0.034 \pm 0.009\,,\\
&R_1(1) = 1.401 \pm 0.034 \pm 0.018\,,\\
&R_2(1) = 0.864 \pm 0.024 \pm 0.008\,,\\
&R_0(1) = 1.14 \pm 0.114
\end{aligned}
\tag{2.23}
$$

We follow the helicity methods of Ref. [63, 64] for the $B \to P\,l\,\nu$ and $B \to V\,l\,\nu$ semileptonic decays. The differential decay distribution can be written as

$$
\frac{d\Gamma}{dq^2\,d\cos\theta_l} \;=\; \frac{G_F^2\,|V_{q'b}|^2\,|\overrightarrow{p}_{(P,\,V)}|}{2^9\,\pi^3\,m_B^2}\left(1-\frac{m_l^2}{q^2}\right)L_{\mu\nu}\,H^{\mu\nu}\,, \tag{2.24}
$$

where, $L_{\mu\nu}$ and $H_{\mu\nu}$ are usual leptonic and hadronic tensor, respectively. Here, θ_l is the angle between the P (V) meson and the lepton three momentum vector in the q^2 rest frame. The three momentum vector $|\overrightarrow{p}_{(P,\,V)}|$ is defined as $|\overrightarrow{p}_{(P,\,V)}| = \sqrt{\lambda(m_B^2,\,m_{P(V)}^2,\,q^2)}/2\,m_B$, where $\lambda(a,\,b,\,c) = a^2+b^2+c^2-2\,(a\,b+b\,c+c\,a)$.

In the next section, we provide the details of kinematics and helicity method to calculate the different helicity amplitudes for $B \to P\,l\,\nu$ and $B \to V\,l\,\nu$ semileptonic decays.

2.2.3 Kinematics and Helicity Amplitudes

We use the Helicity method of Refs. [63, 64] to calculate the different helicity amplitudes for a B meson decaying to Pseudoscalar(Vector) meson along with a charged lepton and an antineutrino in the final state. We know that, the amplitude square of the decay $B \to P(V)\,l\,\nu$ can be factorised into leptonic ($L_{\mu\nu}$) and hadronic ($H_{\mu\nu}$) tensors. That is

$$
|\mathcal{M}(B \to P(V)\,l\,\nu)|^2 \;=\; |\langle P(V)\,l\,\nu|\mathcal{L}_{\rm eff}|B\rangle|^2 = L_{\mu\nu}H^{\mu\nu}\,. \tag{2.25}
$$

The leptonic and hadronic tensor product $L_{\mu\nu}\,H^{\mu\nu}$ depends on the polar angle $\cos\theta_l$, where θ_l is the angle between the P (V) meson three momentum vector and the lepton three momentum vector in the q^2 rest frame, and can be worked out using the completeness relation of the polarization four vectors $\epsilon(t,\pm,0)$, i.e,

$$
\sum_{m,\,m'=t,\pm,0} \epsilon^{\mu}(m)\,\epsilon^{*\,\nu}(m')\,g_{m\,m'} = g^{\mu\nu}\,, \tag{2.26}
$$

where $g_{m\,m'} = {\rm diag}(+,\,-,\,-,\,-)$. Using this approach, one can factorize $L_{\mu\nu}\,H^{\mu\nu}$ in terms of two Lorentz invariant quantities such that

$$
\begin{aligned}
L_{\mu\nu}\,H^{\mu\nu} \;&=\; L^{\mu'\nu'}\,g_{\mu'\mu}\,g_{\nu'\nu}H^{\mu\nu} = \sum_{m,m',n,n'} L^{\mu'\nu'}\,\epsilon_{\mu'}(m)\,\epsilon^*_{\mu}(m')\,g_{mm'}\,\epsilon^*_{\nu'}(n)\,\epsilon_{\nu}(n')\,g_{nn'}\,H^{\mu\nu}\\
&= \sum_{m,m',n,n'} \Big(L^{\mu'\nu'}\,\epsilon_{\mu'}(m)\,\epsilon^*_{\nu'}(n)\Big)\Big(H^{\mu\nu}\,\epsilon^*_{\mu}(m')\,\epsilon_{\nu}(n')\Big)\,g_{mm'}\,g_{nn'}
\end{aligned}
$$

$$= \sum_{m,\,m',\,n,\,n'} L(m,\,n)\,H(m',\,n')\,g_{m\,m'}\,g_{n\,n'}\,, \tag{2.27}$$

where $L(m,\,n)$ and $H(m',\,n')$ can now be evaluated in different Lorentz frames. We evaluate $L(m,\,n)$ in the $l-\nu$ center of mass frame, i.e, in q^2 rest frame and $H(m',\,n')$ in the B meson rest frame.

In the B meson rest frame, the helicity basis ϵ is taken to be

$$\begin{aligned}
\epsilon(0) &= \frac{1}{\sqrt{q^2}}(|p_M|, 0, 0, -q_0)\,, \qquad\qquad \epsilon(\pm) = \pm\frac{1}{\sqrt{2}}(0, \pm 1, -i, 0)\,, \\
\epsilon(t) &= \frac{1}{\sqrt{q^2}}(q_0, 0, 0, -|p_M|)\,,
\end{aligned} \tag{2.28}$$

where $q_0 = (m_B^2 - m_M^2 + q^2)/\,2m_B$ and $q = p_B - p_M$ is the momentum transfer, respectively. Here m_M and p_M denotes the mass and the four momentum of the final state Pseudoscalar(Vector) meson M, respectively. Again, we have $|p_M| = \lambda^{1/2}(m_B^2, m_M^2, q^2)/2m_B$. In the B meson rest frame, the B and M meson four momenta p_B and p_M are

$$p_B = (m_B, 0, 0, 0)\,, \qquad\qquad p_M = (E_M, 0, 0, |\vec{p}_M|)\,, \tag{2.29}$$

where the $E_M = (m_B^2 + m_M^2 - q^2)/\,2m_B$. For vector meson in the final state, the polarization four vectors obey the following orthonormality condition

$$\epsilon_\alpha^*(m)\,\epsilon^\alpha(m') = -\,\delta_{mm'} \tag{2.30}$$

and the completeness relation

$$\sum_{m,m'} \epsilon_\alpha(m)\,\epsilon_\beta(m')\,\delta_{mm'} = -g_{\alpha\beta} + \frac{(p_V)_\alpha (p_V)_\beta}{m_V^2}\,. \tag{2.31}$$

The leptonic tensor $L(m,\,n)$ is evaluated in the $l-\nu_l$ center of mass frame, i.e, in the q^2 rest frame. In this frame, the helicity basis ϵ is taken to be

$$\begin{aligned}
\epsilon(0) &= (0, 0, 0, -1)\,, \qquad\qquad \epsilon(\pm) = \pm\frac{1}{\sqrt{2}}(0, \pm 1, -i, 0)\,, \\
\epsilon(t) &= (1, 0, 0, 0)\,.
\end{aligned} \tag{2.32}$$

In the q^2 rest frame, the four momenta of the lepton and the anti-neutrino pair can be written as

$$\begin{aligned}
p_l^\mu &= (E_l,\, |p_l|\,\sin\theta_l,\, 0,\, -|p_l|\,\cos\theta_l)\,, \\
p_\nu^\mu &= (|p_l|,\, -|p_l|\,\sin\theta_l,\, 0,\, |p_l|\,\cos\theta_l)\,,
\end{aligned} \tag{2.33}$$

where the lepton energy $E_l = (q^2 + m_l^2)/2\sqrt{q^2}$ and the magnitude of its three momenta is $|p_l| = (q^2 - m_l^2)/2\sqrt{q^2}$.

The resulting differential decay distribution for $B \to P\,l\,\nu$ in terms of the helicity amplitudes

H_0, H_t, and H_S is

$$\frac{d\Gamma}{dq^2\, d\cos\theta_l} = 2\,N\,|\overrightarrow{p}_P|\left\{H_0^2\,\sin^2\theta_l\left(G_V^2+\widetilde{G}_V^2\right)+\frac{m_l^2}{q^2}\Big[H_0\,G_V\,\cos\theta_l-\Big(H_t\,G_V+\frac{\sqrt{q^2}}{m_l}\,H_S\,G_S\Big)\Big]^2\right.$$
$$\left.+\frac{m_l^2}{q^2}\Big[H_0\,\widetilde{G}_V\,\cos\theta_l-\Big(H_t\,\widetilde{G}_V+\frac{\sqrt{q^2}}{m_l}\,H_S\,\widetilde{G}_S\Big)\Big]^2\right\} \tag{2.34}$$

where

$$N=\frac{G_F^2\,|V_{q'b}|^2\,q^2}{256\,\pi^3\,m_B^2}\left(1-\frac{m_l^2}{q^2}\right)^2, \qquad H_0=\frac{2\,m_B\,|\overrightarrow{p}_P|}{\sqrt{q^2}}\,F_+(q^2)\,,$$
$$H_t=\frac{m_B^2-m_P^2}{\sqrt{q^2}}\,F_0(q^2)\,, \qquad H_S=\frac{m_B^2-m_P^2}{m_b(\mu)-m_{q'}(\mu)}\,F_0(q^2)\,. \tag{2.35}$$

We determine the differential decay rate $d\Gamma/dq^2$ by performing the $\cos\theta_l$ integration, i.e,

$$\frac{d\Gamma^P}{dq^2} = \frac{8\,N\,|\overrightarrow{p}_P|}{3}\left\{H_0^2\left(G_V^2+\widetilde{G}_V^2\right)\left(1+\frac{m_l^2}{2\,q^2}\right)\right.$$
$$\left.+\frac{3\,m_l^2}{2\,q^2}\left[\Big(H_t\,G_V+\frac{\sqrt{q^2}}{m_l}\,H_S\,G_S\Big)^2+\Big(H_t\,\widetilde{G}_V+\frac{\sqrt{q^2}}{m_l}\,H_S\,\widetilde{G}_S\Big)^2\right]\right\}, \tag{2.36}$$

where, in the SM, $G_V=1$ and all other couplings are zero. One obtains

$$\Big(\frac{d\Gamma^P}{dq^2}\Big)_{\rm SM} = \frac{8\,N\,|\overrightarrow{p}_P|}{3}\left\{H_0^2\Big(1+\frac{m_l^2}{2\,q^2}\Big)+\frac{3\,m_l^2}{2\,q^2}\,H_t^2\right\}. \tag{2.37}$$

Our formulae for the differential branching ratio in the presence of NP couplings in Eq. (2.34) and Eq. (2.36) differ slightly from those given in Ref. [50]. The term containing G_S and $\widetilde{G}_S$ is positive in Eq. (2.34) and Eq. (2.36), whereas, it is negative in Ref. [50]. Although, the SM formula is same, the numerical differences may not be negligible once the NP couplings $S_{L,\,R}$ and $\widetilde{S}_{L,\,R}$ are introduced. It is worth mentioning that, for $l=e,\,\mu$, the term containing m_l^2/q^2 can be safely ignored. However, same is not true for $B\to P\tau\nu$ decay mode as the mass of τ lepton is quite large and one can not neglect the m_τ^2/q^2 term from the decay amplitude. We assume that the NP affects only the third generation lepton and hence these NP couplings are absent in final states with electron and muon.

Similarly, the differential decay distribution for $B\to V\,l\,\nu$ in terms of the helicity amplitudes $\mathcal{A}_0$, $\mathcal{A}_\parallel$, $\mathcal{A}_\perp$, $\mathcal{A}_P$, and $\mathcal{A}_t$ is

$$\frac{d\Gamma}{dq^2\, d\cos\theta_l} = N\,|\overrightarrow{p}_V|\left\{2\,\mathcal{A}_0^2\,\sin^2\theta_l\Big(G_A^2+\widetilde{G}_A^2\Big)+\Big(1+\cos^2\theta_l\Big)\Big[\mathcal{A}_\parallel^2\Big(G_A^2+\widetilde{G}_A^2\Big)+\mathcal{A}_\perp^2\Big(G_V^2+\widetilde{G}_V^2\Big)\Big]\right.$$
$$-4\,\mathcal{A}_\parallel\mathcal{A}_\perp\cos\theta_l\Big(G_A\,G_V-\widetilde{G}_A\,\widetilde{G}_V\Big)+\frac{m_l^2}{q^2}\sin^2\theta_l\Big[\mathcal{A}_\parallel^2\Big(G_A^2+\widetilde{G}_A^2\Big)+\mathcal{A}_\perp^2\Big(G_V^2+\widetilde{G}_V^2\Big)\Big]$$
$$+\frac{2m_l^2}{q^2}\Big[\Big\{\mathcal{A}_0\,G_A\cos\theta_l-\Big(\mathcal{A}_t\,G_A+\frac{\sqrt{q^2}}{m_l}\,\mathcal{A}_P\,G_P\Big)\Big\}^2$$
$$\left.+\Big\{\mathcal{A}_0\,\widetilde{G}_A\cos\theta_l-\Big(\mathcal{A}_t\,\widetilde{G}_A+\frac{\sqrt{q^2}}{m_l}\,\mathcal{A}_P\,\widetilde{G}_P\Big)\Big\}^2\Big]\right\} \tag{2.38}$$

where

$$\mathcal{A}_0 = \frac{1}{2\,m_V\,\sqrt{q^2}}\Big[\Big(m_B^2 - m_V^2 - q^2\Big)(m_B+m_V)A_1(q^2) \;-\; \frac{4M_B^2|\vec{p}_V|^2}{m_B+m_V}A_2(q^2)\Big]\,,$$
$$\mathcal{A}_\parallel = \frac{2(m_B+m_V)A_1(q^2)}{\sqrt{2}}\,, \qquad \mathcal{A}_\perp = -\frac{4m_B V(q^2)|\vec{p}_V|}{\sqrt{2}(m_B+m_V)}\,,$$
$$\mathcal{A}_t = \frac{2m_B|\vec{p}_V|A_0(q^2)}{\sqrt{q^2}}\,, \qquad \mathcal{A}_P = -\frac{2m_B|\vec{p}_V|A_0(q^2)}{(m_b(\mu)+m_c(\mu))}\,. \tag{2.39}$$

We perform the $\cos\theta_l$ integration and obtain the differential decay rate $d\Gamma/dq^2$, that is

$$\frac{d\Gamma^V}{dq^2} \;=\; \frac{8\,N\,|\overrightarrow{p}_V|}{3}\left\{\mathcal{A}_{AV}^2 + \frac{m_l^2}{2\,q^2}\Big[\mathcal{A}_{AV}^2 + 3\mathcal{A}_{tP}^2\Big] + \widetilde{\mathcal{A}}_{AV}^2 + \frac{m_l^2}{2\,q^2}\Big[\widetilde{\mathcal{A}}_{AV}^2 + 3\widetilde{\mathcal{A}}_{tP}^2\Big]\right\} \tag{2.40}$$

where

$$\mathcal{A}_{AV}^2 = \mathcal{A}_0^2\,G_A^2 + \mathcal{A}_\parallel^2\,G_A^2 + \mathcal{A}_\perp^2\,G_V^2\,, \qquad \widetilde{\mathcal{A}}_{AV}^2 = \mathcal{A}_0^2\,\widetilde{G}_A^2 + \mathcal{A}_\parallel^2\,\widetilde{G}_A^2 + \mathcal{A}_\perp^2\,\widetilde{G}_V^2\,,$$
$$\mathcal{A}_{tP} = \mathcal{A}_t\,G_A + \frac{\sqrt{q^2}}{m_l}\,\mathcal{A}_P\,G_P\,, \qquad \widetilde{\mathcal{A}}_{tP} = \mathcal{A}_t\,\widetilde{G}_A + \frac{\sqrt{q^2}}{m_l}\,\mathcal{A}_P\,\widetilde{G}_P\,. \tag{2.41}$$

In the SM, $G_V = G_A = 1$ and all other NP couplings are zero. We obtain

$$\Big(\frac{d\Gamma^V}{dq^2}\Big)_{\rm SM} \;=\; \frac{8\,N\,|\overrightarrow{p}_V|}{3}\left\{(\mathcal{A}_0^2 + \mathcal{A}_{||}^2 + \mathcal{A}_\perp^2)\Big(1 + \frac{m_l^2}{2\,q^2}\Big) + \frac{3\,m_l^2}{2\,q^2}\,\mathcal{A}_t^2\right\}. \tag{2.42}$$

We want to mention that our formulae for the $B \to V\,l\,\nu$ differential decay width in Eq. (2.38) and Eq. (2.40) differ slightly from those reported in Ref. [50]. Our formulae, however, agree with those reported in Ref. [35]. In Eq. (2.38), we have $(1+\cos^2\,\theta_l)$ instead of $(1+\cos\theta_l)^2$ reported in Ref. [50]. Again, note that our definition of $G_P = S_L - S_R$, different from that of $g_P = S_R - S_L$ [50], leads to a sign discrepancy in $\mathcal{A}_{tP}$ ($\widetilde{\mathcal{A}}_{tP}$). Depending on the NP couplings G_P and $\widetilde{G}_P$, the numerical estimates might differ from Ref. [50].

We define some physical observables such as differential branching ratio DBR(q^2), the ratio of branching fractions $R(q^2)$, and the forward-backward asymmetry $A_{FB}(q^2)$.

$$DBR(q^2) = \Big(\frac{d\Gamma}{dq^2}\Big)/\Gamma_{tot}\,, \qquad R(q^2) = \frac{DBR(q^2)\Big(B \to (P,\,V)\,\tau\,\nu\Big)}{DBR(q^2)\Big(B \to (P,\,V)\,l\,\nu\Big)}$$
$$[A_{FB}]_{(P,\,V)}(q^2) = \frac{\Big(\int_{-1}^{0} - \int_0^1\Big)d\cos\theta_l \frac{d\Gamma^{(P,\,V)}}{dq^2\,d\cos\theta_l}}{\frac{d\Gamma^{(P,\,V)}}{dq^2}}\,. \tag{2.43}$$

For $B \to P\,l\,\nu$ decay mode, the forward backward asymmetry in the presence of NP is

$$A_{FB}^P(q^2) \;=\; \frac{3\,m_l^2}{2\,q^2}\frac{H_0\,G_V\left[\Big(H_t\,G_V + \frac{\sqrt{q^2}}{m_l}\,H_S\,G_S\Big) + \Big(H_t\,\widetilde{G}_V + \frac{\sqrt{q^2}}{m_l}\,H_S\,\widetilde{G}_S\Big)\right]}{H_0^2\,(G_V^2 + \widetilde{G}_V^2)(1 + \frac{m_l^2}{2\,q^2}) + \frac{3\,m_l^2}{2\,q^2}\left[\Big(H_t\,G_V + \frac{\sqrt{q^2}}{m_l}\,H_S\,G_S\Big)^2 + \Big(H_t\,\widetilde{G}_V + \frac{\sqrt{q^2}}{m_l}\,H_S\,\widetilde{G}_S\Big)^2\right]} \tag{2.44}$$

where, in the SM, $G_V = 1$ and all other couplings are zero. We obtain

$$\left(A_{FB}^{P}\right)_{\rm SM}(q^2) \;=\; \frac{3\,m_l^2}{2\,q^2}\,\frac{H_0\,H_t}{H_0^2\left(1+\frac{m_l^2}{2\,q^2}\right)+\frac{3\,m_l^2}{2\,q^2}\,H_t^2}\,. \tag{2.45}$$

Similarly, for $B \to V\,l\,\nu$ decay mode, in the presence of NP

$$A_{FB}^{V}(q^2) \;=\; \frac{3}{2}\frac{\mathcal{A}_\parallel\,\mathcal{A}_\perp\left(G_A\,G_V-\widetilde{G}_A\widetilde{G}_V\right)+\frac{m_l^2}{q^2}\mathcal{A}_0\,G_A\Big[\mathcal{A}_t\,G_A-\frac{\sqrt{q^2}}{m_l}\,\mathcal{A}_P\,G_P+\mathcal{A}_t\,\widetilde{G}_A-\frac{\sqrt{q^2}}{m_l}\,\mathcal{A}_P\,\widetilde{G}_P\Big]}{\mathcal{A}_{AV}^2+\frac{m_l^2}{2\,q^2}\Big[\mathcal{A}_{AV}^2+3\mathcal{A}_{tP}^2\Big]+\widetilde{\mathcal{A}}_{AV}^2+\frac{m_l^2}{2\,q^2}\Big[\widetilde{\mathcal{A}}_{AV}^2+3\widetilde{\mathcal{A}}_{tP}^2\Big]} \tag{2.46}$$

In the SM, $G_A = G_V = 1$ while all other NP couplings are zero. Thus we obtain

$$\left(A_{FB}^{V}\right)_{\rm SM}(q^2) \;=\; \frac{3}{2}\,\frac{\mathcal{A}_\parallel\,\mathcal{A}_\perp+\frac{m_l^2}{q^2}\mathcal{A}_0\,\mathcal{A}_t}{\left\{(\mathcal{A}_0^2+\mathcal{A}_{||}^2+\mathcal{A}_\perp^2)\Big(1+\frac{m_l^2}{2\,q^2}\Big)+\frac{3\,m_l^2}{2\,q^2}\,\mathcal{A}_t^2\right\}}\,. \tag{2.47}$$

We see that, in the SM, for the light leptons $l = e,\,\mu$, the forward backward asymmetry is vanishingly small due to the m_l^2/q^2 term for the $B \to P\,l\,\nu$ decay modes. However, for $B \to V\,l\,\nu$, the first term will contribute and we will get a non-zero value for the forward backward asymmetry. Any non-zero value of the A_{FB} parameter for the $B \to P\,l\,\nu$ decay modes will be a hint of NP in all generation leptons. We, however, ignore the NP effects in case of $l = e,\,\mu$. We strictly assume that only third generation leptons get modified due to NP couplings.

We wish to determine various NP effects in a model independent way. The theoretical uncertainties in the calculation of the decay branching fractions come from various input parameters. Firstly, there are uncertainties associated with well known input parameters such as quark masses, meson masses, and life time of the mesons. We ignore these uncertainties as these are not important for our analysis. Secondly, there are uncertainties that are associated with not so well known hadronic input parameters such as form factors, decay constants and the CKM elements. In order to realize the effect of the above mentioned uncertainties on various observables, we use a random number generator and perform a random scan of all the allowed hadronic as well as the CKM elements. In our random scan of the theoretical parameter space, we vary all the hadronic inputs such as $B \to (P,\,V)$ form factors, f_{B_q} decay constants, and CKM elements $|V_{qb}|$ within 3σ from their central values. In order to determine the allowed NP parameter space, we impose the experimental constraints coming from the measured ratio of branching fractions R_π^l, R_D, and R_{D^*} simultaneously. This is to ensure that the resulting NP parameter space can simultaneously accommodate all the existing data on $b \to u$ and $b \to c$ leptonic and semileptonic decays. We impose the experimental constraints in such a way that we ignore those theoretical models which are not compatible within 3σ of the experimental constraints for the 3σ random scan.

2.3 Results and discussion

For definiteness, we summarize the input parameters for our numerical analysis. We use the following inputs from Ref. [26].

$$
\begin{aligned}
&m_b = 4.18\,\text{GeV}\,, && m_c = 1.275\,\text{GeV}\,, && m_\pi = 0.13957\,\text{GeV}\\
&m_{B^-} = 5.27925\,\text{GeV}\,, && m_{B^0} = 5.27955\,\text{GeV}\,, && m_{B_c} = 6.277\,\text{GeV}\,,\\
&m_{D^0} = 1.86486\,\text{GeV}\,, && m_{D^{*\,0}} = 2.00698\,\text{GeV}\,, && \tau_{B^0} = 1.519\times 10^{-12}\,\text{Sec}\,,\\
&\tau_{B^-} = 1.641\times 10^{-12}\,\text{Sec}\,, && \tau_{B_c} = 0.453\times 10^{-12}\,\text{Sec}\,, &&
\end{aligned}
\tag{2.48}
$$

where $m_b \equiv m_b(m_b)$ and $m_c \equiv m_c(m_c)$ denote the running b and c quark masses in $\overline{\text{MS}}$ scheme. We employ a renormalization scale $\mu = m_b$ for which the strong coupling constant $\alpha_s(m_b) = 0.224$. Using the two loop expression for the running quark mass [73], we find $m_c(m_b) = 0.91\,\text{GeV}$. Thus, the coefficients $V_{L,\,R}$, $\widetilde{V}_{L,\,R}$, $S_{L,\,R}$, and $\widetilde{S}_{L,\,R}$ are defined at the scale $\mu = m_b$. The error associated with the quark masses, meson masses, and the mean life time of mesons are not important and we ignore them in our analysis. In Table 2.1 and Table 2.2, we present the most important theoretical and experimental inputs with their uncertainties that are used for our random scan.

CKM Elements:		Meson Decay constants (in GeV):	
$\lvert V_{ub}\rvert$ (Exclusive)	$(3.23 \pm 0.31)\times 10^{-3}$ [26]	f_B	0.1906 ± 0.0047 [74–76]
$\lvert V_{cb}\rvert$ (Average)	$(40.9 \pm 1.1)\times 10^{-3}$ [26]	f_{B_c}	0.395 ± 0.015 [77]
Inputs for $(B \to \pi)$ Form Factors:		Inputs for $(B \to D^*)$ Form Factors:	
$F_+(0) = F_0(0)$	0.281 ± 0.028 [58]	$h_{A_1}(1)\lvert V_{cb}\rvert$	$(34.6 \pm 1.02)\times 10^{-3}$ [79]
b_1	-1.62 ± 0.70 [58]	ρ_1^2	1.214 ± 0.035 [79]
b_1^0	-3.98 ± 0.97 [58]	$R_1(1)$	1.401 ± 0.038 [79]
Inputs for $(B \to D)$ Form Factors:		$R_2(1)$	0.864 ± 0.025 [79]
$V_1(1)\lvert V_{cb}\rvert$	$(43.0 \pm 2.36)\times 10^{-3}$ [78]	$R_0(1)$	1.14 ± 0.114 [35]
ρ_1^2	1.20 ± 0.098 [78]		

Table 2.1: Theory Input parameters

Ratio of branching ratios:	
R_π^l	0.73 ± 0.15 [33]
R_D	0.440 ± 0.072 [34]
R_{D^*}	0.332 ± 0.030 [34]

Table 2.2: Experimental Input parameters

We wish to study the effects of each new physics parameter on various observables and the $B_c \to \tau\nu$ and $B^0 \to \pi\tau\nu$ decays in a model independent way. We also consider the ratio of

branching fractions of $B^0 \to \pi\tau\nu$ to $B^0 \to \pi\, l\nu$ decays, defined as

$$R_\pi = \frac{\mathcal{B}(B \to \pi\tau\nu)}{\mathcal{B}(B \to \pi\, l\, \nu)}\,, \tag{2.49}$$

which, in the SM, only depends on the ratio of form factors $F_0(q^2)/F_+(q^2)$. The decay mode $B \to \pi\tau\nu$ is particularly important because it originates from the same flavor changing interaction as the $B \to \tau\nu$ decay mode and hence can be used as an indicator for NP operators. Similarly, the $B_c \to \tau\nu$ is important as it is mediated via $b \to c$ transition decays, same as $B \to D\,\tau\,\nu$ and $B \to D^*\,\tau\,\nu$ decays, and, in principle, can help identifying the nature of NP in $b \to c$ processes. The SM prediction for the branching ratios and ratio of branching ratios are reported in Table. 2.3, where, for the central values

	Central value	1σ range
$\mathcal{B}(B \to \tau\nu)$	6.70×10^{-5}	$(5.22, 8.45) \times 10^{-5}$
$\mathcal{B}(B_c \to \tau\nu)$	1.63×10^{-2}	$(1.43, 1.85) \times 10^{-2}$
$\mathcal{B}(B \to \pi\, l\, \nu)$	12.77×10^{-5}	$(7.39, 21.28) \times 10^{-5}$
$\mathcal{B}(B \to \pi\,\tau\,\nu)$	8.91×10^{-5}	$(4.93, 15.40) \times 10^{-5}$
$\mathcal{B}(B \to D\, l\, \nu)$	2.32×10^{-2}	$(1.89, 2.81) \times 10^{-2}$
$\mathcal{B}(B \to D\,\tau\,\nu)$	0.72×10^{-2}	$(0.62, 0.84) \times 10^{-2}$
$\mathcal{B}(B \to D^*\, l\, \nu)$	4.93×10^{-2}	$(4.51, 5.39) \times 10^{-2}$
$\mathcal{B}(B \to D^*\,\tau\,\nu)$	1.25×10^{-2}	$(1.14, 1.37) \times 10^{-2}$
R_π^l	0.486	(0.328, 0.733)
R_π	0.698	(0.654, 0.764)
R_D	0.313	(0.300, 0.327)
R_D^*	0.253	(0.245, 0.261)

Table 2.3: Branching ratio and ratio of branching ratios within the SM.

we have used the central values of all the input parameters from Eq. (2.48) and from Table. 2.1. We vary all the theory inputs such as B_q meson decay constants, $B \to (P, V)$ transition form factors and the CKM matrix elements $|V_{qb}|$ within 1σ of their central values and obtain the 1σ allowed ranges in all the different observables in Table. 2.3. The uncertainties associated with the input parameters for the calculation of the form factors, reported in the subsection 2.2.1 and subsection 2.2.2, are added in quadrature and tabulated in Table 2.1.

We now proceed to describe four different scenarios of New Physics and the effect of these NP parameters. We consider all the NP parameters to be real for our analysis. We assume that only the third generation leptons get corrections from the NP couplings in the $b \to (u,\, c)\, l\nu$ processes and for $l = e^-, \mu^-$ cases the NP is absent. We use 3σ experimental constraint coming from the ratio of branching ratios R_π^l, R_D and R_{D^*} to find the allowed ranges of all the NP couplngs. We then show how different observables behave with various NP couplings under four different NP Scenarios that we consider for our analysis. We also give predictions for the branching ratios of $B_c \to \tau\nu$ and $B \to \pi\tau\nu$ decays and the ratio R_π for all the different NP scenarios.

2.3.1 Scenario A

We vary V_L and V_R while keeping all other NP couplings to zero. The allowed ranges of V_L and V_R that satisfies 3σ constraint coming from R_π^l, R_D and R_D^* are shown in the left panel of Fig. 2.1. We see that the experimental values put a severe constraint on the (V_L, V_R) parameter space. In

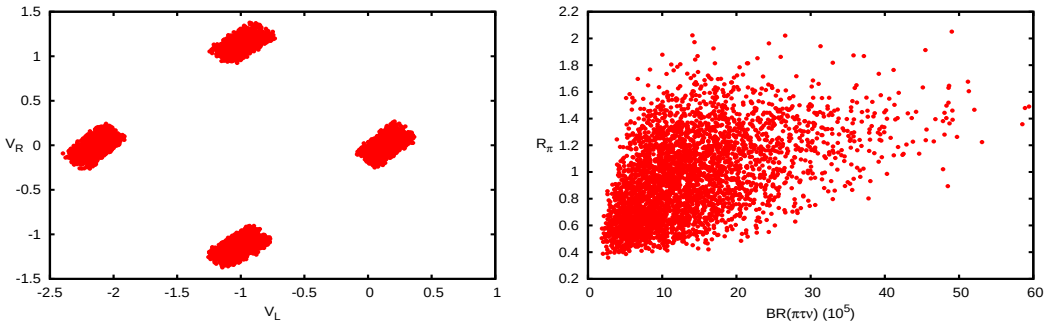

Figure 2.1: Allowed regions of V_L and V_R are shown in the left panel once the 3σ experimental constraint is imposed. The corresponding ranges in $\mathcal{B}(B \to \pi\tau\nu)$ and the ratio R_π in the presence of these NP couplings are shown in the right panel.

the presence of such NP couplings, the $\Gamma(B_q \to \tau\nu)$, $d\Gamma/dq^2(B \to P\,\tau\nu)$, and $d\Gamma/dq^2(B \to V\,\tau\nu)$, where P stands for pseudoscalar and V stands for vector meson, can be written as

$$\begin{aligned}
\Gamma(B_q \to \tau\nu) &= \Gamma(B_q \to \tau\nu)|_{\rm SM}\, G_A^2\,, \\
\frac{d\Gamma}{dq^2}(B \to P\,\tau\,\nu) &= \Big[\frac{d\Gamma}{dq^2}(B \to P\,\tau\,\nu)\Big]_{\rm SM}\, G_V^2\,, \\
\frac{d\Gamma}{dq^2}(B \to V\,\tau\,\nu) &= \frac{8\,N\,|\overrightarrow{p}_V|}{3}\Big\{(\mathcal{A}_0^2\,G_A^2 + \mathcal{A}_{||}^2\,G_A^2 + \mathcal{A}_\perp^2\,G_V^2)\Big(1+\frac{m_\tau^2}{2\,q^2}\Big) + \frac{3\,m_\tau^2}{2\,q^2}\,\mathcal{A}_t^2\,G_A^2\Big\}
\end{aligned} \tag{2.50}$$

It is evident that, the value of $\mathcal{B}(B_c \to \tau\nu)$ varies as G_A^2, whereas, $\mathcal{B}(B \to \pi\tau\nu)$ and the ratio R_π varies as G_V^2 in the presence of these NP couplings. The ranges in $B \to \pi\tau\nu$ branching ratio and the ratio R_π in the presence of V_L and V_R are shown in the right panel of Fig. 2.1. The resulting ranges in $\mathcal{B}(B_c \to \tau\nu)$, $\mathcal{B}(B \to \pi\tau\nu)$, and R_π are

$$\begin{aligned}
&\mathcal{B}(B_c \to \tau\nu) = (1.02,\, 3.95)\%\,, \qquad\qquad \mathcal{B}(B \to \pi\tau\nu) = (1.86,\, 59.42)\times 10^{-5}\,, \\
&R_\pi = (0.36,\, 2.05)\,.
\end{aligned}$$

We see a significant deviation from the the SM expectation in such New Physics scenario. Measurement of the $\mathcal{B}(B_c \to \tau\nu)$, $\mathcal{B}(B \to \pi\tau\nu)$ and the ratio R_π will put additional constraint on the NP parameters. We want to see the effects of these NP couplings on various observables that we defined in section 2.2. In Fig. 2.2, we show in blue bands the SM range and show in red bands the range of each observable once the NP couplings V_L and V_R are switched on. It is clear from Fig. 2.2 that, the differential branching ratios (DBR) and the ratio of branching ratio get considerable deviations once we include the NP couplings. This is expected and can be understood very easily from Eq. (2.50). In the presence of V_L and V_R alone, the DBR and the ratio for $B \to P\,\tau\,\nu$ decays depends on only G_V coupling and is proportional to G_V^2. Whereas, for $B \to V\tau\nu$ decay mode the DBR and the

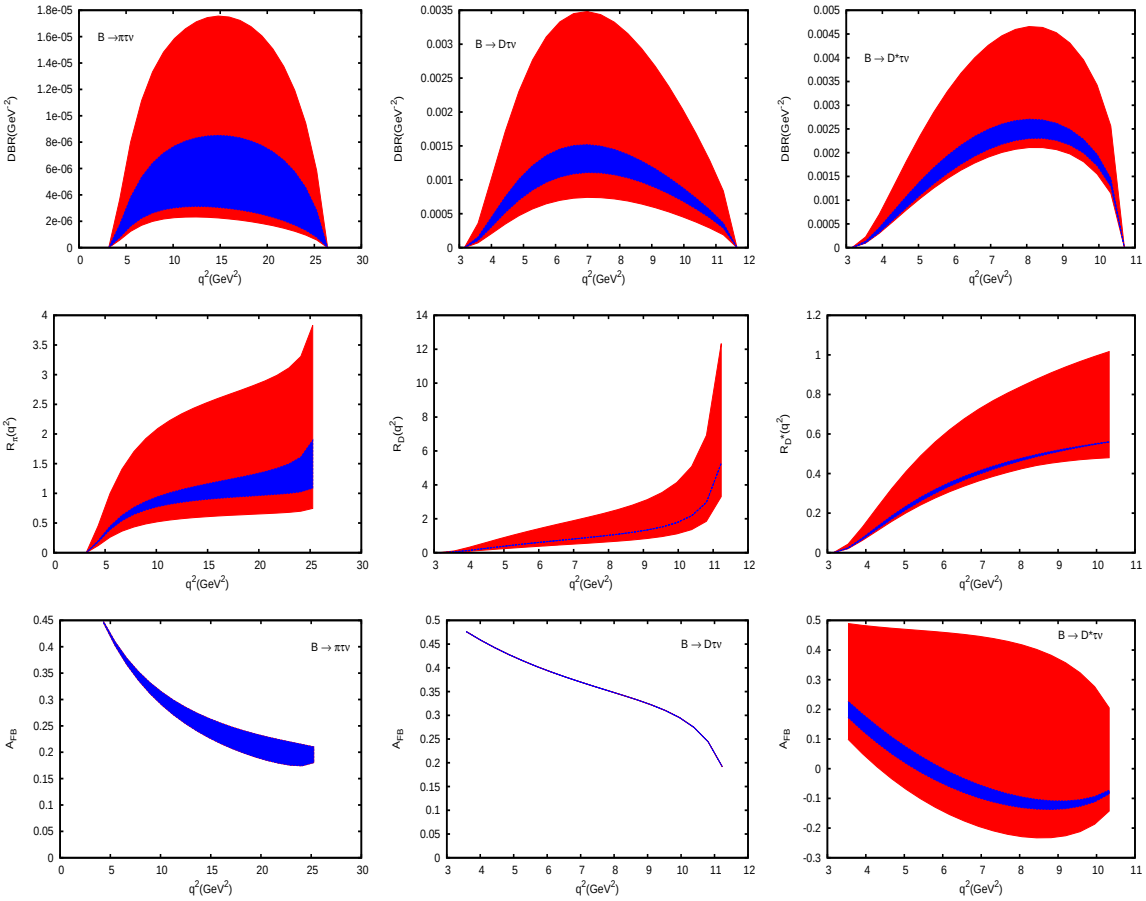

Figure 2.2: Range in DBR(q^2), $R(q^2)$, and the forward backward asymmetry $A_{FB}(q^2)$ for the $B \to \pi\tau\nu$, $B \to D\tau\nu$, and $B \to D^*\tau\nu$ decay modes. The darker (blue) interior region corresponds to the SM prediction, whereas, the lighter (red), larger region corresponds to the allowed (V_L, V_R) NP couplings of Fig. 2.1.

ratio depends on G_V as well as G_A couplings and is proportional to G_V^2 and G_A^2 as can be seen from Eq. (2.50). We see that the DBR for each decay mode can increase by 100% at the peak of its distribution. Similar conclusions can be made for the ratio of branching ratios as well where we see a 100% increase at the peak of its distribution. The forward backward asymmetry, as we expected, does not vary with V_L and V_R for the $B \to \pi\tau\nu$ and the $B \to D\tau\nu$ decay modes. Since it depends on G_V couplings only, the NP dependency gets cancelled in the ratio as can be seen from Eq. (2.44). However, for $B \to D^*\tau\nu$, the deviation is quite large. Again, it can be very easily understood from Eq. (2.46). It is mainly because of the presence of G_V as well as G_A couplings. We see a zero crossing at $q^2 \approx 6.0\,\text{GeV}^2$ in the SM for this decay mode. However, in the presence of such NP, depending on V_L and V_R, there may or may not be a zero crossing as is evident from Fig. 2.2.

Again, we want to emphasize on the fact that a pure G_V coupling will contribute to the $B \to P\,\tau\nu$ as well as $B \to V\,\tau\nu$ decay processes, whereas, a pure G_A coupling will contribute to the $B \to \tau\nu$ as well as the $B \to V\,\tau\,\nu$ decay modes. We do not consider pure G_V and G_A couplings for our analysis as a pure G_V or a pure G_A type NP couplings will not be able to accomodate all the existing data since current experiments on $b \to u$ and $b \to c$ semi-(leptonic) decays suggests that there could be new physics in all the three decay modes. Hence, if NP is present in R_π^l, R_D, and R_{D^*}, one can rule out the possibility of having a pure G_V or a pure G_A type of NP couplings.

2.3.2 Scenario B

Here we consider non zero S_L and S_R couplings and keep all other NP couplings to zero. The allowed ranges of S_L and S_R that satisfies the 3σ experimental constraints are shown in the left panel of Fig. 2.3. In the presence of S_L and S_R, the $\Gamma(B_q \to \tau\nu)$, $d\Gamma/dq^2(B \to P\,\tau\nu)$, and $d\Gamma/dq^2(B \to V\,\tau\nu)$

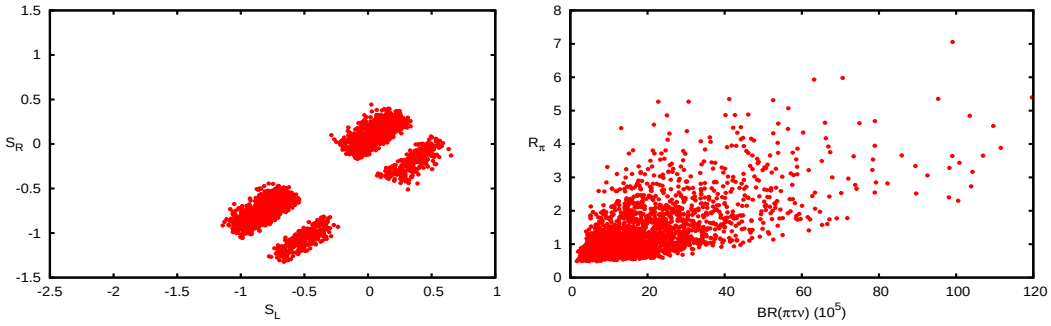

Figure 2.3: Allowed ranges of (S_L, S_R) is shown in the left panel once the experimental constraint is imposed. The right panel shows the ranges of $B \to \pi\tau\nu$ branching fractions and the ratio R_π with these NP couplings.

can be written as

$$\Gamma(B_q \to \tau\nu) = \Gamma(B_q \to \tau\nu)|_{\text{SM}} \left[1 - \frac{m_B^2}{m_\tau\,(m_b + m_q)}\,G_P\right]^2,$$

$$\frac{d\Gamma}{dq^2}(B \to P\,\tau\,\nu) = \frac{8\,N\,|\overrightarrow{p}_P|}{3}\left\{H_0^2\left(1 + \frac{m_\tau^2}{2\,q^2}\right) + \frac{3\,m_\tau^2}{2\,q^2}\,H_t^2 + \frac{3}{2}\left(H_S^2\,G_S^2 + \frac{2\,m_\tau}{\sqrt{q^2}}\,H_t\,H_S\,G_S\right)\right\},$$

$$\frac{d\Gamma}{dq^2}(B \to V\,\tau\,\nu) \;=\; \frac{8\,N\,|\overrightarrow{p}_V|}{3}\Bigg\{(\mathcal{A}_0^2+\mathcal{A}_{||}^2+\mathcal{A}_{\perp}^2)\Big(1+\frac{m_\tau^2}{2\,q^2}\Big)+\frac{3\,m_\tau^2}{2\,q^2}\,\mathcal{A}_t^2$$
$$+\frac{3}{2}\Big(\mathcal{A}_P^2\,G_P^2+\frac{2\,m_\tau}{\sqrt{q^2}}\,\mathcal{A}_t\,\mathcal{A}_P\,G_P\Big)\Bigg\} \tag{2.51}$$

We see that $B \to \tau\nu$ and $B \to D^*\tau\nu$ depend on pure G_P coupling, whereas, $B \to \pi\tau\nu$ and $B \to D\tau\nu$ depend on pure G_S coupling. Hence, we do not consider pure G_P and pure G_S NP couplings for our anaysis as these will not simultaneously explain all the existing data. The effects

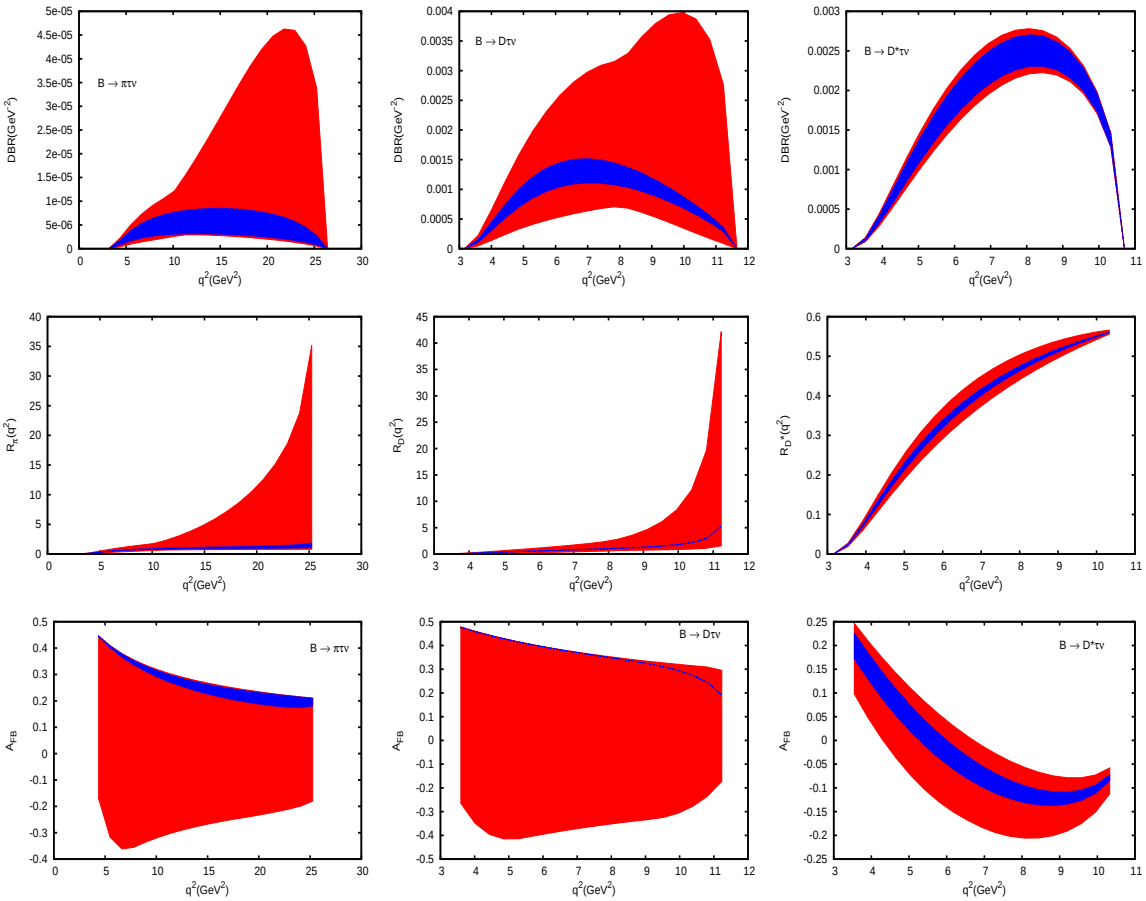

Figure 2.4: Range in DBR(q^2), $R(q^2)$, and the forward backward asymmetry $A_{FB}(q^2)$ for the $B \to \pi\tau\nu$, $B \to D\tau\nu$, and $B \to D^*\tau\nu$ decay modes. The darker (blue) interior region corresponds to the SM prediction, whereas, the lighter (red), larger region corresponds to the allowed (S_L, S_R) NP couplings of Fig. 2.3.

of these NP couplings on the $\mathcal{B}(B \to \pi\tau\nu)$ and the ratio R_π is shown in the right panel of Fig. 2.3. In the presence of such NP, the 3σ allowed ranges of the branching ratio of $B_c \to \tau\nu$, $B \to \pi\tau\nu$, and the ratio R_π of the branching ratios of $B \to \pi\tau\nu$ to the corresponding $B \to \pi\,l\,\nu$ are

$$\mathcal{B}(B_c \to \tau\nu) = (0.21,\, 13.66)\%\,, \qquad \mathcal{B}(B \to \pi\tau\nu) = (1.69,\, 119.66) \times 10^{-5}\,,$$
$$R_\pi = (0.49,\, 7.06)\,.$$

We see that the $\mathcal{B}(B_c \to \tau\nu)$, $\mathcal{B}(B \to \pi\tau\nu)$, and the ratio R_π are quite sensitive to the S_L and S_R NP couplings. The deviation from the SM is quite large once these NP couplings are switched on.

We now wish to see how different observables behave with S_L and S_R. The corresponding DBR, the ratio $R(q^2)$, and the forward backward asymmetries $A_{FB}(q^2)$ as a function of q^2 are shown in Fig. 2.4. We see that deviation from the SM is much larger in case of $B \to \pi\tau\nu$ and $B \to D\tau\nu$ decay modes than the $B \to D^*\tau\nu$ decay mode. We see that the variation is quite similar in $B \to \pi\tau\nu$ and $B \to D\tau\nu$ decay mode. It is expected as both the decay modes depend on the NP couplings through G_S, whereas, the $B \to D^*\tau\nu$ depends on the NP couplings through G_P and hence the variation is quite different from the $B \to \pi\tau\nu$ and $B \to D\tau\nu$ decay modes. Again, the peak of the distribution of differential branching ratio for the $B \to \pi\tau\nu$ and $B \to D\tau\nu$ can shift to higher q^2 region once the NP couplings are introduced.

Again in the SM, as mentioned earlier, we see a zero crossing in the forward backward asymmetry for the $B \to D^*\tau\nu$ decay mode. Moreover, we observe no such zero crossing in case of $B \to \pi\tau\nu$ and $B \to D\tau\nu$ decay modes. However, once the NP couplings S_L and S_R are switched on, we see a zero crossing for the $B \to \pi\tau\nu$ as well as the $B \to D\tau\nu$ decay modes. Depending on the value of the NP couplings, there may be a zero crossing or there could be a total change of sign of the A_{FB} parameter as can be seen from Fig. 2.4. Thus, we see that, the forward backward asymmetry in case of $B \to \pi\tau\nu$ and $B \to D\tau\nu$ is very sensitive to the S_L and S_R couplings. In case of $B \to D^*\tau\nu$ decay mode, however, the sensitivity is much smaller than the $B \to \pi\tau\nu$ and $B \to D\tau\nu$ modes. It is worth mentioning that, depending on the value of the NP couplings, there can be a zero crossing for the $B \to D^*\tau\nu$ decay process which is marginally different from the SM as is evident from Fig. 2.4.

2.3.3 Scenario C

We set all the other NP couplings to zero while varying $\widetilde{V}_L$ and $\widetilde{V}_R$. These couplings are related to the right handed neutrino interactions. As already mentioned in section 2.2, the decay rate depends quadratically on these NP couplings. The linear term that comes from the interference betweeen SM and the NP is negligible due to the mass of neutrino. The allowed ranges of $\widetilde{V}_L$ and $\widetilde{V}_R$ are shown in the left panel of Fig. 2.5. It is evident that the parameter space is much less restricted than Scenario A ($V_{L,\,R} \neq 0$) and Scenario B ($S_{L,\,R} \neq 0$).

In the presence of such NP couplings, the $\Gamma(B_q \to \tau\nu)$, $d\Gamma/dq^2(B \to P\,\tau\nu)$, and $d\Gamma/dq^2(B \to V\,\tau\nu)$, where P stands for pseudoscalar and V stands for vector meson, can be written as

$$\begin{aligned}
\Gamma(B_q \to \tau\nu) &= \Gamma(B_q \to \tau\nu)|_{\rm SM} \left(1 + \widetilde{G}_A^2\right), \\
\frac{d\Gamma}{dq^2}(B \to P\,\tau\,\nu) &= \left(\frac{d\Gamma}{dq^2}(B \to P\,\tau\,\nu)\right)_{\rm SM} \left(1 + \widetilde{G}_V^2\right), \\
\frac{d\Gamma}{dq^2}(B \to V\,\tau\,\nu) &= \frac{8\,N\,|\overrightarrow{p}_V|}{3}\Bigg\{\left[\mathcal{A}_0^2\,(1+\widetilde{G}_A^2) + \mathcal{A}_{||}^2\,(1+\widetilde{G}_A^2) + \mathcal{A}_\perp^2\,(1+\widetilde{G}_V^2)\right]\left(1 + \frac{m_\tau^2}{2\,q^2}\right) \\
&\quad + \frac{3\,m_\tau^2}{2\,q^2}\,\mathcal{A}_t^2\,(1+\widetilde{G}_A^2)\Bigg\}. \qquad (2.52)
\end{aligned}$$

It is evident from Eq. (2.52) that the $B \to \tau\nu$ decay branching ratio depends on the NP couplings

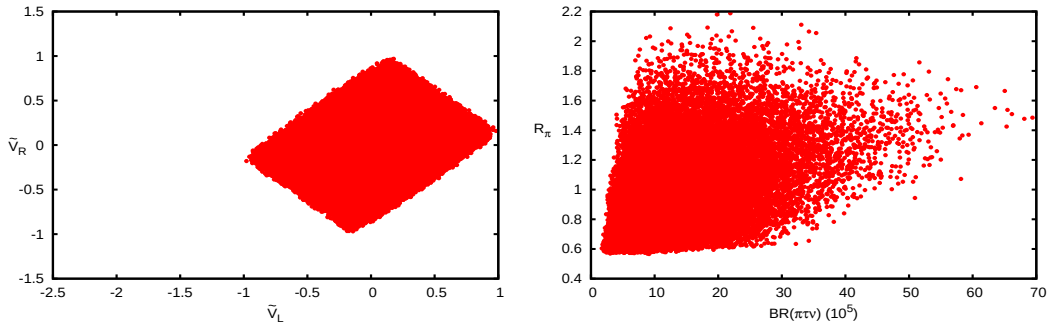

Figure 2.5: Range in $\widetilde{V}_L$ and $\widetilde{V}_R$ is shown in the left panel once the 3σ experimental constraint is imposed. The resulting range in the $\mathcal{B}(B \to \pi\tau\nu)$ and R_π is shown in the right panel with these NP couplings.

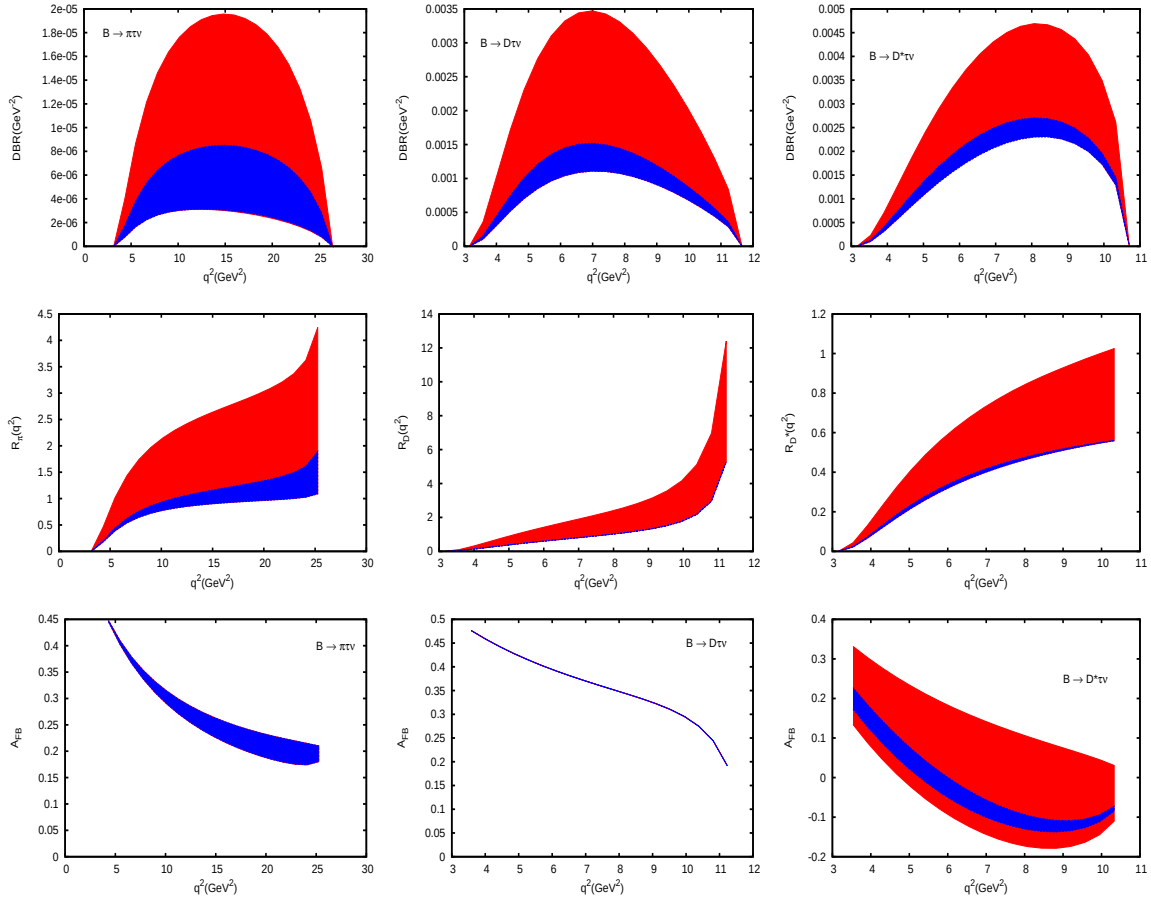

Figure 2.6: Range in DBR(q^2), $R(q^2)$, and $A_{FB}(q^2)$ for the $B \to \pi\tau\nu$, $B \to D\tau\nu$, and the $B \to D^*\tau\nu$ decay modes. The dark (blue) band corresponds to the SM range, whereas, the light (red) band corresponds to the NP couplings ($\widetilde{V}_L$, $\widetilde{V}_R$) that are shown in the left panel of Fig. 2.5.

through $\widetilde{G}_A^2$ term and the $B \to D^*\tau\nu$ branching ratio depend on $\widetilde{V}_L$ and $\widetilde{V}_R$ couplings through $\widetilde{G}_A^2$ as well as $\widetilde{G}_V^2$ term, whereas, the $B \to \pi\tau\nu$ and $B \to D\tau\nu$ branching ratios depend on these couplings through $\widetilde{G}_V^2$ term. The corresponding 3σ allowed ranges of $\mathcal{B}(B \to \pi\tau\nu)$ and the ratio R_π is shown in the right panel of Fig. 2.5. The ranges are

$$\mathcal{B}(B_c \to \tau\nu) = (1.09,\, 4.13)\%\,, \qquad \mathcal{B}(B \to \pi\tau\nu) = (1.71,\, 69.39) \times 10^{-5}\,,$$
$$R_\pi = (0.57,\, 2.19)\,,$$

and are quite similar to Scenario A. Again, a significant deviation from the SM prediction is expected in such NP scenario.

The allowed ranges of all the different observables with these NP couplings are shown in Fig. 2.6. We see that the differential branching ratio, the ratio of branching ratio, and the forward backward asymmetry parameters vary quite significantly with the inclusion of the NP couplings. The q^2 distribution looks quite similar to what we obtain for Scenario A. Although, the differential branching ratio and the ratio of branching ratios are quite sensitive to $\widetilde{V}_L$ and $\widetilde{V}_R$, the forward backward asymmetry for the $B \to \pi\tau\nu$ and $B \to D\tau\nu$ does not depend on the NP couplings at all. However, for the $B \to D^*\tau\nu$ decay mode, all the three observables are very sensitive to these right handed neutrino couplings. Again, depending on these NP couplings, there may be a zero crossing in the q^2 distribution of the A_{FB} parameter which can be quite different from the SM prediction.

2.3.4 Scenario D

We include the New Physics effects coming from the $\widetilde{S}_L$ and $\widetilde{S}_R$ alone while keeping all the other NP couplings to zero. We impose the experimental constraint coming from the measured data of R_π^l, R_D, and R_{D^*} and the resulting allowed ranges of $\widetilde{S}_L$ and $\widetilde{S}_R$ are shown in the left panel of Fig. 2.7. Similar to $\widetilde{V}_L$ and $\widetilde{V}_R$, these couplings also arise due to the right handed neutrino interactions. The decay rate depends on these NP couplings quadratically and hence the parameter space is less constrained. In the presence of $\widetilde{S}_L$ and $\widetilde{S}_R$, the $\Gamma(B_q \to \tau\nu)$, $d\Gamma/dq^2(B \to P\,\tau\nu)$, and

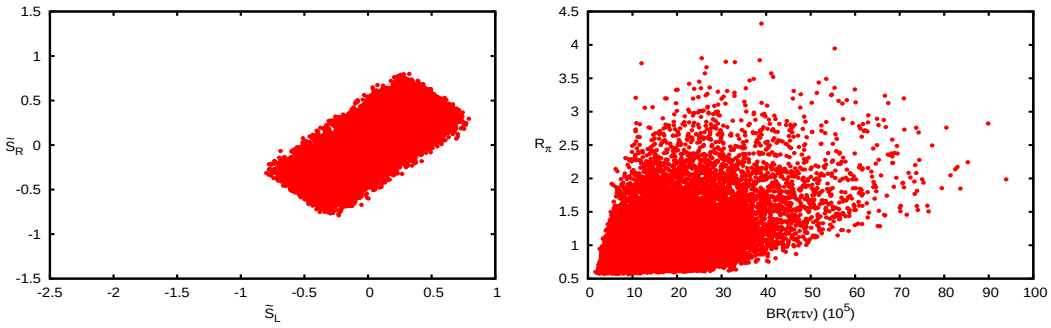

Figure 2.7: Left panel shows the allowed range in $\widetilde{S}_L$ and $\widetilde{S}_R$ with the 3σ experimental constraint imposed. The resulting range in $B \to \pi\tau\nu$ branching ratio and the ratio R_π is shown in the right panel once the NP $\widetilde{S}_L$ and $\widetilde{S}_R$ are included.

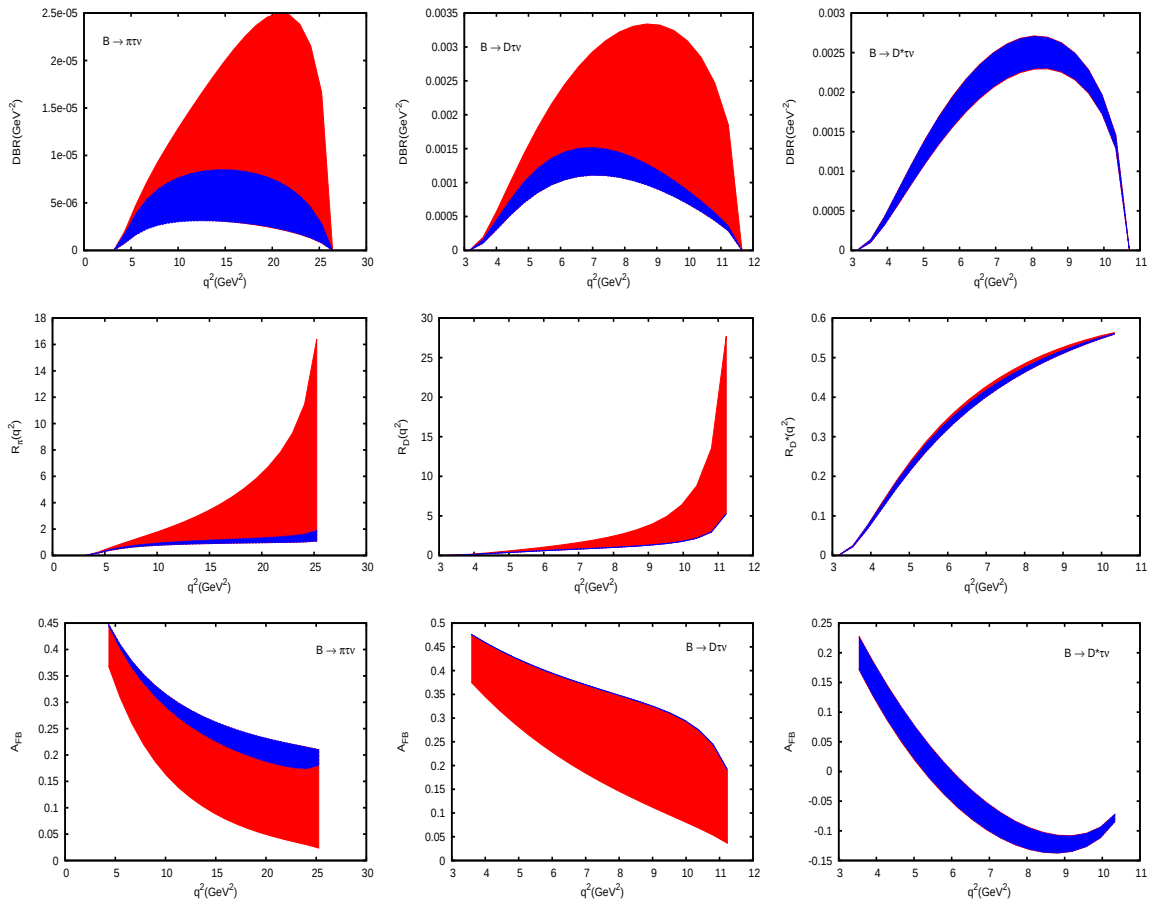

Figure 2.8: Range in various observables such as DBR(q^2), $R(q^2)$, and $A_{FB}(q^2)$ for the $B \to \pi\tau\nu$, $B \to D\tau\nu$, and the $B \to D^*\tau\nu$ decays. The allowed range in each observable is shown in light (red) band once the NP couplings ($\widetilde{S}_L$, $\widetilde{S}_R$) are varied within the allowed ranges as shown in the left panel of Fig. 2.7. The corresponding SM prediction is shown in dark (blue) band.

$d\Gamma/dq^2(B \to V\,\tau\nu)$ can be written as

$$\begin{aligned}
\Gamma(B_q \to \tau\nu) &= \Gamma(B_q \to \tau\nu)|_{\rm SM}\left[1 + \frac{m_B^4}{m_\tau^2\,(m_b+m_q)^2}\,\widetilde{G}_P^2\right], \\
\frac{d\Gamma}{dq^2}(B \to P\,\tau\,\nu) &= \frac{8\,N\,|\overrightarrow{p}_P|}{3}\left\{H_0^2\Big(1+\frac{m_\tau^2}{2\,q^2}\Big) + \frac{3\,m_\tau^2}{2\,q^2}\,H_t^2 + \frac{3}{2}\,H_S^2\,\widetilde{G}_S^2\right\}, \\
\frac{d\Gamma}{dq^2}(B \to V\,\tau\,\nu) &= \frac{8\,N\,|\overrightarrow{p}_V|}{3}\left\{(\mathcal{A}_0^2 + \mathcal{A}_{||}^2 + \mathcal{A}_\perp^2)\Big(1+\frac{m_\tau^2}{2\,q^2}\Big) + \frac{3\,m_\tau^2}{2\,q^2}\,\mathcal{A}_t^2 + \frac{3}{2}\mathcal{A}_P^2\,\widetilde{G}_P^2\right\}. \quad (2.53)
\end{aligned}$$

The 3σ allowed ranges of the $B \to \pi\tau\nu$ branching ratio and the ratio R_π are shown in the right panel of Fig. 2.7. The ranges of $\mathcal{B}(B_c \to \tau\nu)$, $\mathcal{B}(B \to \pi\tau\nu)$, and R_π are

$$\begin{aligned}
&\mathcal{B}(B_c \to \tau\nu) = (1.11,\,16.71)\%\,, \qquad\qquad \mathcal{B}(B \to \pi\tau\nu) = (1.70,\,93.90)\times 10^{-5}\,, \\
&R_\pi = (0.56,\,4.32)\,.
\end{aligned}$$

The effect of these NP couplings on various observables are quite similar to the scenario where only the S_L and S_R are non zero. The differential branching ratio, the ratio of branching ratios, and the forward backward aymmetry parameters deviate quite significantly from the SM prediction for the $B \to \pi\tau\nu$ and $B \to D\tau\nu$ decay modes, whereas, there is no or very little deviation of these observables from the SM value in case of $B \to D^*\tau\nu$ decay process. We see that the $B \to \tau\nu$ and $B \to D^*\tau\nu$ decay branching ratios depend on these NP couplings through $\widetilde{G}_P^2$ terms, but, the $B \to \pi\tau\nu$ and $B \to D\tau\nu$ decay branching fractions depend on these NP couplings through $\widetilde{G}_S^2$ terms. Hence, we see similar behaviour for the $B \to \pi\tau\nu$ and $B \to D\tau\nu$ decay modes. However, as expected, the variation in the $B \to D^*\tau\nu$ decay mode is quite different from the $B \to \pi\tau\nu$ and the $B \to D\tau\nu$ decay modes. Again, we see that the peak of the distribution of $B \to \pi\tau\nu$ and $B \to D\tau\nu$ decay branching ratios shift towards large q^2 region. Although, effect of these right handed couplings are quite similar to its left handed counterpart, there are some differences. We do not see any zero crossing in the q^2 distribution of the A_{FB} parameter for the $B \to \pi\tau\nu$ and $B \to D\tau\nu$ decay modes.

2.4 Conclusion

B decay measurements have been providing us a lot of useful information regarding the nature of New Physics. Several recent measurements in the rare processes have put severe constraint on the NP parameters. Precision measurements in B meson decays have been a great platform for indirect evidences of beyond the Standard Model physics. The recent measurements of the ratio of the branching ratio R_D of $B \to D\,\tau\,\nu$ to that of $B \to D\,l\,\nu$ and R_D^* of $B \to D^*\,\tau\,\nu$ to that of $B \to D^*\,l\,\nu$ differ from the Standard Model expectation at 3.4σ level. It is still not conclusive enough that New Physics is indeed present in this $b \to c\,\tau\,\nu$ processes. More precise measurements will reveal the nature of the New Physics. Similar New Physics effects have been observed in $b \to u\,\tau\,\nu$ processes as well. The measurement of the branching ratio of $B \to \tau\nu$ and the ratio R_π^l of the branching ratio of $B \to \tau\nu$ to $B \to \pi\,l\,\nu$ decays differ from Standard Model expectation at more than 2.5σ level. A lot of phenomenological studies have been done in order to explain all these discrepancies. In this chapter, we consider an effective Lagrangian for the $b \to q\,l\,\nu$ transition processes in the presence of NP, where $q = u,\,c$, and perform a combined analysis of $B \to \tau\nu$, $B \to D\tau\nu$ and $B \to D^*\tau\nu$

decay processes. Our work differs significantly from others as we include the right handed neutrino couplings. We assume that New Physics is present only in the third generation leptons. We look at four different New Physics (NP) scenarios. The results of our analysis are as follows.

We assume New Physics in the third generation lepton only and see the effect of each New Physics couplings on various observables. We first find the allowed ranges of each NP couplings using 3σ constraint coming from the most recent data of R_π^l, R_D, and R_{D^*}. For non zero V_L and V_R couplings, the differential branching ratio and the ratio of branching ratios are quite sensitive to these NP couplings for each decay mode. However, the forward backward asymmetry for the $B \to \pi\tau\nu$ and $B \to D\tau\nu$ is not sensitive to these couplings at all. The forward backward asymmetry is quite sensitive to these NP couplings for $B \to D^*\tau\nu$ decays and the deviation from the Standard Model prediction can be quite significant depending on the value of V_L and V_R. Although, we see a zero crossing in the q^2 distribution, it may or may not be there depending on the NP couplings. Again, even if we see a zero crossing, it can deviate quite significantly from the Standard Model prediction.

In case of S_L and S_R couplings, all the observables such as the differential branching ratio, ratio of branching ratios, and the forward backward asymmetry are quite sensitive to the NP couplings for the $B \to \pi\tau\nu$ and $B \to D\tau\nu$ decays. However, the sensitivity is somewhat reduced for the $B \to D^*\tau\nu$ decay mode. Although, in the Standard Model, there is no zero crossing in the forward backward asymmetry parameter for the $B \to \pi\tau\nu$ and $B \to D\tau\nu$ decay modes, however, depending on the value of S_L and S_R, one might see a zero crossing for both the decay modes. For the $B \to D^*\tau\nu$ mode, the zero crossing can be similar or marginally different from the Standard Model one.

For the right handed neutrino couplings ($\widetilde{V}_L$, $\widetilde{V}_R$) and ($\widetilde{S}_L$, $\widetilde{S}_R$), the effects are quite similar to its left handed counterpart (V_L, V_R) and (S_L, S_R). However, the sensitivity is somewhat reduced.

Although, current experimental results are pointing towards the third generation leptons for possible New Physics, there could be, in principle, New Physics in the first two generations as well. If there is NP in all generation leptons, then it might be possible to identify it by measuring the forward backward asymmetry for $B \to \pi\, l\, \nu$, $B \to D\, l\, \nu$, and $B \to D^*\, l\, \nu$ decay modes, where l could be either an electron or a muon. It will provide useful information regarding the NP couplings (S_L, S_R) and ($\widetilde{S}_L$, $\widetilde{S}_R$). Similarly, measurement of the branching ratio of $B_c \to \tau\nu$ and $B \to \pi\tau\nu$ and the ratio R_π will put additional constraint on the nature of NP couplings. Retaining our current approach, we could also sharpen our estimates once improved measurements of various branching ratios and ratio of branching ratios become available. At the same time, reducing the theoretical uncertainties in various form factors and decay constants will also improve our estimates in future.

Chapter 3

Flavour changing baryonic decay $B^- \to \Lambda\bar{p}\mu^+\mu^-$

3.1 Introduction

Over the last decade, weak decays of B meson to meson-meson final states have not only confirmed and established the Cabibbo-Kobayashi-Maskawa (CKM) mechanism of quark flavor mixing and CP violation in the quark sector to a very high degree of precision but also provided a strong ground to test the nature of flavor changing neutral currents (FCNC) via $b \to s\,l\bar{l}$ transition decays. Due to the large mass of B meson, it can also decay to final states that contain a baryon-antibaryon pair. Although almost 7% [26] of all the B meson decays contain baryons in the final state, but the exploration in this field is less in comparison to decays with mesons in the final state. In particular, we have very little knowledge about the mechanism behind these baryonic decays and more generally, about the mechanism behind hadron fragmentation into baryons.

ARGUS [80] reported the first baryonic decay mode which was later ruled out by CLEO [81]. Exclusive decay of B mesons to a charmed baryon was first reported by CLEO [82] in which they measured the branching ratios of $B^- \to \Lambda_c^+\,\bar{p}\,\pi^-$ and $\bar{B}^0 \to \Lambda_c^+\,\bar{p}\,\pi^+\,\pi^-$ decay modes. In recent years, many exclusive baryonic B meson decays have been found by the two b-factories, BABAR [83] and Belle [84]. Several theoretical approaches such as flavor symmetry approach [85–88], pole model [89, 90], the diquark model [91], QCD sum rule [92], and the factorization formalism [93, 94] have been proposed in order to explain the mechanism behind these baryonic B decays.

Baryonic B decays have two very common and unique features. First, there is an enhancement at the threshold in dibaryon invariant mass distribution and it is experimentally observed in many three body decay modes [95–109]. Second, the largest branching fraction for baryonic B decays come with moderate multiplicities of $3-4$ hadrons in the final state. Baryonic B meson decay branching fraction hierarchy is $\mathrm{Br}_{3-\mathrm{body}} < \mathrm{Br}_{5-\mathrm{body}} < \mathrm{Br}_{4-\mathrm{body}}$ [110]. This is quite different from B meson decays to meson only final states and a proper theoretical understanding is yet to be achieved. Similarly, branching fraction of a three body final state is larger than its two body counterpart. The three body decays are more preferable due to the threshold enhancement in the dibaryon in-

variant mass distribution which sharply peaks at low values with emitted meson carrying much energy. However, for a two body decay, the invariant mass of the baryon-antibaryon pair is M_B and hence these decay modes are not preferred. Several theoretical approaches have been proposed to explain the threshold enhancement in the dibaryon invariant mass distribution [111–124]. In principle, the threshold enhancement mechanism can be very easily understood in terms of a simple short distance picture [125]. The observed angular distributions in various decay modes such as $B^- \to p\,\bar{p}\,\pi^-$, $\Lambda_c^+\,\bar{p}\,\pi^+$, and $\Lambda\,\bar{p}\,\gamma$ [98,102,103] decays are consistent with this short distance picture, however, this simple picture fails to explain the observed angular correlations in the penguin dominated $B \to p\,\bar{p}\,K^-$ [97,103] and $B^- \to \Lambda\,\bar{p}\,\pi^-$ [101] decays. It is worth mentioning that the threshold enhancement mechanism plays a crucial role in case of baryonic B decays and understanding this mechanism will be the key to interpret the physics behind these baryonic B decays.

In the Standard Model (SM), the inclusive FCNC processes are mediated via electroweak box and penguin type diagrams. Tree level diagrams do not contribute to these decay processes. New physics (NP) particles, in principle, can enter through these loop processes and compete with the SM processes. This can lead to modifications of branching fractions or angular distributions of the particles in these decay modes. Consequently, the exclusive rare radiative decays such as $B_s^0 \to \phi\gamma$ and rare leptonic and semileptonic decays such as $B_{(d,s)} \to l^+\,l^-$ and $B^0 \to K^{*^0}\,l^+\,l^-$ are potentially good places to look for NP. Very recently, the LHCb [126] and CMS [127] have reported new results on $B_{d,\,s} \to \mu^+\,\mu^-$ decays and branching ratio of $B_d \to \mu^+\,\mu^-$ decay is found to be higher than the SM value by a factor of 3.5. Although the branching ratio of $B_s \to \mu^+\,\mu^-$ decay mode is in good agreement with the SM prediction [128], but recent measurement [129] suggests a sizable width difference $\Delta\,\Gamma_s = 0.116 \pm 0.018\ (\text{stat}) \pm 0.006\ (\text{syst})\ \text{ps}^{-1}$ of B_s meson which points towards NP. A lot of phenomenological work have been done in this regard [130–137]. Again, the recent measurement of the angular observable in $B_d \to K^*\,\mu^+\,\mu^-$ decay mode by LHCb [138] differs from the SM expectation. These results, if persist in future precision experiments, would be a definite hint of physics beyond the SM and, in principle, will affect any FCNC decays mediated via $b \to s\,l\,\bar{l}$ transition process. Lot of theoretical studies have been done to interpret the data using various NP scenarios [139–149]. The theoretical prediction of a semileptonic $B \to M\,l\,\bar{l}$ decay branching fraction depends mainly on the hadronic $B \to M$ transition form factors, which, in principle, can be calculated using various models such as quark models, lattice QCD, light cone sum rules, and heavy quark effective theory. Like mesonic decays, one can also study the baryonic semileptonic decay modes such as $B \to \mathcal{B}\bar{\mathcal{B}}'\,l\,\bar{l}$ and investigate the theoretical modeling of $B \to \mathcal{B}\,\bar{\mathcal{B}}'$ transition form factors. In Ref. [150], the authors have used perturbative QCD approach for the $B \to p\bar{p}$ transition form factors and predicted the SM branching ratio of four body exclusive semileptonic baryonic $B^- \to p\bar{p}\,l\,\nu_l$ decays. The SM prediction of $(1.0, 1.0, 0.5) \times 10^{-4}$ for $l = e$, μ, and τ, however, differs significantly from the recently measured branching fraction of $(5.8^{+2.4}_{-2.1}(\text{stat.}) \pm 0.9(\text{syst.})) \times 10^{-6}$ [151]. Hence, a careful investigation of the theoretical modeling of the baryonic transition form factors in B decays is necessary in light of this new information. More recently, in Ref. [152], the authors have calculated the branching ratio of the rare $B^- \to \Lambda\,\bar{p}\nu\bar{\nu}$ decay process within the SM using the same approach as in Ref. [150] for the $B \to \Lambda\,\bar{p}$ transition form factors. Moreover, the exclusive modes of baryonic and mesonic decays are good places to search for exotic baryons beyond the SM such as dibaryon, pentaquark, and exotic mesons (glueball, tetraquark). In this chapter, we focus

mainly on the baryonic B decays, particularly $B \to \Lambda \bar{p}\, \mu^+ \mu^-$ decay mode, as an exclusive B decay mediated via the $b \to s\, l\, \bar{l}$ transition to test the nature of the FCNCs. In this context, we use the most general effective Hamiltonian in the presence of NP and see the effect of each NP coupling on various observables in a model independent way. We predict the branching ratio of $B \to \Lambda \bar{p}\, \mu^+ \mu^-$ decay mode and obtain asymmetries in angular distributions and triple product correlations in the SM and in the presence of NP.

The chapter is organized as follows. We begin, in section 3.2, with a description of the effective Hamiltonian for $b \to s\, l\, \bar{l}$ transition decay process and briefly review the $B \to \mathcal{B}\bar{\mathcal{B}}'$ transition form factors and their QCD counting rules. We then define several observables in $B^- \to \Lambda \bar{p}\, \mu^+ \mu^-$ decays. In section 3.3, we present all the input parameters that are used for our numerical simulations and report the branching ratio and various asymmetries for the $B^- \to \Lambda\, \bar{p}\, \mu^+ \mu^-$ decay mode. We conclude with a summary of our results in section 3.4.

3.2 Theory

Exclusive $B^- \to \Lambda \bar{p}\, \mu^+ \mu^-$ decays mediated via $b \to s\, l\, \bar{l}$ transition process is governed by the electroweak box and penguin type diagrams. The relevant Feynman diagrams responsible for this decay process are shown in Fig 3.2. We employ the effective Hamiltonian for $\Delta B = \Delta S = 1$

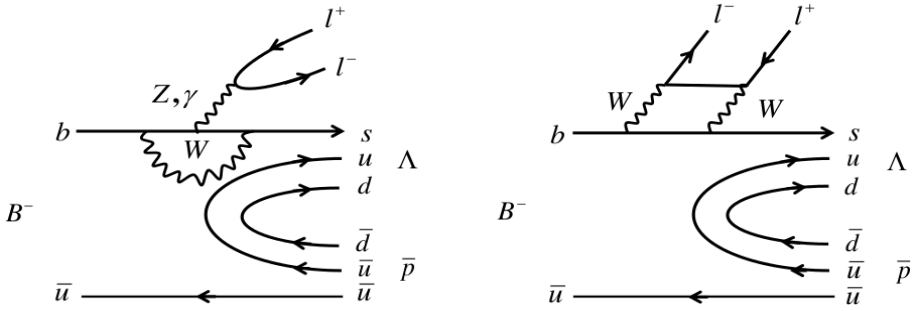

Figure 3.1: Penguin and box diagram contributing to the $B \to \Lambda \bar{p}\, \mu^+ \mu^-$ decay mode.

transition and write the amplitude for $b \to s\, l\, \bar{l}$ transition as [153–156]

$$\mathcal{M}(b \to s\, l\bar{l}) \;=\; \frac{\alpha\, G_F}{\sqrt{2}\pi}\, \lambda_t \sum_i \Big[C_i\, \mathcal{O}_i \,+\, C_i{}'\, \mathcal{O}_i{}' \Big] \,+\, h.c.\,, \tag{3.1}$$

where G_F is the Fermi constant and $\lambda_t = V_{ts}^* V_{tb}$, where V_{ts} and V_{tb} are CKM matrix elements. The electromagnetic coupling constant is denoted by α. The relevant operators considered in our analysis are given by

$$\begin{aligned}
\mathcal{O}_7 &= -2\, i\, m_b \frac{p^\nu}{p^2}\, \bar{s}\sigma_{\mu\nu}\, b_R\, \bar{l}\gamma^\mu\, l\,, & \mathcal{O}'_7 &= -2\, i\, m_b \frac{p^\nu}{p^2}\, \bar{s}\sigma_{\mu\nu}\, b_L\, \bar{l}\gamma^\mu\, l\,,\\
\mathcal{O}_8 &= \bar{s}\gamma_\mu\, b_R\, \bar{l}\gamma^\mu\, l\,, & \mathcal{O}'_8 &= \bar{s}\gamma_\mu\, b_L\, \bar{l}\gamma^\mu\, l\,,\\
\mathcal{O}_9 &= \bar{s}\gamma_\mu\, b_R\, \bar{l}\gamma^\mu\, \gamma_5\, l\,, & \mathcal{O}'_9 &= \bar{s}\gamma_\mu\, b_L\, \bar{l}\gamma^\mu\, \gamma_5\, l\,,\\
\mathcal{O}_S &= m_b\, \bar{s}\, b_R\, \bar{l}\, l\,, & \mathcal{O}'_S &= m_b\, \bar{s}\, b_L\, \bar{l}\, l\,,
\end{aligned}$$

$$\mathcal{O}_P = m_b\,\bar{s}\,b_R\,\bar{l}\,\gamma_5\,l\,, \qquad\qquad \mathcal{O}'_P = m_b\,\bar{s}\,b_L\,\bar{l}\,\gamma_5\,l\,, \tag{3.2}$$

where, $\mathcal{O}_7$ ($\mathcal{O}'_7$) and $\mathcal{O}_8$ ($\mathcal{O}'_8$) represent the magnetic penguin operators and $\mathcal{O}_9$ ($\mathcal{O}'_9$) represents the electromagnetic penguin operator. Here, m_b is the mass of the b quark and $b_{R,\,L} = b\,(1 \pm \gamma_5)/2$. The operators $\mathcal{O}_i{}'$ are obtained from the operators $\mathcal{O}_i$ by making the replacements $b_R \leftrightarrow b_L$. The invariant mass square of the lepton pair is denoted by $p^2 = M^2_{l\bar{l}}$. The Wilson coefficients are denoted by C_7, C_8, and C_9 for the unprimed operators, whereas, C'_7, C'_8, and C'_9 for the primed operators, respectively. Similarly, C_S (C'_S) and C_P (C'_P) denote the Wilson coefficients corresponding to the scalar $\mathcal{O}_S$ ($\mathcal{O}'_S$) and pseudoscalar $\mathcal{O}_P$ ($\mathcal{O}'_P$) operators, respectively. The primed operators $\mathcal{O}'_{7,8,9}$ and $\mathcal{O}_{S,\,P}$ ($\mathcal{O}'_{S,\,P}$) are highly suppressed in the SM.

With the effective Hamiltonian of Eq. (3.1), the amplitude for $B^- \to \Lambda\bar{p}\,l\bar{l}$ can be factorized into hadronic and leptonic parts as

$$\begin{aligned}
\mathcal{A}(B^- \to \Lambda\bar{p}\,l\,\bar{l}) \;=\; & \frac{\alpha\,G_F}{\sqrt{2}\pi}\,\lambda_t \Bigg\{ -2\,i\,\frac{C_7\,m_b}{p^2}\,\langle\Lambda\bar{p}|\bar{s}\sigma_{\mu\nu}\,p^\nu\,b_R|\bar{B}\rangle\,\bar{l}\gamma^\mu\,l + C_8\,\langle\Lambda\bar{p}|\bar{s}\gamma_\mu\,b_R|\bar{B}\rangle\bar{l}\gamma^\mu\,l \\
& + C_9\,\langle\Lambda\bar{p}|\bar{s}\gamma_\mu\,b_R|\bar{B}\rangle\,\bar{l}\gamma^\mu\,\gamma_5\,l \;+\; C_S\,m_b\,\langle\Lambda\bar{p}|\bar{s}\,b_R|\bar{B}\rangle\,\bar{l}\,l \\
& + C_P\,m_b\,\langle\Lambda\bar{p}|\bar{s}\,b_R|\bar{B}\rangle\,\bar{l}\gamma_5\,l \;-\; 2\,i\,\frac{C_7{}'\,m_b}{p^2}\,\langle\Lambda\bar{p}|\bar{s}\sigma_{\mu\nu}\,p^\nu\,b_L|\bar{B}\rangle\,\bar{l}\gamma^\mu\,l \\
& + C_8{}'\,\langle\Lambda\bar{p}|\bar{s}\gamma_\mu\,b_L|\bar{B}\rangle\bar{l}\gamma^\mu\,l + C_9{}'\,\langle\Lambda\bar{p}|\bar{s}\gamma_\mu\,b_L|\bar{B}\rangle\,\bar{l}\gamma^\mu\,\gamma_5\,l \\
& + C_S{}'\,m_b\,\langle\Lambda\bar{p}|\bar{s}\,b_L|\bar{B}\rangle\,\bar{l}\,l \;+\; C_P{}'\,m_b\,\langle\Lambda\bar{p}|\bar{s}\,b_L|\bar{B}\rangle\,\bar{l}\gamma_5\,l \Bigg\}\,.
\end{aligned} \tag{3.3}$$

The explicit form of the matrix element for $B \to \mathcal{B}\bar{\mathcal{B}}'$ depends on the parametrization. We pattern our analysis after that of Geng *et al*, Ref. [122, 152], and, indeed, adopt a common notation. With Lorentz invariance, the most general form of the $B \to \mathcal{B}\bar{\mathcal{B}}'$ transition matrix elements due to the scalar, pseudoscalar, vector, and axial vector currents are [122, 152]

$$\begin{aligned}
&\langle\mathcal{B}\bar{\mathcal{B}}'|\bar{s}\,b|\bar{B}\rangle = i\bar{u}(p_{\mathcal{B}})(f_A\;\not{p} + f_P)\,\gamma_5\,v(p_{\bar{\mathcal{B}}'})\,,\\
&\langle\mathcal{B}\bar{\mathcal{B}}'|\bar{s}\,\gamma_5\,b|\bar{B}\rangle = i\bar{u}(p_{\mathcal{B}})(f_V\;\not{p} + f_S)v(p_{\bar{\mathcal{B}}'})\,,\\
&\langle\mathcal{B}\bar{\mathcal{B}}'|\bar{s}\gamma_\mu b|\bar{B}\rangle = i\bar{u}(p_{\mathcal{B}})\Big[g_1\gamma_\mu + g_2\,i\sigma_{\mu\nu}\,p^\nu + g_3\,p_\mu + g_4\,q_\mu + g_5\,r_\mu\Big]\gamma_5\,v(p_{\bar{\mathcal{B}}'})\,,\\
&\langle\mathcal{B}\bar{\mathcal{B}}'|\bar{s}\gamma_\mu\gamma_5\,b|\bar{B}\rangle = i\bar{u}(p_{\mathcal{B}})\Big[f_1\gamma_\mu + f_2\,i\sigma_{\mu\nu}\,p^\nu + f_3\,p_\mu + f_4\,q_\mu + f_5\,r_\mu\Big]v(p_{\bar{\mathcal{B}}'})\,,
\end{aligned} \tag{3.4}$$

where $q = p_{\mathcal{B}} + p_{\bar{\mathcal{B}}'}$, $p = p_{\bar{B}} - q$, and $r = p_{\bar{\mathcal{B}}'} - p_{\mathcal{B}}$. In the large t limit, where $t \equiv q^2 \equiv m^2_{\mathcal{B}\bar{\mathcal{B}}'}$, the various form factors such as f_i and g_i vary as $1/t^3$ since we need three hard gluons to induce $B \to \mathcal{B}\bar{\mathcal{B}}'$ transition: two for creating the baryon antibaryon pair and one additional gluon for the spectator quark in B meson. There are experimental evidences of the threshold enhancement in many three body baryonic B decays, which, in principle, can be linked to the asymptotic behavior of the various form factors in pQCD counting rules. However, non-observation of the threshold enhancement in $\Sigma^{++}\,\bar{p}\,\pi^-$ decay mode and asymmetric angular distributions in $B^- \to p\bar{p}\,K^-$, $B \to \Lambda_c^+\,\bar{p}\,\pi^-$, and $B \to \Lambda\,\bar{p}\,\gamma$ decay modes suggest that the form factors depend not only on the dibaryon invariant mass t but also depend on the invariant mass of one of the baryons and the invariant mass of the emitted meson. The momentum dependence of the form factors has been studied within the pole model framework where the dominant contributions come from the baryon and meson intermediate

states. The t dependence of the form factors arises due to the meson intermediate state whereas the dependence of the form factors on the invariant mass of one of the baryons and the emitted meson comes from the low lying baryon intermediate state. In this chapter, we follow Refs. [122, 123, 152] and parameterize the form factors in a power series of the inverse of the dibaryon invariant mass squared $m^2_{\mathcal{B}\bar{\mathcal{B}}'}$. The dependence of the form factors on other variables such as the invariant mass of one of the baryons and the invariant mass of the lepton pair are contained in the coefficients, D_{f_i} and D_{g_i}. In this parameterization, the form factors f_i and g_i are written as

$$f_i \;=\; \frac{D_{f_i}}{t^3}\,, \qquad\qquad g_i = \frac{D_{g_i}}{t^3}\,, \tag{3.5}$$

where, the constants D_{f_i} and D_{g_i} can be expressed in terms of the reduced parameters $D_{||}$ and $D^j_{||}$ by using $SU(3)$ flavor and $SU(2)$ spin symmetries. That is

$$\begin{aligned} D_{g_1} &= D_{f_1} = -\sqrt{\frac{3}{2}}\, D_{||}\,, \\ D_{g_j} &= -D_{f_j} = -\sqrt{\frac{3}{2}}\, D^j_{||}\,, \quad (j = 2,\, 3,\, 4,\, 5) \end{aligned} \tag{3.6}$$

where these constants are determined by the measured data in $\bar{B} \to p\bar{p}M$ decays [122]. We refer to Refs. [123] for all omitted details. Using equation of motion, one can relate f_A, f_V, f_S, and f_P to f_i and g_i as

$$\begin{aligned} (m_b - m_s)\, f_A &= g_1\,, & (m_b - m_s)\, f_P &= g_3\, p^2 + g_4\, (p\cdot q) + g_5\, (r\cdot p)\,, \\ -(m_b + m_s)\, f_V &= f_1\,, & -(m_b + m_s)\, f_S &= f_3\, p^2 + f_4\, (p\cdot q) + f_5\, (r\cdot p)\,, \end{aligned} \tag{3.7}$$

where the terms containing g_2 and f_2 vanish because of the antisymmetric nature of $\sigma_{\mu\nu}$. Similarly, using the equation of motion, we write the tensor currents in terms of scalar, pseudoscalar, vector, and axial vector currents. That is

$$\begin{aligned} \langle \mathcal{B}\bar{\mathcal{B}}'|\bar{s}\, p^\nu\, i\,\sigma_{\mu\nu}\, b|\bar{B}\rangle &= q'_\mu \langle \mathcal{B}\bar{\mathcal{B}}'|\bar{s}\, b|\bar{B}\rangle - (m_b + m_s)\langle \mathcal{B}\bar{\mathcal{B}}'|\bar{s}\,\gamma_\mu\, b|\bar{B}\rangle\,, \\ \langle \mathcal{B}\bar{\mathcal{B}}'|\bar{s}\, p^\nu\, i\,\sigma_{\mu\nu}\gamma_5\, b|\bar{B}\rangle &= q'_\mu \langle \mathcal{B}\bar{\mathcal{B}}'|\bar{s}\,\gamma_5\, b|\bar{B}\rangle + (m_b - m_s)\langle \mathcal{B}\bar{\mathcal{B}}'|\bar{s}\,\gamma_\mu\gamma_5\, b|\bar{B}\rangle\,, \end{aligned} \tag{3.8}$$

with $q' = p_{\bar{B}} + q$. Here m_b and m_s denote mass of b and s quark, respectively. Here we assume that all the quarks inside the meson and baryons are on their mass shell.

The differential decay rate for the four body decay can be expressed as

$$d\Gamma \;=\; \frac{|\mathcal{M}|^2}{2^{18}\,\pi^8\, M_B^3\, q^2\, p^2}\lambda^{1/2}(M_B^2,\, q^2,\, p^2)\,\lambda^{1/2}(q^2,\, M_{\mathcal{B}}^2,\, M_{\bar{\mathcal{B}}'}^2)\,\lambda^{1/2}(p^2,\, M_l^2,\, M_{\bar{l}}^2)\, dq^2\, dp^2 \prod_1^3 d\Omega_i\,, \tag{3.9}$$

where $\lambda(x,y,z) = x^2 + y^2 + z^2 - 2\,x\,y - 2\,y\,z - 2\,z\,x$ and $d\Omega_i = d(\cos\theta_i)\, d\phi_i$. Here θ_1 (ϕ_1) is the polar (azimuthal) angle between the $\Lambda\,\bar{p}$ plane and $l\bar{l}$ plane in the B meson rest frame. We define θ_2 (ϕ_2) as the polar (azimuthal) angle between the outgoing Λ and $\Lambda\bar{p}$ system in the rest frame of the $\Lambda\,\bar{p}$ whereas θ_3 (ϕ_3) as the polar (azimuthal) angle between the outgoing l and $l\bar{l}$ system in the

rest frame of the $l\,\bar{l}$. Now the branching ratio is given by

$$\mathrm{BR} = \frac{\Gamma(B^- \to \Lambda\,\bar{p}\,l\,\bar{l})}{\Gamma_{B^-}}\,, \tag{3.10}$$

where Γ_{B^-} is the total decay width of B^- meson. We define asymmetries in angular distributions as

$$A_\theta = \frac{\int_0^1 \frac{d(\mathrm{BR})}{d\cos\theta}\,d\cos\theta - \int_{-1}^0 \frac{d(\mathrm{BR})}{d\cos\theta}\,d\cos\theta}{\int_0^1 \frac{d(\mathrm{BR})}{d\cos\theta}\,d\cos\theta + \int_{-1}^0 \frac{d(\mathrm{BR})}{d\cos\theta}\,d\cos\theta}\,, \tag{3.11}$$

where, $\theta = \theta_L$ and θ_B. Here θ_B defines the angle between p_Λ and the $\Lambda\bar{p}$ line of flight direction in the rest frame of $\Lambda\bar{p}$ system and θ_L defines the angle between p_l and the $l\bar{l}$ line of flight direction in the rest frame of $l\bar{l}$ system. We also define the triple product correlation which is a CP-odd, T-odd

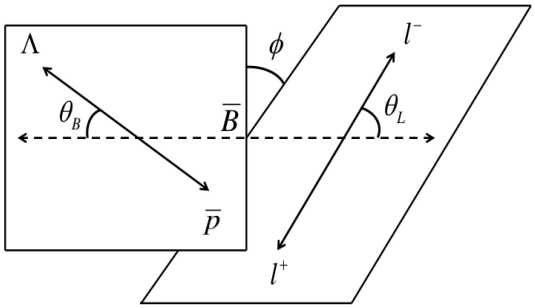

Figure 3.2: Three angles ϕ, θ_B and θ_L in the phase space for the four-body $B \to \Lambda\bar{p}\,\mu^+\,\mu^-$ decay mode.

observable, i.e,

$$T \;=\; \frac{\vec{p}_l \cdot (\vec{p}_\Lambda \times \vec{p}_{\bar{p}})}{|\vec{p}_l||\vec{p}_\Lambda \times \vec{p}_{\bar{p}}|}\,, \tag{3.12}$$

where $\vec{p}_\Lambda$ and $\vec{p}_p$ denote the three momentum of the baryons and $\vec{p}_l$ denotes the three momentum of the lepton. In the SM, this decay mode does not contain any CP phase since it depends on the product of V_{ts} and V_{tb}. Thus the CP odd, T-odd observable will be vanishingly small in the SM.

The azimuthal angle ϕ between the decay planes of the dibaryon and dilepton is also sensitive to the CP violating coupling. We define two unit vectors $\hat{\eta}_1$ and $\hat{\eta}_2$ perpendicular to the $\Lambda\bar{p}$ and $l\bar{l}$ decay plane. That is

$$\hat{\eta}_1 \;=\; \frac{\vec{p}_\Lambda \times \vec{p}_{\bar{p}}}{|\vec{p}_\Lambda \times \vec{p}_{\bar{p}}|}\,, \tag{3.13}$$

$$\hat{\eta}_2 \;=\; \frac{\vec{p}_l \times \vec{p}_{\bar{l}}}{|\vec{p}_l \times \vec{p}_{\bar{l}}|}\,. \tag{3.14}$$

The azimuthal angle ϕ is defined as the angle between these two unit vectors, that is

$$\phi = \cos^{-1}(\hat{\eta}_1.\hat{\eta}_2)\,. \tag{3.15}$$

We define asymmetries in the triple product correlation and azimuthal angular distribution as

$$A_T = \frac{\int_0^1 \frac{d(\mathrm{BR})}{dT}\, dT - \int_{-1}^0 \frac{d(\mathrm{BR})}{dT}\, dT}{\int_0^1 \frac{d(\mathrm{BR})}{dT}\, dT + \int_{-1}^0 \frac{d(\mathrm{BR})}{dT}\, dT}\,,$$
$$A_\phi = \frac{\int_0^1 \frac{d(\mathrm{BR})}{d\cos\phi}\, d\cos\phi - \int_{-1}^0 \frac{d(\mathrm{BR})}{d\cos\phi}\, d\cos\phi}{\int_0^1 \frac{d(\mathrm{BR})}{d\cos\phi}\, d\cos\phi + \int_{-1}^0 \frac{d(\mathrm{BR})}{d\cos\phi}\, d\cos\phi}\,. \tag{3.16}$$

We will discuss more about the triple product asymmetries and the angular asymmetries in section 3.3.

We want to see the effect of various NP couplings on all the above mentioned observables in a qualitative way. The recent $B \to K^* \mu^+ \mu^-$ anomaly reported by LHCb got a lot of attention and various phenomenological work have been done in order to understand the data and to identify the NP parameter that is responsible for the deviation from the SM expectation [139–149]. Although, NP affects all the Wilson coefficients, there seems to be a general agreement among various groups that NP contributes dominantly to the Wilson coefficient C_9. Our main goal here is to understand how different NP couplings modify the branching fraction and various observables in the $B^- \to \Lambda \bar{p}\, \mu^+ \mu^-$ decay mode. Our NP framework is defined by considering that NP enters in $\mathcal{O}_i$ with $i = 7,\, 8,\, 9,\, S,\, P$ together with their chirally flipped operators $\mathcal{O}'_i$. We study the impact of each NP coupling on various observables. To do this we set all other NP parameters to zero and vary one NP parameter alone within the allowed range. This will allow us to have a better control of the NP parameters and once confronted with the data, we will be able to find the minimal set of operators that are compatible with the data. We assume the NP couplings to be real for our analysis. We now proceed to discuss the results.

3.3 Results and discussion

For definiteness, we summarize all the input parameters that we have used for our numerical simulations. For the CKM matrix elements, we use $|V_{ts}| = (42.9 \pm 2.6) \times 10^{-3}$ and $|V_{tb}| = 0.89 \pm 0.07$ from Ref. [26]. For the lepton and hadron masses, we use $M_B = 5.27925\,\mathrm{GeV}$, $M_\Lambda = 1.115683\,\mathrm{GeV}$, $M_p = 0.93827\,\mathrm{GeV}$, and $M_\mu = 0.105658\,\mathrm{GeV}$ [26], respectively. For quark masses, we use $m_b = 4.18\,\mathrm{GeV}$ and $m_s = 0.095\,\mathrm{GeV}$ [26]. For the Wilson coefficients, we use the values reported in Ref. [157]. That is

$$C_7 = -0.313\,, \qquad C_8 = 4.344\,, \qquad C_9 = -4.669\,. \tag{3.17}$$

The Wilson coefficients associated with the primed operators $\mathcal{O}'_i$ and the scalar and pseudoscalar operators $O_{S,P}$, $O'_{S,P}$ are assumed to be zero in the SM. For the baryonic form factors f_i and g_i, we use the values of $D_{||}$'s reported in Ref. [152]. That is

$$D_{||} = 67.7 \pm 16.3\,\mathrm{GeV}^5\,, \qquad D^2_{||} = -187.3 \pm 26.6\,\mathrm{GeV}^4\,, \qquad D^3_{||} = -840.1 \pm 132.1\,\mathrm{GeV}^4\,,$$
$$D^4_{||} = -10.1 \pm 10.8\,\mathrm{GeV}^4\,, \qquad D^5_{||} = -157.0 \pm 27.1\,\mathrm{GeV}^4\,. \tag{3.18}$$

First, we report the value of the branching ratio and various asymmetries within the SM. In the SM, the relevant operators for our analysis are the non-primed operators ($\mathcal{O}_i$), where $i = 7,\, 8,$ and 9,

respectively. All the primed operators ($\mathcal{O}_i'$) and the scalar ($\mathcal{O}_S$, $\mathcal{O}_S'$) and the pseudoscalar ($\mathcal{O}_P$, $\mathcal{O}_P'$) operators are ignored. The SM prediction of the branching ratio and various asymmetries for the $B \to \Lambda\bar{p}\,\mu^+\,\mu^-$ decay mode is reported in Table. 3.1, where, for the central values we have used the central values of all the input parameters. The theoretical uncertainties in the calculation of the decay branching fractions come from various input parameters. First, there are uncertainties associated with well-known input parameters such as quark masses, meson masses, and lifetime of the mesons. We ignore these uncertainties as these are not important for our analysis. Second, there are uncertainties that are associated with not so well-known hadronic input parameters such as form factors and the CKM elements. In order to realize the effect of the above-mentioned uncertainties on various observables, we vary these theory inputs within 1σ of their central values and obtain the 1σ allowed ranges in all the different observables. The results are reported in Table. 3.1.

SM values	BR$\times 10^{-7}$	$A_{\theta_L} \times 10^{-2}$	$A_{\theta_B} \times 10^{-2}$	$A_T \times 10^{-5}$	$A_\phi \times 10^{-2}$
Central value	1.08	2.79	-6.71	2.71	4.85
1σ range	$(0.57, 1.90)$	$(2.72, 2.89)$	$(-5.62, -7.53)$	$(2.49, 3.14)$	$(4.76, 4.88)$

Table 3.1: Branching ratio and various angular asymmetries for $B^- \to \Lambda\bar{p}\,\mu^+\,\mu^-$ within the SM.

We find that the dominant contribution to the branching ratio comes from the first term in the $b \to s\,l\bar{l}$ decay amplitude. It is expected as this term is inversely proportional to the invariant mass square of the lepton pair. In Fig. 3.3, we show the invariant mass distributions and various angular distributions of the $B^- \to \Lambda\bar{p}\,\mu^+\,\mu^-$ decay mode, where the shaded regions represent the theoretical uncertainties coming from the $B \to \mathcal{B}\bar{\mathcal{B}}'$ transition form factors and the CKM matrix elements. The enhancement at the threshold of both the dilepton as well as the dibaryon invariant mass is quite clear. The dibaryon invariant mass peaks at the threshold because the $B \to \Lambda\bar{p}$ transition form factors f_i and g_i are proportional to $1/t^3$, where t is the square of the invariant mass of the baryon - antibaryon pair. Whereas, the dilepton mass peaks at the threshold because of the $1/p^2$ dependence in the $b \to s\,l\,\bar{l}$ transition decay amplitude. In the low energy region, the decay $B \to \Lambda\,\bar{p}\,\mu^+\,\mu^-$ receives dominant contribution near the dilepton mass threshold. Again, we find that the contributions coming from the vector and axial vector couplings are much larger than the contributions coming from the scalar and pseudoscalar couplings in the $B \to \mathcal{B}\bar{\mathcal{B}}'$ transition. We also plot the angular distributions for $B^- \to \Lambda\bar{p}\,\mu^+\,\mu^-$ decay mode as functions of $\cos\theta_B$ and $\cos\theta_L$ which are shown in Fig. 3.3. The angular asymmetries A_{θ_B} and A_{θ_L} calculated within the SM are reported in Table. 3.1. The angular asymmetries are quite small and this is what we expect. In $B^- \to \Lambda\,\bar{p}\,\mu^+\,\mu^-$ decays, the Λ and p pick up the energetic s and u quarks, respectively. The threshold enhancement ensures that, in the rest frame of the B meson, the Λ and $\bar{p}$ move collinearly. Thus, in the boosted frame of $\Lambda\,\bar{p}$, the dilepton will move away from the dibaryon system and hence the distribution should be symmetric as functions of $\cos\theta_B$ and $\cos\theta_L$. We also show the angular distribution for $B^- \to \Lambda\bar{p}\,\mu^+\,\mu^-$ decay mode as a function of the triple product correlation T and the azimuthal angle $\cos\phi$. The triple product asymmetry A_T and the azimuthal angular asymmetry A_ϕ calculated within the SM are reported in Table. 3.1. These are vanishingly small as expected. Any deviation from the SM expectation will be a definite hint of beyond the SM physics.

Now we proceed to discuss the effect of various NP couplings on the above mentioned observables in a qualitative way. For definiteness, we report the 95% CL range of each NP coupling that are taken from Refs. [158, 159]. We assume that all the coefficients are real.

$$
\begin{aligned}
&C_7^{\rm NP} = (-0.15,\, 0.03), \qquad C_8^{\rm NP} = (-1.1,\, 1.6), \qquad C_9^{\rm NP} = (-1.2,\, 1.6),\\
&C_7' = (-0.4,\, 0.3), \qquad C_8' = (-2.0,\, 4.0), \qquad C_9' = (-3.0,\, 1.0),\\
&C_S,\, C_S' = (-0.7,\, 0.7)\,, \qquad C_P,\, C_P' = (-1.0,\, 1.0)
\end{aligned}
\tag{3.19}
$$

The branching ratio for the $B^- \to \Lambda\bar{p}\,\mu^+\,\mu^-$ decay mode is listed in Table. 3.2 with the various NP couplings. The range in each observable is obtained by using the range of NP parameters in Eq. (3.19). It is clear that the deviation from the SM prediction is more if one include the NP effects in C_S, C_P, C_S', and C_P' simultaneously.

$C_7^{\rm NP}$	$C_8^{\rm NP}$	$C_9^{\rm NP}$	C_7'	C_8'	C_9'	C_S, C_S', C_P, C_P'
(0.50, 3.44)	(0.57, 2.09)	(0.49, 2.23)	(1.65, 3.01)	(0.65, 2.24)	(0.60, 2.02)	(1.50, 4.30)

Table 3.2: Branching ratio ($\times 10^{-7}$) of $B^- \to \Lambda\bar{p}\,\mu^+\,\mu^-$ once the NP is switched on.

We consider various NP scenarios. First, we assume that NP affects the Wilson coefficient C_7 only. In Fig. 3.3, we show the effect of NP associated with the operator $\mathcal{O}_7$. In this case, the NP will modify the dipole operator coefficient C_7 only. We allow for sizable modifications to the dipole Wilson coefficient. We show the effect of NP on various observables for $C_7^{\rm NP} = -0.15$ and 0.03. We see an enhancement of about 100% at the threshold of the invariant mass distribution of the lepton pair. This is expected as the dipole operators in $B \to \Lambda\bar{p}\,\mu^+\mu^-$ decay amplitude is directly proportional to $1/p^2$, where p^2 is the invariant mass square of the lepton pair. Similar enhancement is seen in the invariant mass distribution of the baryon pair as well. Again, it is worth mentioning that, NP has a significant effect on the angular distributions for θ_L and θ_B. The NP effects on these observables are illustrated in the middle panel of Fig. 3.3. For $C_7^{\rm NP} = -0.15$, the shape of the distribution curve changes drastically. Once the NP is switched on, the angular distribution curve peaks at $\cos\theta_L = -1$, whereas, SM distribution peaks at $\cos\theta_L = 1$. Thus, it is clear that once the NP coupling is present, there can be a significant deviation from the SM expectation and depending on the value of the NP coupling, the shape of the distribution curve may or may not change. However, we do not expect to see a sizable deviation in the shape of the $\cos\theta_B$ distribution curve. Similarly, although, there is deviation from the SM expectation in the azimuthal angular distribution and the triple product correlation, these distribution curves remain symmetric with respect to the origin. This is expected as the NP coupling $C_7^{\rm NP}$ is real and we do not expect to see any CP violation.

In Fig. 3.4, we show the effect of NP associated with the semileptonic operator $\mathcal{O}_8$, i.e, we assume that NP affects the Wilson coefficient C_8 only. We show the effect on various observables for two different values of the NP coupling. We set $C_8^{\rm NP} = -1.1$ and 1.6. Although, we observe a slight change in the invariant mass distribution curve, as can be seen from Fig. 3.4, such kind of NP coupling mainly affects the angular distribution, leaving all other observables approximately SM

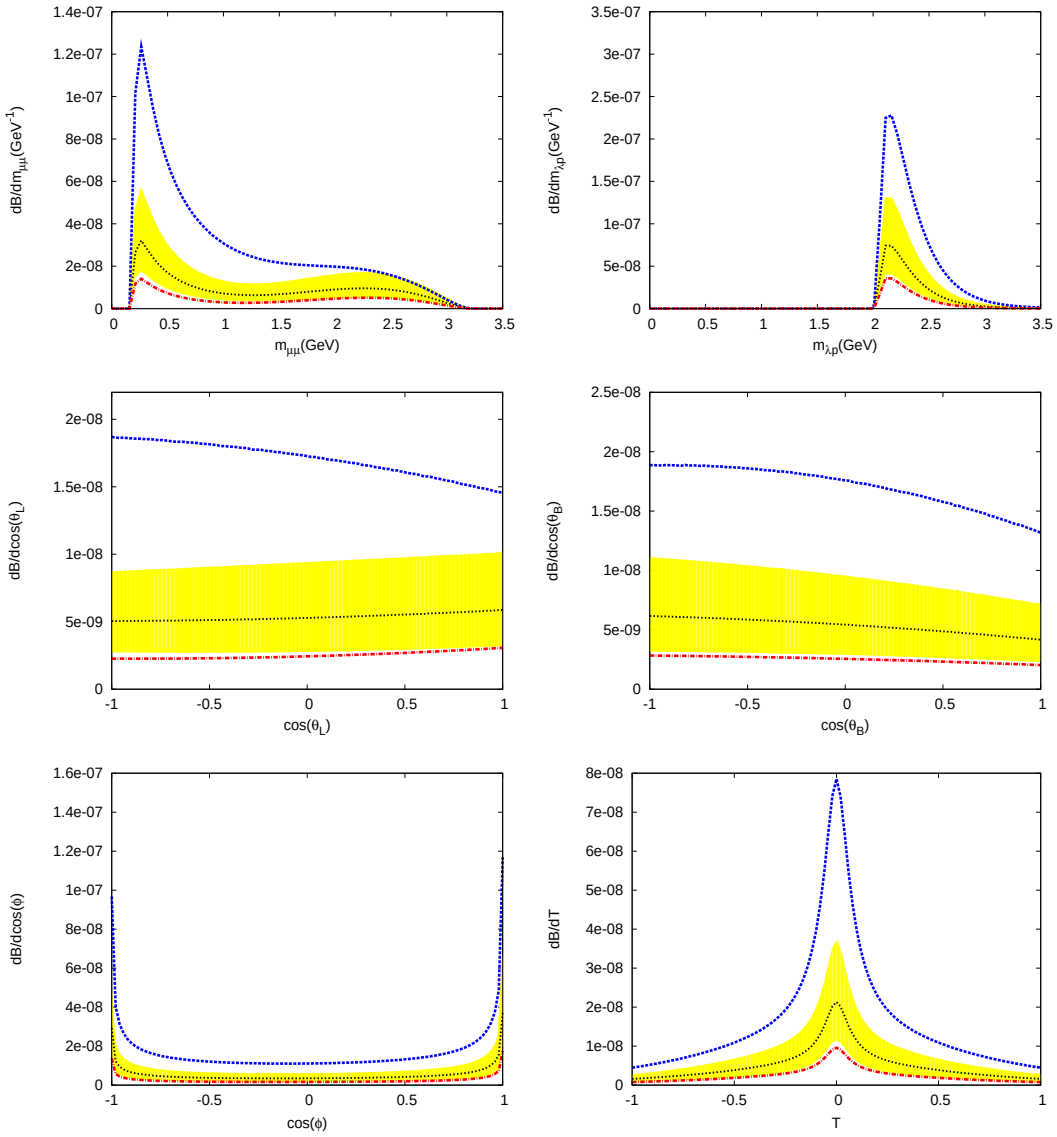

Figure 3.3: Effect of NP coupling $C_7^{\rm NP}$ on various observables. The shaded region (yellow band) represents the SM prediction with the theoretical uncertainties coming from the transition form factors and the CKM matrix elements. The black curve corresponds to the central values of the SM, whereas the red and the blue curve correspond to $C_7^{\rm NP} = 0.03$ and -0.15, respectively.

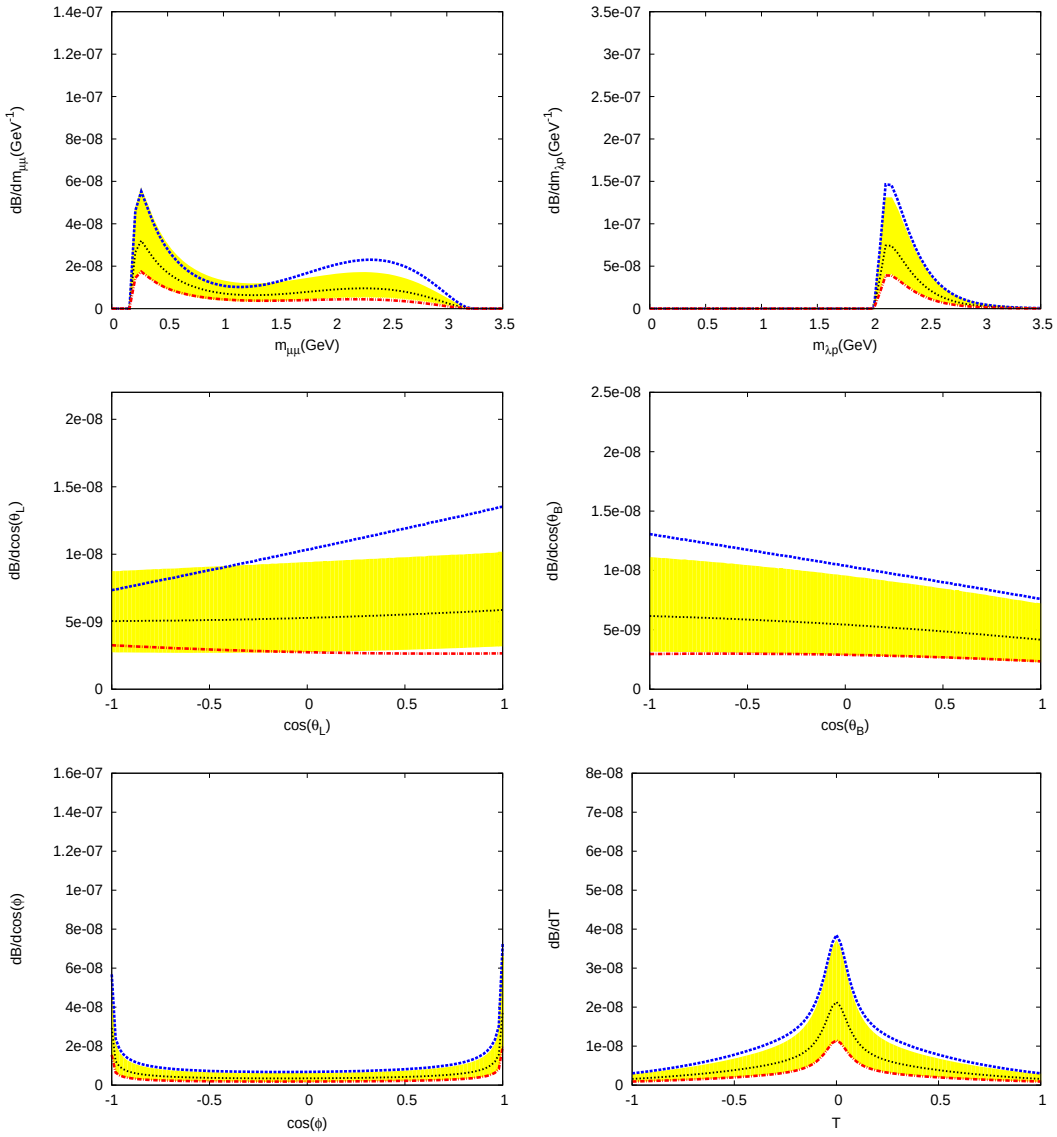

Figure 3.4: Effect of NP coupling $C_8^{\rm NP}$ on various observables. The shaded region (yellow band) represents the SM prediction with the theoretical uncertainties coming from the transition form factors and the CKM matrix elements. The black curve corresponds to the central values of the SM, whereas the red and the blue correspond to $C_8^{\rm NP} = -1.1$ and 1.6, respectively.

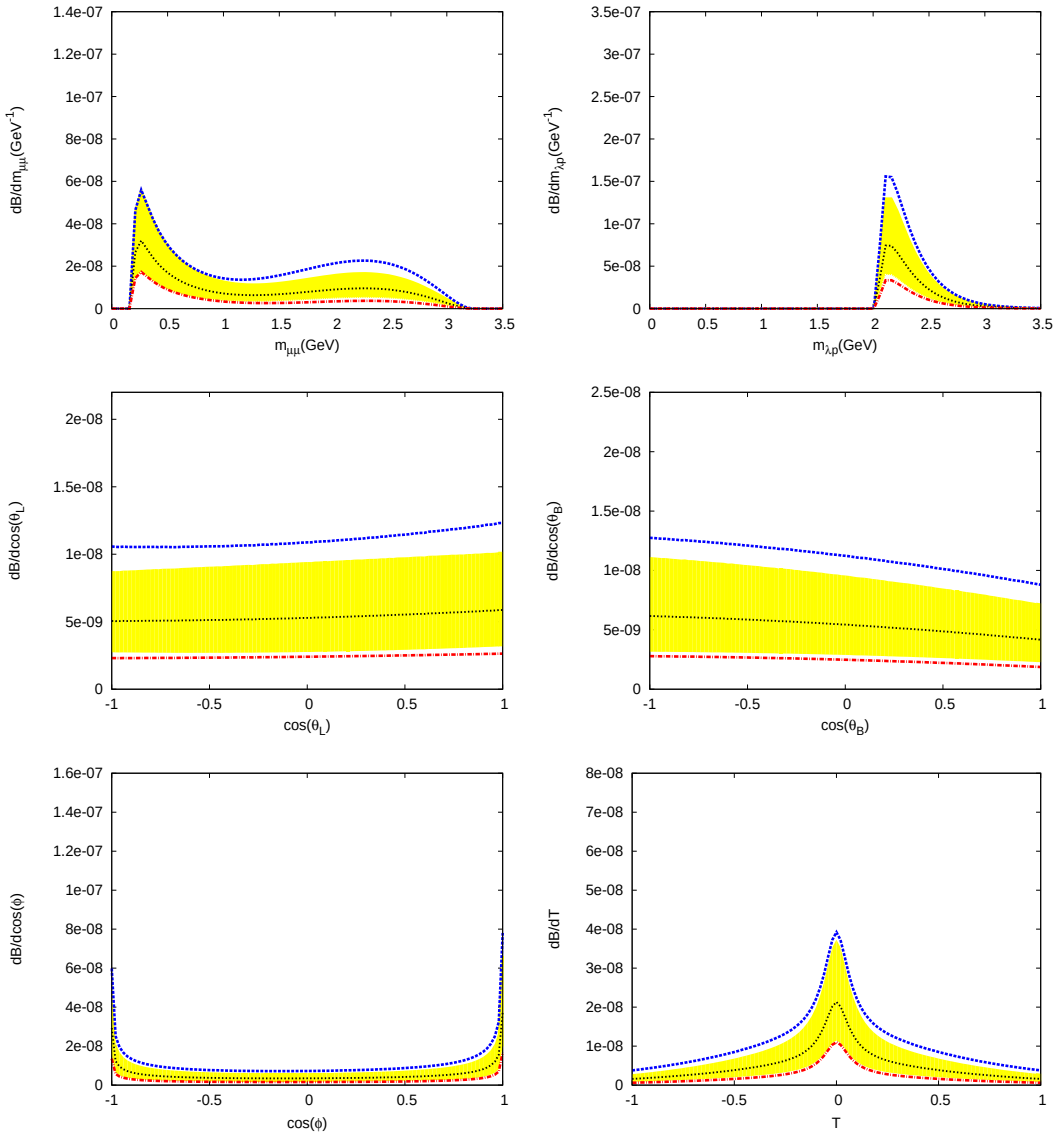

Figure 3.5: Effect of NP coupling $C_9^{\rm NP}$ on various observables. The shaded region (yellow band) represents the SM prediction with the theoretical uncertainties coming from the transition form factors and the CKM matrix elements. The black curve corresponds to the central values of the SM, whereas the red and the blue correspond to $C_9^{\rm NP} = 1.6$ and -1.2, respectively.

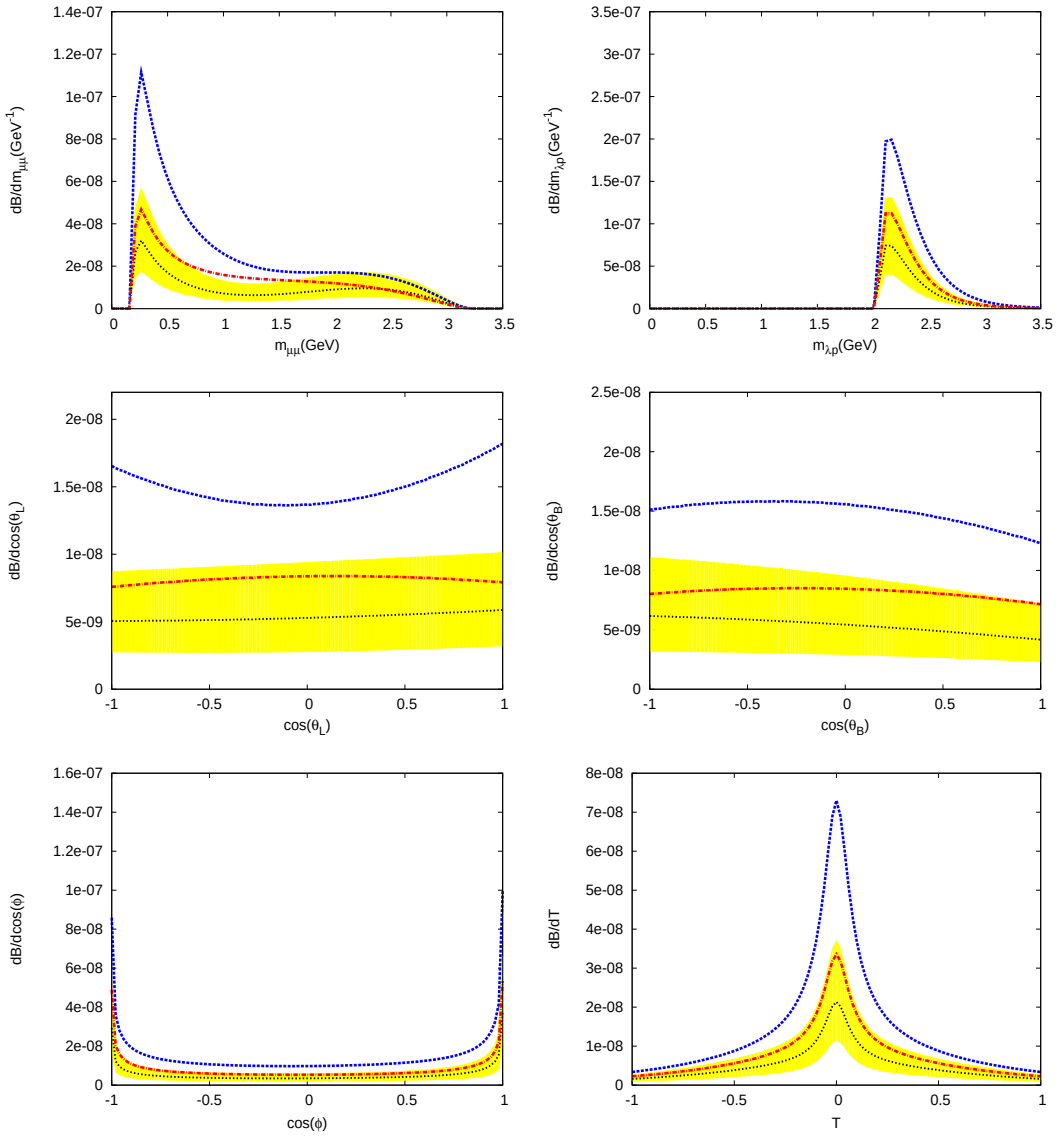

Figure 3.6: Effect of NP coupling C_7' on various observables. The shaded region (yellow band) represents the SM prediction with the theoretical uncertainties coming from the transition form factors and the CKM matrix elements. The black curve corresponds to the central values of the SM, whereas the red and the blue correspond to $C_7' = -0.4$ and 0.3, respectively.

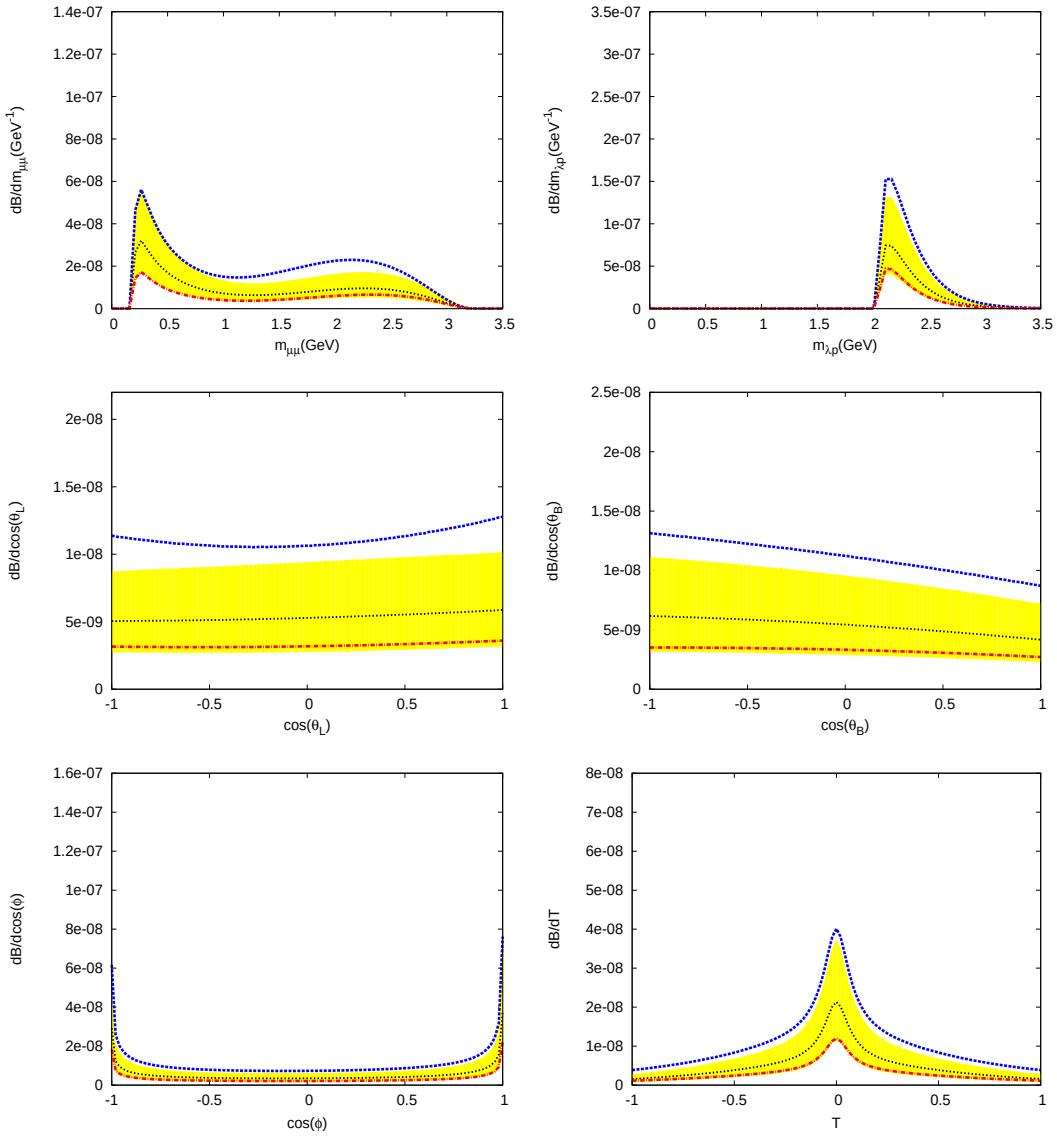

Figure 3.7: Effect of NP coupling C_8' on various observables. The shaded region (yellow band) represents the SM prediction with the theoretical uncertainties coming from the transition form factors and the CKM matrix elements. The black curve corresponds to the central values of the SM, whereas the red and the blue correspond to $C_8' = -2.0$ and 4.0, respectively.

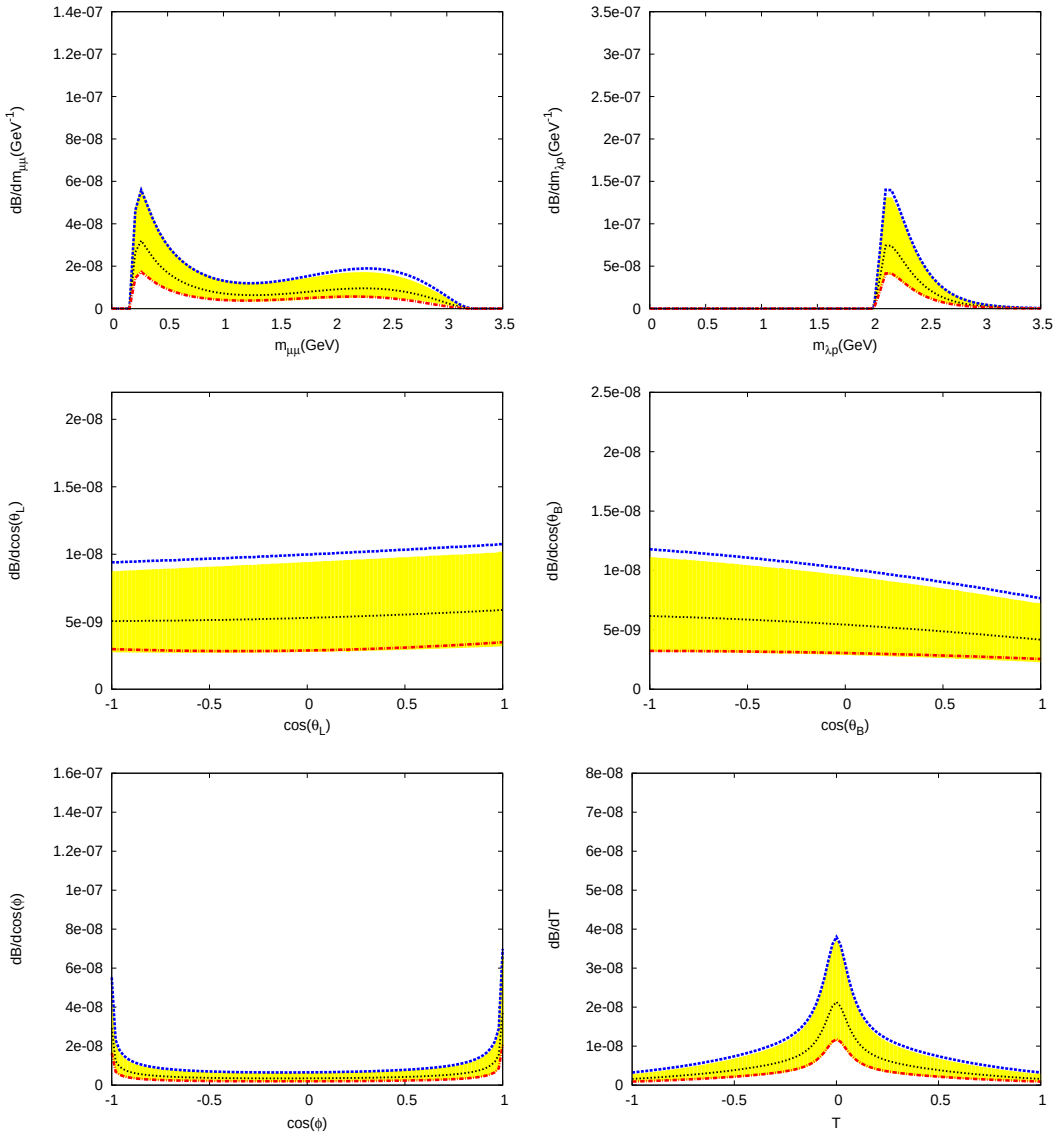

Figure 3.8: Effect of NP coupling C_9' on various observables. The shaded region (yellow band) represents the SM prediction with the theoretical uncertainties coming from the transition form factors and the CKM matrix elements. The black curve corresponds to the central values of the SM, whereas the red and the blue correspond to $C_9' = -3.0$ and 1.0, respectively.

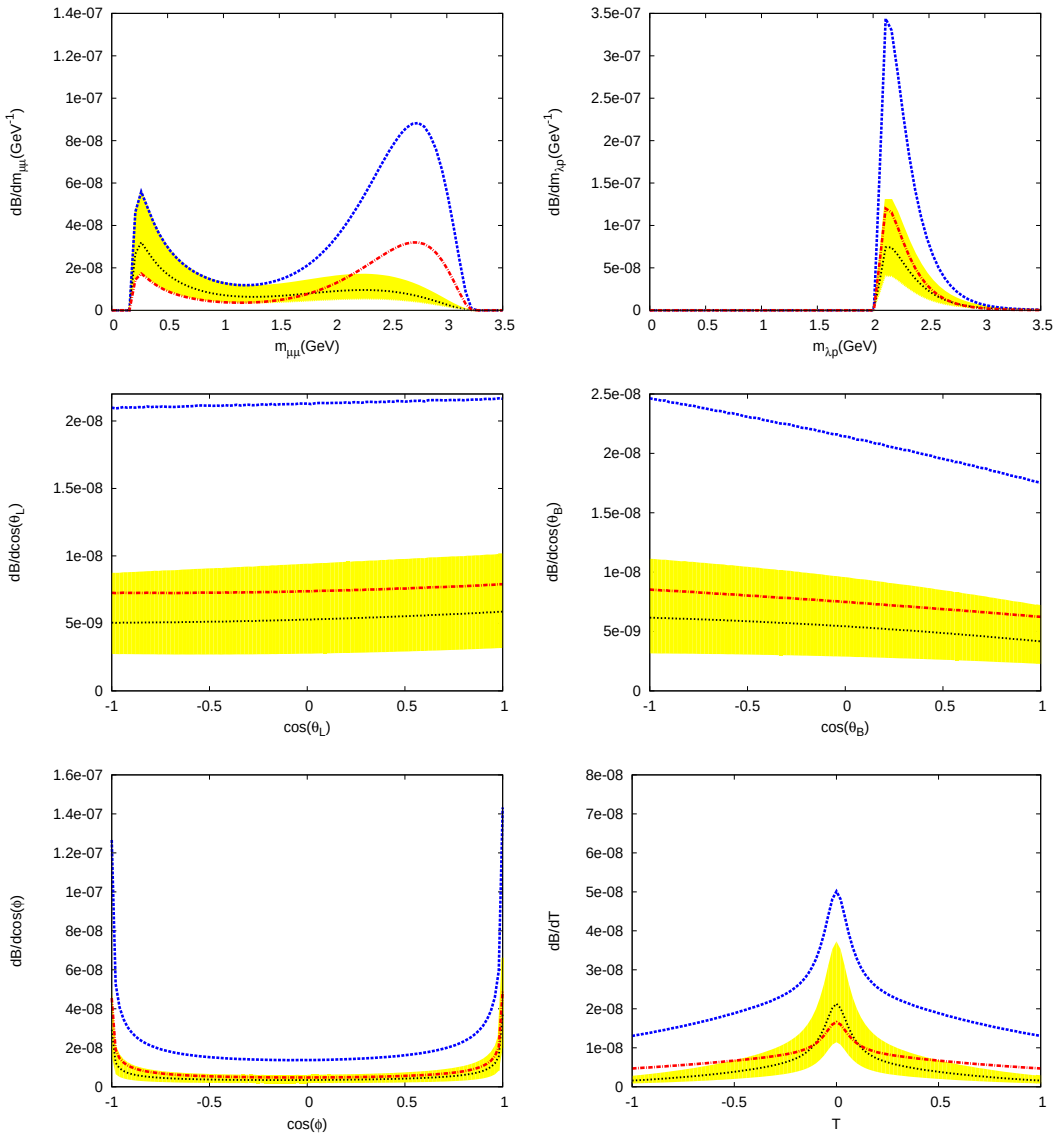

Figure 3.9: Effect of NP couplings C_S, C_P, C'_S, and C'_P on various observables. The shaded region (yellow band) represents the SM prediction with the theoretical uncertainties coming from the transition form factors and the CKM matrix elements. The black curve corresponds to the central values of the SM. The red curve corresponds to C_S, $C'_S = -0.7$ and C_P, $C'_P = -1.0$, whereas the blue curve corresponds to C_S, $C'_S = 0.7$ and C_P, $C'_P = 1.0$.

like. We see that the angular distributions for θ_B and θ_L are significantly different from the SM once the NP coupling is switched on. Again, for the azimuthal angular distribution and triple product correlation, the distribution curves remain symmetric with respect to the origin as expected since the NP coupling $C_8^{\rm NP}$ is real.

Similar pattern is observed once the NP coupling associated with the operator $\mathcal{O}_9$ is switched on. We use NP in C_9 and see the effects on various observables for $C_9^{\rm NP} = -1.2$ and 1.6, respectively. We see a significant deviation from the SM in the angular distribution, leaving all other observables approximately SM like. The effects of this NP coupling on various observables are shown in Fig. 3.5.

Now we look at the primed operators $\mathcal{O}_i'$. In the SM, the Wilson coefficients associated with these chirally flipped operators are suppressed and are assumed to be zero. Once we switched on the NP in these primed operators, the angular distribution differs significantly from the SM. We show the effects of these NP parameters on various observables in Fig. 3.6, Fig. 3.7, and Fig. 3.8, respectively. There is deviation in the invariant mass distribution for NP in C_7'. Although, we see an enhancement of more than 100% in the branching ratio from the SM expectation, the shape remains similar to that of the SM as can be seen from Fig. 3.6. The effect of C_8' and C_9' on the angular distributions as functions of $\cos\theta_L$ and $\cos\theta_B$ is significant as can be seen from Fig. 3.7 and Fig. 3.8. However, the effect of these NP is negligible on all other observables such as invariant mass distribution, the azimuthal angular distribution, and the triple product correlation.

In Fig. 3.9, we show the NP effect associated with the primed and non-primed scalar and pseudoscalar operators on various observables. We consider simultaneous NP effects in all the four Wilson coefficients, i.e, we consider NP in C_S, C_P, C_S', and C_P' simultaneously. In the SM, these are suppressed and are assumed to be zero for our analysis. However, it may not be negligible in the presence of NP. We see that the invariant mass spectra as functions of the invariant masses $m_{\Lambda\bar{p}}$ and $m_{\mu^+\mu^-}$ differ significantly from their SM expectation. We see a huge peak at large invariant mass of the lepton pair. Thus, in the presence of such NP, the peak of the distribution is no longer at the threshold. Although, there is significant deviation of the angular distributions for θ_L and θ_B from the SM expectation, the shape of the distribution curves remain similar to the SM. Similarly, we do not see any asymmetry in the azimuthal angular distribution and triple product correlation.

3.4 Conclusion

Flavor changing neutral current process mediated via $b \to (d,\, s)\, l\bar{l}$ transition decay process is a loop mediated process and, in principle, can get significant corrections from NP effects. A lot of experimental as well as theoretical work have been done in this context with a meson in the final state. Recent measurements of $B_{d,s} \to \mu^+\,\mu^-$ and $B \to K^*\,\mu^+\,\mu^-$ decays differ from the standard model expectation and if they persist in future precision experiments, it will be a definite hint of beyond the standard model physics. This will, in turn, affect any FCNC decays mediated via $b \to s\, l\, \bar{l}$ transition process such as baryonic $B \to \mathcal{B}\bar{\mathcal{B}}'\, l\bar{l}$ decays. In this context, we construct the most general effective Hamiltonian for the semileptonic $B^- \to \Lambda\bar{p}\,\mu^+\mu^-$ decay process and look at the effect of NP couplings on various observables in a qualitative way. We assume that all the Wilson

coefficients of the operators get modified due to NP effects and see the effect of each NP coupling on various observables. We also assume that all the NP couplings are real. This $B^- \to \Lambda\bar{p}\,\mu^+\,\mu^-$ decay mode is important for several reasons. First, the study of such modes is complementary to the study of $B \to K^*\,\mu^+\,\mu^-$ mediated via $b \to s\,l\,\bar{l}$ transition process. Second, its empirical study can be complementary to other baryonic B decays and one can, in principle, investigate the theoretical modeling of the $B \to \mathcal{B}\,\bar{\mathcal{B}}'$ transition form factors.

Within the SM, we find the branching ratio of $B^- \to \Lambda\bar{p}\,\mu^+\mu^-$ decay mode to be 1.08×10^{-7}. We see that the deviation from the SM prediction is quite significant if we include the NP in C_S, C_P, C'_S, and C'_P simultaneously. The asymmetries in the triple product correlations are found to be vanishingly small as expected since, in the SM, this decay mode depends only on V_{ts} and V_{tb}, CKM matrix elements. Again, we see that the azimuthal angular distribution and the triple product correlation remain symmetric with respect to the origin once we include the NP effects. This is expected because all the NP couplings are real and hence we do not expect to find any CP violation in this decay mode. The effect of $C_7^{\rm NP}$ on the invariant mass distribution and the angular distributions as functions of $\cos\theta_L$ and $\cos\theta_B$ is quite significant. Again, in case of NP in C_8 and C_9, we see that only the angular distributions as functions of $\cos\theta_L$ and $\cos\theta_B$ are significantly different from the SM prediction. Similar pattern is observed in case of NP in all the primed coefficients. However, if we switch on NP in C_S, C_P, C'_S, and C'_P simultaneously, we see a significant deviation from the SM prediction in the invariant mass spectrum as function of the invariant mass $m_{\mu^+\,\mu^-}$. The peak of the distribution shifts towards the large invariant mass of the lepton pair.

Current experimental results suggest new physics in FCNC decays mediated via $b \to (s,\,d)\,l\,\bar{l}$ transition processes. Precision measurements in future B experiments will help in identifying the nature of the new physics. Again, a better theoretical understanding of the $B \to \mathcal{B}\,\bar{\mathcal{B}}'$ transition form factors will improve our estimates in future.

Chapter 4

$B_s \to D_s^{(*)} l\nu_l$ semileptonic decays

4.1 Introduction

The semileptonic decays of bottom mesons are excellent attempts to further confirm validity of the Standard Model and to search for New Physics beyond the Standard Model. These decays allow us to measure Cabibbo-Kobayashi-Maskawa(CKM) matrix elements, mixing parameters as well as the origin of CP violation. Among the different semileptonic decay channels of $B_q \to D_q\, l\nu_l$ $(q = s, d, u)$, the decays with quark level transition $b \to c$ are the most compelling decay channels because this transition is a more dominant transition among b decays. Recently the BaBar measurement [34] of ratio of branching fractions showed 3.4 σ discrepancy with the standard model expectation, that brought up a lot of studies in $B \to D^{(*)}\, l\, \bar{\nu}_l$ semileptonic decays [33, 49–55, 160, 161]. The measured ratios are

$$R_D = \frac{\mathcal{B}(\bar{B} \to D\tau^-\bar{\nu}_\tau)}{\mathcal{B}(\bar{B} \to D\, l^-\bar{\nu}_l)} = 0.440 \pm 0.058 \pm 0.042\,,$$
$$R_{D^*} = \frac{\mathcal{B}(\bar{B} \to D^*\tau^-\bar{\nu}_\tau)}{\mathcal{B}(\bar{B} \to D^*\, l^-\bar{\nu}_l)} = 0.332 \pm 0.024 \pm 0.018\,, \tag{4.1}$$

where the first error is statistical and the second one is systematic.

The SM predicted values for R_D and R_{D^*} are [35, 62]

$$R_D = 0.297 \pm 0.017\,, \qquad R_{D^*} = 0.252 \pm 0.003\,. \tag{4.2}$$

The transition form factors play a significant role in the semi-leptonic decays and the $B_s \to D_s^{(*)}\, l\, \nu$ semileptonic decays have been studied within the SM with different approaches of form factor calculation and using different models. The problem has been studied in the framework of constituent quark meson (CQM) model [162] and form factors related to it have been calculated using QCD sum rules approach [163,164], light cone sum rules(LCSR) approach [165], covariant light-front quark model(CLFQM) [166], method of an instantaneous approximated Mandelstam formulation of transition matrix elements and the instantaneous Bethe-Salpeter equation [167]. Recently the problem has been studied in the lattice QCD method [168] and in the perturabative QCD factorization approach [169].

In the past few years, semileptonic $B \to D^{(*)}\, l\, \nu$ decays, have been extensively studied following BaBar measurement rather than $B_s \to D_s^{(*)}\, l\, \nu$ semileptonic decays. However both of these semileptonic decays are related to each other by $SU(3)_F$ flavor symmetry. Both decays involve the same quark level transition $b \to c\, l\, \nu$ but the only difference is in the spectator quark. For $B \to D^{(*)}\, l\, \nu$ decays, the spectator quark is u or d while for $B_s \to D_s^{(*)}\, l\, \nu$ decays, the spectator quark is s. In principle, they should have similar properties and features in the limit of $SU(3)_F$ flavor symmetry. But the B_s meson decays have smaller soft photon pollution than the non-strange B meson decays [170] which is one of the advantage in studying B_s decays. Moreover, the significant deviations between the SM prediction and BaBar measurement [34] for the measurement of the ratios such as R_D and R_{D^*} also motivated us to study for $B_s \to D_s^{(*)}\, l\, \nu_l$ decay modes to estimate the numerical values branching ratios and ratios of branching ratio which could be measurable in the up-coming Super-B experiments, where the SM predictions could be verified. Any deviation from SM expectations will possibly be an indirect evidence of New Physics(NP) beyond the SM. In this chapter, we study $B_s \to D_s^{(*)}\, l\, \nu_l$ semileptonic decays within the Standard Model and calculate the branching ratios of different decay modes. We define ratios of branching fractions R_{D_s}, $R_{D_s^*}$, R_τ and R_l as:

$$
\begin{aligned}
R_{D_s} &= \frac{\mathcal{B}(\bar{B}_s \to D_s \tau^- \bar{\nu}_\tau)}{\mathcal{B}(\bar{B}_s \to D_s\, l^- \bar{\nu}_l)}, \qquad & R_{D_s^*} &= \frac{\mathcal{B}(\bar{B}_s \to D_s^* \tau^- \bar{\nu}_\tau)}{\mathcal{B}(\bar{B}_s \to D_s^*\, l^- \bar{\nu}_l)}, \\
R_\tau &= \frac{\mathcal{B}(\bar{B}_s \to D_s \tau^- \bar{\nu}_\tau)}{\mathcal{B}(\bar{B}_s \to D_s^*\, \tau^- \bar{\nu}_\tau)}, \qquad & R_l &= \frac{\mathcal{B}(\bar{B}_s \to D_s l^- \bar{\nu}_l)}{\mathcal{B}(\bar{B}_s \to D_s^*\, l^- \bar{\nu}_l)},
\end{aligned}
\tag{4.3}
$$

and we estimate their numerical values within the SM that could be measurable in future Super-B experiments. Moreover, we study physical observables such as differential branching ratio (DBR) and forward-backward asymmetry and their implications. The ratios R_{D_s}, $R_{D_s^*}$ are defined for same mesonic mode and different leptonic mode that signify the mass effect arising due to heavy lepton τ against light lepton, e^- or μ^-, whereas the ratios R_τ, R_l are defined for different mesonic mode and same leptonic mode that signify the effects arising from the different form factors of $B_s \to D_s$ and $B_s \to D_s^*$ transitions.

The chapter is organised as follows. In section 4.2, we start with a brief description of the effective Lagrangian for the $b \to c\, l\, \nu$ processes and then write all the relevant formulae of the decay rates for various decay modes within SM. We define several observables in $B_s \to D_s \tau(l)\nu$, and $B_s \to D_s^* \tau(l)\nu$ decays, where $l = e^-, \mu^-$. The numerical prediction of the branching ratios and the ratios of branching ratio for the different decay modes are presented in section 4.3. We conclude with a summary of our results in section 4.4.

4.2 Effective Lagrangian and decay amplitude

The most general effective Lagrangian governing $B_s \to D_s^{(*)}\, l\, \nu_l$ decay with quark level transition, $b \to c\, l\, \nu$, can be written as [73]

$$
\mathcal{L}_{\text{eff}} \;=\; -\frac{G_F}{\sqrt{2}}\, V_{cb} \left\{ \bar{l}\, \gamma_\mu\, (1 - \gamma_5)\, \nu_l\, \bar{c}\, \gamma^\mu\, (1 - \gamma_5)\, b \right\} + \text{h.c.}\,, \tag{4.4}
$$

where G_F is the Fermi constant and V_{cb} is the Cabibbo-Kobayashi-Maskawa (CKM) Matrix element.

The transition form factors for $B_s \to D_s^{(*)}\, l\, \nu$ can be parametrised as [171]

$$\begin{aligned}
\langle D_s(p')|\bar{c}\,\gamma_\mu\, b|B_s(p)\rangle &= F_+(q^2)\left[(p+p')_\mu - \frac{m^2_{B_s}-m^2_{D_s}}{q^2}\,q_\mu\right] + F_0(q^2)\,\frac{m^2_{B_s}-m^2_{D_s}}{q^2}\,q_\mu\,,\\
\langle D_s^*(p',\epsilon^*)|\bar{c}\,\gamma_\mu\, b|B_s(p)\rangle &= \frac{2\,i\,V(q^2)}{m_{B_s}+m_{D_s^*}}\,\varepsilon_{\mu\nu\rho\sigma}\,\epsilon^{*\nu}\,p'^{\rho}\,p^{\sigma}\,,\\
\langle D_s^*(p',\epsilon^*)|\bar{c}\,\gamma_\mu\,\gamma_5\, b|B_s(p)\rangle &= 2\,m_{D_s^*}\,A_0(q^2)\,\frac{\epsilon^*.q}{q^2}\,q_\mu \;+\; (m_{B_s}+m_{D_s^*})\,A_1(q^2)\left[\epsilon^*_\mu \;-\; \frac{\epsilon^*.q}{q^2}\,q_\mu\right]\\
&\quad - A_2(q^2)\,\frac{\epsilon^*.q}{(m_{B_s}\,+\,m_{D_s})}\Big[(p+p')_\mu \;-\; \frac{m^2_{B_s}\,-\,m^2_{D_s}}{q^2}\,q_\mu\Big]\,, \qquad (4.5)
\end{aligned}$$

where $q = p - p'$ is the momentum transfer. Using Lorentz invariance and parity, one can show for the $B_s \to D_s$ matrix element, the axial vector current vanishes, whereas for the $B_s \to D_s^*$ matrix element the scalar current vanishes. Again, using the equation of motion, the scalar and pseudoscalar matrix elements are given by,

$$\begin{aligned}
\langle D_s(p')|\bar{c}\,b|B_s(p)\rangle &= \frac{m^2_{B_s}-m^2_{D_s}}{m_b(\mu)-m_c(\mu)}\,F_0(q^2)\,,\\
\langle D_s^*(p',\epsilon^*)|\bar{c}\,\gamma_5\, b|B_s(p)\rangle &= -\,\frac{2\,m_{D_s}\,A_0(q^2)}{m_b(\mu)+m_c(\mu)}\epsilon^*.q\;. \qquad (4.6)
\end{aligned}$$

We follow Ref. [172] for the $B_s \to (D_s, D_s^*)$ form factors in which the form factors are evaluated in the framework of relativistic quark model based on the quasipotential approach. Using the Isgur-Wise functions of the model in these relations, the form factors can be approximated with certainty by the following expressions.

(a) $\quad F_+(q^2),\, V(q^2),\, A_0(q^2) = F(q^2)\,,$

$$F(q^2) = \frac{F(0)}{\left(1-\frac{q^2}{M^2}\right)\left(1-\sigma_1\,\frac{q^2}{{M_{B_c^*}}^2}+\sigma_2\,\frac{q^4}{{M_{B_c^*}}^4}\right)}\,. \qquad (4.7)$$

(b) $\quad F_0(q^2),\, A_1(q^2),\, A_2(q^2) = F(q^2)\,,$

$$F(q^2) = \frac{F(0)}{\left(1-\sigma_1\,\frac{q^2}{{M_{B_c^*}}^2}+\sigma_2\,\frac{q^4}{{M_{B_c^*}}^4}\right)}\,. \qquad (4.8)$$

where $M = M_{B_c^*} = 6.332\,\mathrm{GeV}$, for form factors $F_+(q^2)$, $V(q^2)$ and $M = M_{B_c} = 6.272\,\mathrm{GeV}$, for the form factor $A_0(q^2)$. We use the input values with their uncertainty error-bar for $F_+(0)$, $F_0(0)$ and $A_0(0)$, $A_1(0)$, $A_2(0)$ at maximum recoil point $q^2 = 0$ reported in Ref. [172] and we consider ten percent of error for the uncertainties associated with $\sigma_{1,2}$ in our analysis. The values of $F(0)$ and $\sigma_{1,2}$ are given in Table 4.1.

We use the helicity methods of Ref. [63, 64] for the $B_s \to D_s\, l\, \nu$ and $B_s \to D_s^*\, l\, \nu$ semileptonic decays and we refer to our earlier work [160] for the details of helicity amplitudes calculation.

The differential decay rate for $B_s \to D_s\, l\, \nu$ is:

$$\frac{d\Gamma^{D_s}}{dq^2} \;=\; \frac{8\,N\,|\overrightarrow{p}_{D_s}|}{3}\left\{ H_0^2\left(1+\frac{m_l^2}{2\,q^2}\right)+\frac{3\,m_l^2}{2\,q^2}\,H_t^2\right\}. \tag{4.9}$$

where

$$\begin{aligned}
&|\overrightarrow{p}_{D_s^{(*)}}| = \sqrt{\lambda(m_{B_s}^2,\, m_{D_s^{(*)}}^2,\, q^2)}/2\,m_{B_s},\\
&\lambda(a,\,b,\,c) = a^2+b^2+c^2-2\,(a\,b+b\,c+c\,a),\\
&N = \frac{G_F^2\,|V_{cb}|^2\,q^2}{256\,\pi^3\,m_{B_s}^2}\left(1-\frac{m_l^2}{q^2}\right)^2,\\
&H_0 = \frac{2\,m_{B_s}\,|\overrightarrow{p}_{D_s}|}{\sqrt{q^2}}\,F_+(q^2),\\
&H_t = \frac{m_{B_s}^2-m_{D_s}^2}{\sqrt{q^2}}\,F_0(q^2).
\end{aligned} \tag{4.10}$$

Here we note that the term containing m_l^2/q^2 is negligible for $l = e,\,\mu$, which is not true for $l=\tau$ case, as it has a quite large mass.

Similarly the differential decay rate of $B_s \to D_s^*\, l\, \nu$ is:

$$\frac{d\Gamma^{D_s^*}}{dq^2} \;=\; \frac{8\,N\,|\overrightarrow{p}_{D_s^*}|}{3}\left\{\mathcal{A}_{AV}^2+\frac{m_l^2}{2\,q^2}\Big[\mathcal{A}_{AV}^2+3\mathcal{A}_t^2\Big]\right\} \tag{4.11}$$

where

$$\begin{aligned}
&\mathcal{A}_{AV}^2 = \mathcal{A}_0^2+\mathcal{A}_\parallel^2+\mathcal{A}_\perp^2\,, \qquad\qquad \mathcal{A}_t = \frac{2m_{B_s}|\vec{p}_{D_s^*}|A_0(q^2)}{\sqrt{q^2}}\,,\\
&\mathcal{A}_0 = \frac{1}{2\,m_{D_s^*}\sqrt{q^2}}\Big[\Big(m_{B_s}^2-m_{D_s^*}^2-q^2\Big)(m_{B_s}+m_{D_s^*})A_1(q^2)\;-\;\frac{4m_{B_s}^2|\vec{p}_{D_s^*}|^2}{m_{B_s}+m_{D_s^*}}A_2(q^2)\Big]\,,\\
&\mathcal{A}_\parallel = \frac{2(m_{B_s}+m_{D_s^*})A_1(q^2)}{\sqrt{2}}\,, \qquad\qquad \mathcal{A}_\perp = -\frac{4m_{B_s}V(q^2)|\vec{p}_{D_s^*}|}{\sqrt{2}(m_{B_s}+m_{D_s^*})}\,.
\end{aligned} \tag{4.12}$$

We define some physical observables such as differential branching ratio DBR(q^2), the ratios of branching fractions $R(q^2)$, $R_{\tau,l}(q^2)$ and the forward-backward asymmetry $A_{FB}(q^2)$ as following.

$$\begin{aligned}
&DBR(q^2) = \Big(\frac{d\Gamma}{dq^2}\Big)/\Gamma_{tot}\,,\\
&R(q^2) = \frac{DBR(q^2)\Big(B_s\to D_s(D_s^*)\,\tau\,\nu\Big)}{DBR(q^2)\Big(B_s\to D_s(D_s^*)\,l\,\nu\Big)}\,,\\
&R_{\tau,l}(q^2) = \frac{DBR(q^2)\Big(B_s\to D_s\,\tau(l)\,\nu\Big)}{DBR(q^2)\Big(B_s\to D_s^*\,\tau(l)\,\nu\Big)},\\
&[A_{FB}]_{(D_s,\,D_s^*)}(q^2) = \frac{\Big(\int_{-1}^0-\int_0^1\Big)d\cos\theta_l\,\frac{d\Gamma^{(D_s,\,D_s^*)}}{dq^2\,d\cos\theta_l}}{\frac{d\Gamma^{(D_s,\,D_s^*)}}{dq^2}}\,.
\end{aligned} \tag{4.13}$$

The forward backward asymmetries for $B_s \to D_s\, l\, \nu$ and $B_s \to D_s^*\, l\, \nu$ decay modes are

$$\begin{aligned} A_{FB}^{D_s}(q^2) &= \frac{3\, m_l^2}{2\, q^2} \frac{H_0\, H_t}{H_0^2 \left(1 + \frac{m_l^2}{2\, q^2}\right) + \frac{3\, m_l^2}{2\, q^2}\, H_t^2}\,, \\ A_{FB}^{D_s^*}(q^2) &= \frac{3}{2} \frac{\mathcal{A}_\parallel\, \mathcal{A}_\perp + \frac{m_l^2}{q^2} \mathcal{A}_0\, \mathcal{A}_t}{\left\{ (\mathcal{A}_0^2 + \mathcal{A}_\parallel^2 + \mathcal{A}_\perp^2)\Big(1 + \frac{m_l^2}{2\, q^2}\Big) + \frac{3\, m_l^2}{2\, q^2}\, \mathcal{A}_t^2 \right\}}\,. \end{aligned} \tag{4.14}$$

In this chapter we calculate the branching ratios of $B_s \to D_s\, l\, \nu_l$ and $B_s \to D_s^*\, l\, \nu_l$ decays within the SM and also we find the numerical values of the ratios R_{D_s, D_s^*}, $R_{\tau,l}$. We present an analysis of physical observables such as differential branching ratio, ratio of differential branching ratio and forward-backward asymmetry.

CKM elements:				
$\lvert V_{cb}\rvert$ (Average)	$(40.9 \pm 1.1) \times 10^{-3}$ [26]			
Inputs for $(B_s \to D_s)$ Form Factors: [172]				
	F_+		F_0	
$F(0)$	0.74 ± 0.02		0.74 ± 0.02	
σ_1	0.20 ± 0.02		0.430 ± 0.043	
σ_2	-0.461 ± 0.0461		-0.464 ± 0.0464	
Inputs for $(B_s \to D_s^*)$ Form Factors: [172]				
	V	A_0	A_1	A_2
$F(0)$	0.95 ± 0.02	0.67 ± 0.01	0.70 ± 0.01	0.75 ± 0.02
σ_1	0.372 ± 0.0372	0.350 ± 0.035	0.463 ± 0.0463	1.04 ± 0.104
σ_2	$-0.561 \pm .0561$	-0.60 ± 0.06	-0.510 ± 0.051	-0.07 ± 0.007

Table 4.1: Theory Input parameters

	Central value	1σ range
$\mathcal{B}(B_s \to D_s\, \tau\, \nu)$	0.695×10^{-2}	$(0.62,\ 0.78) \times 10^{-2}$
$\mathcal{B}(B_s \to D_s^*\, \tau\, \nu)$	1.42×10^{-2}	$(1.28,\ 1.58) \times 10^{-2}$
$\mathcal{B}(B_s \to D_s\, l\, \nu)$	2.54×10^{-2}	$(2.27,\ 2.82) \times 10^{-2}$
$\mathcal{B}(B_s \to D_s^*\, l\, \nu)$	5.92×10^{-2}	$(5.27,\ 6.60) \times 10^{-2}$
R_{D_s}	0.274	(0.255, 0.294)
$R_{D_s^*}$	0.240	(0.236, 0.245)
R_τ	0.487	(0.438, 0.542)
R_l	0.428	(0.384, 0.480)

Table 4.2: Branching ratio and ratio of branching ratios within the SM.

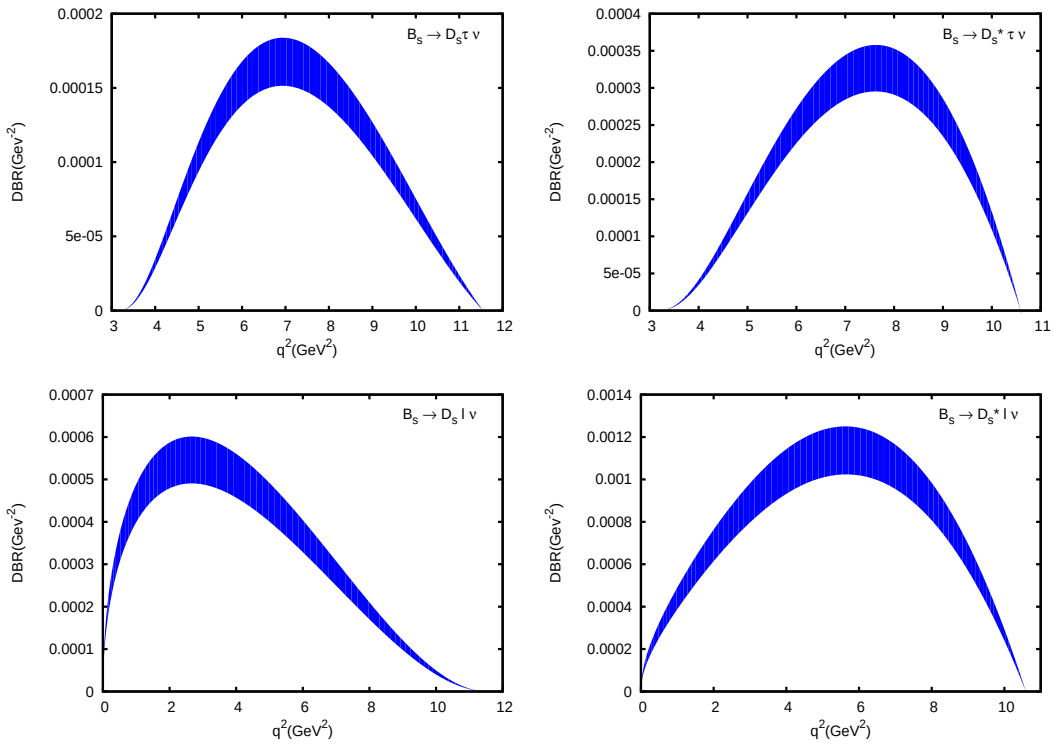

Figure 4.1: The figure show the differential branching ratio (DBR) for the $B_s \to D_s^{(*)}\,\tau(l)\,\nu$

4.3 Results and discussion

We use the following input parameters for our numerical analysis from the Ref. [26].

$$\begin{aligned} m_{B_s} &= 5.36677\,\text{GeV}\,, & m_{D_s^+} &= 1.9685\,\text{GeV} \\ m_{D_s^{*+}} &= 2.1123\,\text{GeV} & m_b(m_b) &= 4.18\,\text{GeV}\,, \\ m_c(m_b) &= 0.91\,\text{GeV}\,, & \tau_{B_s} &= 1.516 \times 10^{-12}\,\text{Sec}\,. \end{aligned} \tag{4.15}$$

The theoretical uncertainties in the calculation of the decay branching fractions come from various input parameters. In our analysis we do not consider the uncertainties due to quark masses, meson masses, and life time of the mesons, rather we take into account all hadronic uncertainties such as CKM matrix element and form factors, since these are not well-known quantities. We allow these hadronic input parameters to vary within their error bars and calculate the branching fraction, ratios of branching ratio $R_{D_s^{(*)}}$, $R_{\tau,l}$ and analyse the differential branching ratio (DBR) and forward-backward asymmetry A_{FB}. The numerical values of the input parameters such as the form factors and CKM matrix elements are given in Table 4.1. The SM prediction for the central values branching ratios and ratios of branching ratios and their 1 σ range values are reported in Table 4.2.

The SM prediction of the differential branching ratios for $B_s \to D_s\,\tau(l)\,\nu$ and $B_s \to D_s^*\,\tau(l)\,\nu$ are shown in the figure 4.1. We see that the dependence of differential branching ratios for all of the decays except for $B_s \to D_s\,l\,\nu$ decay on the hadronic uncertainties of the input parameters is more significant in mid-q^2 region than in the lower and higher q^2 region. In the SM, the DBR

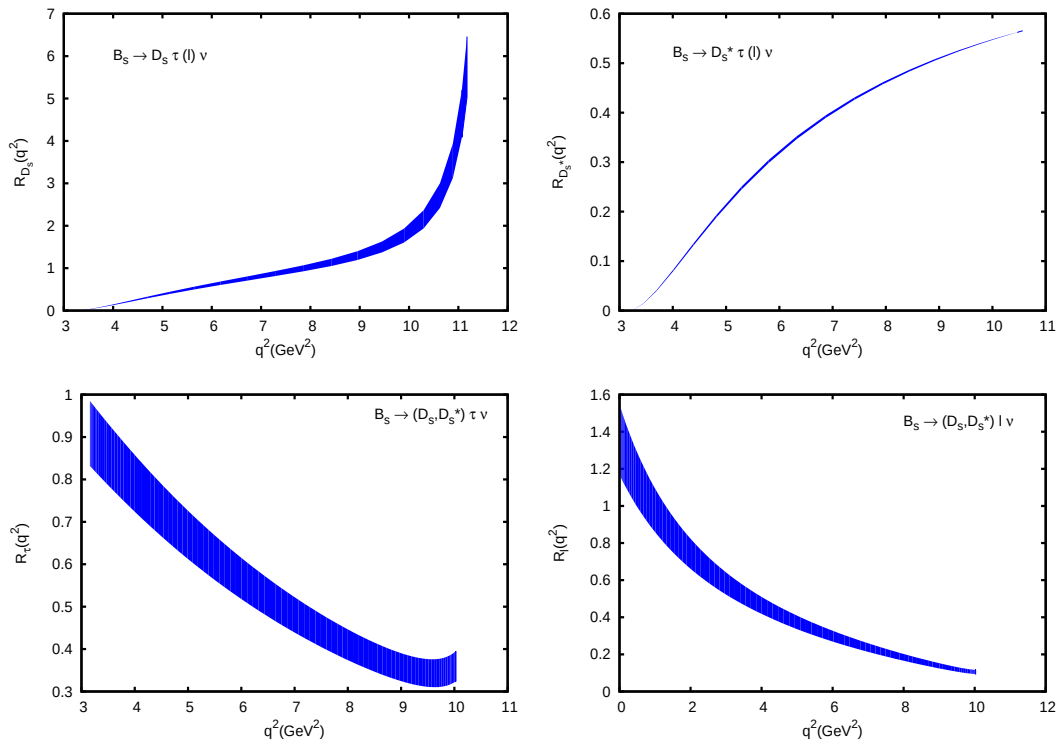

Figure 4.2: The figure show the ratio of branching ratio R_{D_s}, $R_{D_s^*}$, R_τ and R_l for the $B_s \to D_s^{(*)} \tau(l) \nu$

for the $B_s \to D_s \tau \nu$ decay peaks at $q^2 \approx 7$ GeV^2 and the value of the corresponding DBR is 1.84×10^{-4} GeV^{-2}. Similarly for the $B_s \to D_s^* \tau \nu$, we find, the peak is shifted to a higher q^2 region with respect to the peak of $B_s \to D_s \tau \nu$, which is obvious, because the threshold of $B_s \to D_s^*$ is greater than the threshold of $B_s \to D_s$. For $B_s \to D_s^* \tau \nu$ decay, the DBR peaks at $q^2 \approx 7.8$ GeV^2 and the value of DBR is 3.58×10^{-4} GeV^{-2}. In $B_s \to D_s l \nu$ decay the peak is observed in the low q^2 region as the threshold energy of this decay is comparatively smaller, and the DBR distribution peaks at $q^2 \approx 2.6$ Gev^2 with the value of differential branching ratio being 6.0×10^{-4} GeV^{-2}. For $B_s \to D_s^* l \nu$ the DBR peaks at $q^2 \approx 5.6$ GeV^2 and the value of DBR is 1.25×10^{-3} GeV^{-2}.

The ratios of the branching fractions R_{D_s, D_s^*} and $R_{\tau,l}$ defined in the Eq. 4.13 within the SM for $B_s \to D_s \tau(l) \nu$ and $B_s \to D_s^* \tau(l) \nu$ decays are shown in the Figure 4.2. It is clear from the plot that the dependence of $R(q^2)$ on the uncertainties is smaller than the differential branching ratio, since it is a ratio, and therefore the hadronic uncertainties get cancelled for R_{D_s} and $R_{D_s^*}$ while R_τ and R_l will have hadronic uncertainties in the form of form factors of $B_s \to D_s$ and $B_s \to D_s^*$ transitions. For $B_s \to D_s l \nu$ we can see the value of $R_{D_s}(q^2)$ increases slowly up to certain value of $q^2 (\approx 9.5 \text{GeV}^2)$, then suddenly, the increase rate is very rapid, and this is because of low value of differential branching ratio of $B_s \to D_s l \nu$ in high q^2 region. The uncertainty in $R_{D_s^*}(q^2)$ plot for the $B_s \to D_s^* \tau(l) \nu$ is comparatively smaller than for the other. Here, also, we can see the value of $R_{D_s^*}(q^2)$ increase with q^2 according to the differential branching ratio for the corresponding decay modes. In the plot of R_τ we can see the dependency on the uncertainties while for R_l, the dependency is comparatively smaller, which can be explained from the Eq. 4.9 and Eq. 4.11 as the

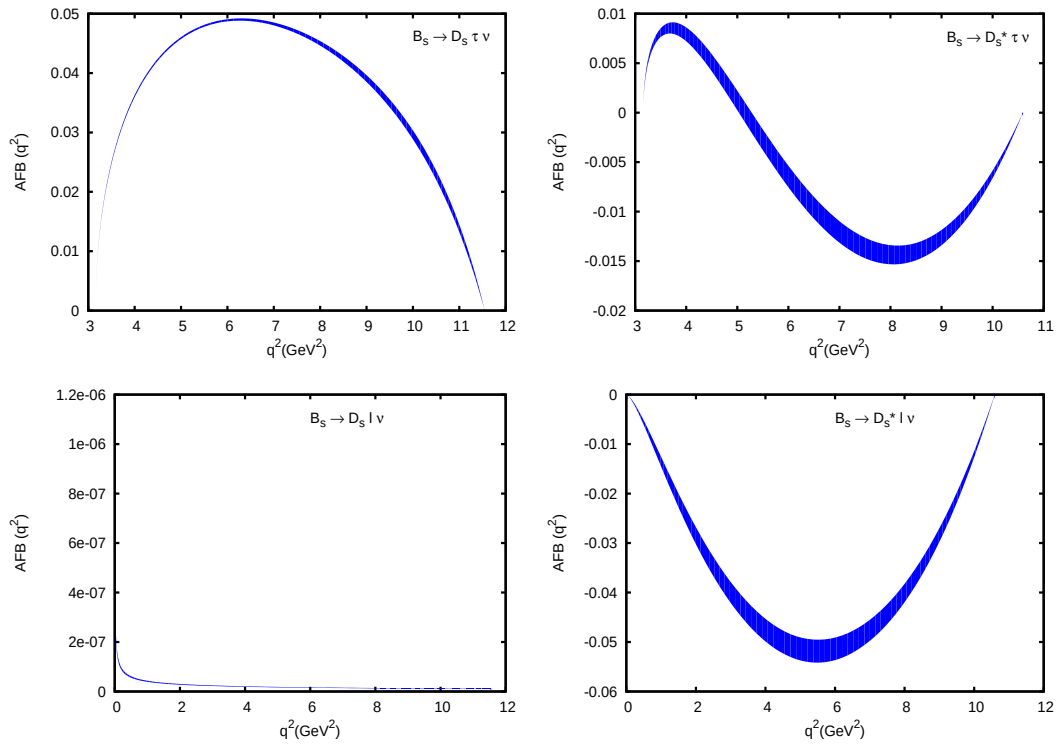

Figure 4.3: The figure show the forward-backward asymmetry (AFB) for the $B_s \to D_s^{(*)} \tau(l)\, \nu$

mass of $l\,(e^-, \mu^-)$ is negligible in comparison to mass of τ lepton.

The SM prediction of the forward-backward asymmetries (AFB) for $B_s \to D_s\, \tau(l)\, \nu$ and $B_s \to D_s^*\, \tau(l)\, \nu$ are shown in the Fig 4.3. The asymmetry for $B_s \to D_s\, l\, \nu$ decay is vanishingly small, as expected, because of small mass of the lepton and any nonzero value of AFB may imply NP in first and second generation of leptons. AFB for $B_s \to D_s^*\, l\, \nu$ is significant, as we can see from the Eq. 4.14. There is a significant asymmetry for $B_s \to D_s\, \tau\, \nu$ decay because of large mass of τ but there is no zero crossing, while, in $B_s \to D_s^*\, \tau\, \nu$ decay, we can find the zero crossing at $q^2 \approx 5.2$ GeV^2.

4.4 Conclusion

In this chapter, we have worked out on the problem of the semileptonic decays $B_s \to D_s\, \tau(l)\, \nu$ and $B_s \to D_s^*\, \tau(l)\, \nu$. Although we did not provide an in-depth analysis of the calculation of form factors, we calculated the branching ratios of the decay modes and the ratios of branching ratio and also studied the differential branching ratios and forward-backward asymmetries. The estimated values are:

$$
\begin{aligned}
&Br(B_s \to D_s\, \tau\, \nu) = \left(6.95^{+0.85}_{-0.75}\right) \times 10^{-3}\,, && Br(B_s \to D_s^*\, \tau\, \nu) = \left(1.42^{+0.16}_{-0.14}\right) \times 10^{-2}\,,\\
&Br(B_s \to D_s\, l\, \nu) = \left(2.54^{+0.28}_{-0.27}\right) \times 10^{-2}\,, && Br(B_s \to D_s^*\, l\, \nu) = \left(5.92^{+0.68}_{-0.65}\right) \times 10^{-2}\,,\\
&R_{D_s} = 0.274^{+0.02}_{-0.019}\,, && R_{D_s^*} = 0.240^{+0.05}_{-0.04}\,, && R_\tau = 0.487^{+0.055}_{-0.045}\,,\\
&R_l = 0.428^{+0.052}_{-0.044}\,. && && (4.16)
\end{aligned}
$$

The branching ratios and the ratios of branching ratio could be measurable in the future Super-B experiments and if the experimental values are not consistent with the SM predictions, then, they are pointing towards NP and one can do an analysis similar to that in the Ref. [160]. One can take the effective Lagrangian in presence of NP couplings and can constrain NP parameter space, once the measurment of various branching ratios and ratios of branching ratios becomes available. Simultaneously, the reduced uncertainty in the various form factor also could sharpen the estimates of branching ratios and ratio of branching ratios and also NP parameter space. Moreover, we would like emphasize on this point that according to our current status of both theoritical and experimental knowledge, NP affects only the third generation of leptons but if NP is present in the first and second generation leptons then one can identify it by measuring the forward-backward asymmetry for the $B_s \to D_s\, l\, \nu$ and $B_s \to D_s^*\, l\, \nu$ decay modes.

Chapter 5

Conclusion

We now summarize and point out the main results of our work in this chapter. We have studied some phenomenological aspects of B decays, including the New Physics in the form of an effective theory and attempted to understand in one such case the multi-particle states with baryon-anti-baryon in the final state. In doing so we have considered few $b \to c$, $b \to u$ and $b \to s$ semi-leptonic and leptonic transitions.

In the Chapter-1 we started with the motivation and a brief introduction to Particle Physics and the Standard Model. Thereafter, we have provided the tools required to undertake the studies done in this thesis. In doing so, we have discussed about the mixing matrix known as CKM matrix and used Wolenstein parametrization. The significance of discrete symmetries such as charge-parity (CP), charge-parity-time (CPT) and flavour changing neutral currents (FCNCs) have been discussed. In the basic formalism we discussed the basic formalism of B meson decays, neutral meson mixing, CP violations in B meson systems etc. Since the form of New Physics, if any, is not clear as of now and therefore we have employed the generic structure of effective theory approach in B decays to see its effect which in principle can provide the guidelines for the model builders.

In the Chapter-2, we have presented an effective theory approach to New Physics in $b \to u$ and $b \to c$ leptonic and semileptonic decays. The recent BaBar [34] measurement of the ratio of branching fractions of $B \to (D,\, D^*)\, \tau\, \nu$ to the corresponding $B \to (D,\, D^*)\, l\nu$ is found to have 3.4σ discrepancy with the SM expectation, which motivated to obtain the information about the nature of New Physics. In this chapter, we have used the most general effective Lagrangian for the $b \to q$, where $q = u$, or c, semi-(leptonic) transition decays in presence of various NP couplings such as V_L, V_R, S_L, S_R and right-handed neutrino couplings ($\widetilde{V}_L$, $\widetilde{V}_R$, $\widetilde{S}_L$, $\widetilde{S}_R$) and have done a combined analysis of $b \to u$ and $b \to c$ semi-(leptonic) decay processes. We have constrained the NP parameter space using the recent data of R^l_π, R_D and R_{D^*}. We have assumed that the NP affects only the third generation of leptons and the NP couplings are real. We have illustrated four different scenarios of the New Physics in which we have shown the allowed parameter space for all NP couplings. The effects of each NP coupling on various observables such as the differential branching ratios, forward-backward asymmetries, ratios of branching ratio are also shown. We have predicted the branching ratio of $B_c \to \tau\nu$ and $B \to \pi\tau\nu$ decay processes in all four different scenarios. We have

also estimated the numerical value of ratio of branching ratio R_π of $B \to \pi\tau\nu$ to the corresponding $B \to \pi\, l\, \nu$ decay mode for all the scenarios in our anaysis.

Due to the large mass of B meson, it can decay to final states containing a baryon-antibaryon pair. The mesonic B decays are more extensively studied in the literature than the baryonic B decays. Moreover, B decays allow us to study the FCNC decay processes. In the Chapter-3, we have studied the exclusive baryonic decay mode of B meson, particularly $B^- \to \Lambda\bar{p}\,\mu^+\,\mu^-$ decay mode, mediated via the $b \to s\, l\, \bar{l}$ transition, to test the nature of the FCNCs. There are several indications of NP in B decays mediated via the $b \to s\, l\, \bar{l}$ transitions which are mentioned in the Introduction section of Chapter-3. In this context, we have taken the most general effective Hamiltonian in the presence of NP and we have showed the effect of each NP coupling on various observables in a model independent way. We have predicted the branching ratio of $B^- \to \Lambda\bar{p}\,\mu^+\,\mu^-$ decay mode and have obtained asymmetries in angular distributions and triple product correlations in the SM and in the presence of NP. Within the SM, we found that the branching ratio of $B^- \to \Lambda\bar{p}\,\mu^+\mu^-$ decay mode to be 1.08×10^{-7} and the deviation from the SM prediction is quite significant if we include the NP in C_S, C_P, C'_S, and C'_P simultaneously.

In the Chapter-4, we have studied the semileptonic decays $B_s \to D_s^{(*)}\, l\, \nu$ within the SM. We have defined observables such as R_{D_s}, $R_{D_s^*}$, and also we have introduced new observable R_τ, R_l. Afterwards, we have estimated the numerical values of branching ratios and ratios of branching ratios which could be measurable in the up-coming Super-B experiments. We have also studied the differential branching ratio and forward-backward asymmetry and their implications.

In conclusion, we have studied some B meson decays in light of the puzzle $R(D)$ and $R(D^*)$, provided by the BaBar data, and attempted to find which are the New Physics operators (from effective theory point of view) which could be responsible for such discrepancy. Later on we have tried to understand the baryon-anti-baryon states in the multi-particle B decays. The intention is to look for the New Physics effects, if any, from an effective theory point of view, as might have been revealing in their meson counterparts. Finally, we have also studied B_s semileptonic decays and introduced some new observables which can be measured in the ongoing or upcoming experiments. Therefore, in this thesis we have tried to visualize the effect of New Physics from a model independent point of view in case of some B meson decays and CP asymmetry parameters with a hope that these findings will help the model builders and enrich our understanding of the flavour sector of the Standard Model.

References

[1] P. W. Higgs, "Broken Symmetries and the Masses of Gauge Bosons," Phys. Rev. Lett. **13**, 508 (1964).

[2] F. Englert and R. Brout, "Broken Symmetry and the Mass of Gauge Vector Mesons," Phys. Rev. Lett. **13**, 321 (1964).

[3] Y. Nir, "CP violation in meson decays," hep-ph/0510413.

[4] M. Kobayashi and T. Maskawa, "CP Violation in the Renormalizable Theory of Weak Interaction," Prog. Theor. Phys. **49**, 652 (1973).

[5] N. Cabibbo, Unitary symmetry and leptonic decays, Phys. Rev. Lett. 10 (1963), no. 12, 531533.

[6] L. -L. Chau and W. -Y. Keung, "Comments on the Parametrization of the Kobayashi-Maskawa Matrix," Phys. Rev. Lett. **53**, 1802 (1984).

[7] L. Wolfenstein, "Parametrization of the Kobayashi-Maskawa Matrix," Phys. Rev. Lett. **51**, 1945 (1983).

[8] A. J. Buras, M. E. Lautenbacher and G. Ostermaier, "Waiting for the top quark mass, $K^+ \to \pi^+ \nu\bar{\nu}$, B_s^0 - $\bar{B}_s^0$ mixing and CP asymmetries in B decays," Phys. Rev. D **50**, 3433 (1994) [hep-ph/9403384].

[9] C. Jarlskog, "Commutator of the Quark Mass Matrices in the Standard Electroweak Model and a Measure of Maximal CP Violation," Phys. Rev. Lett. **55**, 1039 (1985).

[10] R. Aleksan, B. Kayser and D. London, "Determining the quark mixing matrix from CP violating asymmetries," Phys. Rev. Lett. **73**, 18 (1994) [hep-ph/9403341].

[11] C. Jarlskog and R. Stora, "Unitarity Polygons and CP Violation Areas and Phases in the Standard Electroweak Model," Phys. Lett. B **208**, 268 (1988).

[12] E. Noether, "Invariant Variation Problems," Gott. Nachr. **1918**, 235 (1918) [Transp. Theory Statist. Phys. **1**, 186 (1971)] [physics/0503066].

[13] J. H. Christenson, J. W. Cronin, V. L. Fitch and R. Turlay, "Evidence for the 2 pi Decay of the k(2)0 Meson," Phys. Rev. Lett. **13**, 138 (1964).

[14] B. Aubert *et al.* [BaBar Collaboration], "Observation of CP violation in the B^0 meson system," Phys. Rev. Lett. **87**, 091801 (2001) [hep-ex/0107013].

[15] K. Abe *et al.* [Belle Collaboration], "Observation of large CP violation in the neutral B meson system," Phys. Rev. Lett. **87**, 091802 (2001) [hep-ex/0107061].

[16] J. Charles *et al.* [CKMfitter Group Collaboration], "CP violation and the CKM matrix: Assessing the impact of the asymmetric B factories," Eur. Phys. J. C **41**, 1 (2005) [hep-ph/0406184].

[17] M. Bona *et al.* [UTfit Collaboration], "Model-independent constraints on Δ F=2 operators and the scale of new physics," JHEP **0803**, 049 (2008) [arXiv:0707.0636 [hep-ph]].

[18] G. C. Branco, L. Lavoura and J. P. Silva, "CP Violation," Int. Ser. Monogr. Phys. **103**, 1 (1999).

[19] V. Weisskopf and E. Wigner, "Over the natural line width in the radiation of the harmonius oscillator," Z. Phys. **65**, 18 (1930).

[20] V. Weisskopf and E. P. Wigner, "Calculation of the natural brightness of spectral lines on the basis of Dirac's theory," Z. Phys. **63**, 54 (1930).

[21] S. Chatrchyan *et al.* [CMS Collaboration], "Observation of a new boson at a mass of 125 GeV with the CMS experiment at the LHC," Phys. Lett. B **716**, 30 (2012) [arXiv:1207.7235 [hep-ex]].

[22] G. Aad *et al.* [ATLAS Collaboration], "Observation of a new particle in the search for the Standard Model Higgs boson with the ATLAS detector at the LHC," Phys. Lett. B **716**, 1 (2012) [arXiv:1207.7214 [hep-ex]].

[23] G. Aad *et al.* [ATLAS Collaboration], "Combined search for the Standard Model Higgs boson in pp collisions at $\sqrt{s} = 7$ TeV with the ATLAS detector," Phys. Rev. D **86**, 032003 (2012) [arXiv:1207.0319 [hep-ex]].

[24] I. Adachi *et al.* [Belle Collaboration], "Measurement of $B^- \to \tau^- \bar{\nu}_\tau$ with a Hadronic Tagging Method Using the Full Data Sample of Belle," Phys. Rev. Lett. **110**, 131801 (2013) [arXiv:1208.4678 [hep-ex]].

[25] J. P. Lees *et al.* [BaBar Collaboration], "Evidence of $B^+ \to \tau^+ \nu$ decays with hadronic B tags," Phys. Rev. D **88**, no. 3, 031102 (2013) [arXiv:1207.0698 [hep-ex]].

[26] J. Beringer *et al.* (Particle Data Group), Phys. Rev. D **86**, 010001 (2012)

[27] J. Charles, O. Deschamps, S. Descotes-Genon, R. Itoh, H. Lacker, A. Menzel, S. Monteil and V. Niess *et al.*, "Predictions of selected flavour observables within the Standard Model," Phys. Rev. D **84**, 033005 (2011) [arXiv:1106.4041 [hep-ph]]

[28] J. Charles *et al.* [CKMfitter Group Collaboration], "CP violation and the CKM matrix: Assessing the impact of the asymmetric B factories," Eur. Phys. J. C **41**, 1 (2005) [hep-ph/0406184].

[29] M. Bona *et al.* [UTfit Collaboration], "An Improved Standard Model Prediction Of BR($B \to \tau\nu$) And Its Implications For New Physics," Phys. Lett. B **687**, 61 (2010) [arXiv:0908.3470 [hep-ph]].

[30] P. del Amo Sanchez *et al.* [BaBar Collaboration], "Study of $B \to \pi\ell\nu$ and $B \to \rho\ell\nu$ Decays and Determination of $|V_{ub}|$," Phys. Rev. D **83**, 032007 (2011) [arXiv:1005.3288 [hep-ex]].

[31] H. Ha *et al.* [BELLE Collaboration], "Measurement of the decay $B^0 \to \pi^- \ell^+ \nu$ and determination of $|V_{ub}|$," Phys. Rev. D **83**, 071101 (2011) [arXiv:1012.0090 [hep-ex]].

[32] D. Asner *et al.* [Heavy Flavor Averaging Group Collaboration], "Averages of b-hadron, c-hadron, and τ-lepton Properties," arXiv:1010.1589 [hep-ex].

[33] S. Fajfer, J. F. Kamenik, I. Nisandzic and J. Zupan, "Implications of Lepton Flavor Universality Violations in B Decays," Phys. Rev. Lett. **109**, 161801 (2012) [arXiv:1206.1872 [hep-ph]].

[34] J. P. Lees *et al.* [BaBar Collaboration], "Evidence for an excess of $\bar{B} \to D^{(*)} \tau^- \bar{\nu}_\tau$ decays," Phys. Rev. Lett. **109**, 101802 (2012) [arXiv:1205.5442 [hep-ex]].

[35] S. Fajfer, J. F. Kamenik and I. Nisandzic, "On the $B \to D * \tau \bar{\nu}_\tau$ Sensitivity to New Physics," Phys. Rev. D **85**, 094025 (2012) [arXiv:1203.2654 [hep-ph]].

[36] G. C. Branco, P. M. Ferreira, L. Lavoura, M. N. Rebelo, M. Sher and J. P. Silva, "Theory and phenomenology of two-Higgs-doublet models," Phys. Rept. **516**, 1 (2012) [arXiv:1106.0034 [hep-ph]].

[37] W. S. Hou, "Enhanced charged Higgs boson effects in $B^- \to \tau \bar{\nu}, \mu \bar{\nu}$ and $B \to \tau \bar{\nu} + X$," Phys. Rev. D **48**, 2342 (1993).

[38] A. G. Akeroyd and S. Recksiegel, "The Effect of $H^\pm$ on $B^\pm \to \tau^\pm \nu_\tau$ and $B^\pm \to \mu^\pm \nu_\mu$," J. Phys. G **29**, 2311 (2003) [hep-ph/0306037].

[39] M. Tanaka, "Charged Higgs effects on exclusive semitauonic B decays," Z. Phys. C **67**, 321 (1995) [hep-ph/9411405].

[40] U. Nierste, S. Trine and S. Westhoff, "Charged-Higgs effects in a new $B \to D\tau\nu$ differential decay distribution," Phys. Rev. D **78**, 015006 (2008) [arXiv:0801.4938 [hep-ph]].

[41] T. Miki, T. Miura and M. Tanaka, "Effects of charged Higgs boson and QCD corrections in $\bar{B} \to D\tau\bar{\nu}_\tau$," hep-ph/0210051.;

[42] A. Wahab El Kaffas, P. Osland and O. M. Ogreid, "Constraining the Two-Higgs-Doublet-Model parameter space," Phys. Rev. D **76**, 095001 (2007) [arXiv:0706.2997 [hep-ph]].;

[43] O. Deschamps, S. Descotes-Genon, S. Monteil, V. Niess, S. T'Jampens and V. Tisserand, "The Two Higgs Doublet of Type II facing flavour physics data," Phys. Rev. D **82**, 073012 (2010) [arXiv:0907.5135 [hep-ph]].;

[44] G. Blankenburg and G. Isidori, "$B \to \tau\nu$ in two-Higgs doublet models with MFV," Eur. Phys. J. Plus **127**, 85 (2012) [arXiv:1107.1216 [hep-ph]].;

[45] G. D'Ambrosio, G. F. Giudice, G. Isidori and A. Strumia, "Minimal flavor violation: An Effective field theory approach," Nucl. Phys. B **645**, 155 (2002) [hep-ph/0207036].;

[46] A. J. Buras, M. V. Carlucci, S. Gori and G. Isidori, "Higgs-mediated FCNCs: Natural Flavour Conservation vs. Minimal Flavour Violation," JHEP **1010**, 009 (2010) [arXiv:1005.5310 [hep-ph]].;

[47] A. Pich and P. Tuzon, "Yukawa Alignment in the Two-Higgs-Doublet Model," Phys. Rev. D **80**, 091702 (2009) [arXiv:0908.1554 [hep-ph]].;

[48] M. Jung, A. Pich and P. Tuzon, "Charged-Higgs phenomenology in the Aligned two-Higgs-doublet model," JHEP **1011**, 003 (2010) [arXiv:1006.0470 [hep-ph]].

[49] A. Crivellin, C. Greub and A. Kokulu, "Explaining $B \to D\tau\nu$, $B \to D^*\tau\nu$ and $B \to \tau\nu$ in a 2HDM of type III," Phys. Rev. D **86**, 054014 (2012) [arXiv:1206.2634 [hep-ph]].

[50] A. Datta, M. Duraisamy and D. Ghosh, "Diagnosing New Physics in $b \to c\,\tau\,\nu_\tau$ decays in the light of the recent BaBar result," Phys. Rev. D **86**, 034027 (2012) [arXiv:1206.3760 [hep-ph]].

[51] M. Duraisamy and A. Datta, "The Full $B \to D^*\tau^-\bar{\nu_\tau}$ Angular Distribution and CP violating Triple Products," arXiv:1302.7031 [hep-ph].

[52] P. Biancofiore, P. Colangelo and F. De Fazio, "On the anomalous enhancement observed in $B \to D^{(*)}\,\tau\,\bar{\nu}_\tau$ decays," Phys. Rev. D **87**, 074010 (2013) [arXiv:1302.1042 [hep-ph]].

[53] A. Crivellin, "Effects of right-handed charged currents on the determinations of $|V(ub)|$ and $|V(cb)|$," Phys. Rev. D **81**, 031301 (2010) [arXiv:0907.2461 [hep-ph]].

[54] A. Celis, M. Jung, X. -Q. Li and A. Pich, "Sensitivity to charged scalars in $B \to D^{(*)}\tau\nu_\tau$ and $B \to \tau\nu_\tau$ decays," JHEP **1301**, 054 (2013) [arXiv:1210.8443 [hep-ph]].

[55] X. -G. He and G. Valencia, "B decays with τ-leptons in non-universal left-right models," Phys. Rev. D **87**, 014014 (2013) [arXiv:1211.0348 [hep-ph]].

[56] T. Bhattacharya, V. Cirigliano, S. D. Cohen, A. Filipuzzi, M. Gonzalez-Alonso, M. L. Graesser, R. Gupta and H. -W. Lin, "Probing Novel Scalar and Tensor Interactions from (Ultra)Cold Neutrons to the LHC," Phys. Rev. D **85**, 054512 (2012) [arXiv:1110.6448 [hep-ph]].

[57] V. Cirigliano, J. Jenkins and M. Gonzalez-Alonso, "Semileptonic decays of light quarks beyond the Standard Model," Nucl. Phys. B **830**, 95 (2010) [arXiv:0908.1754 [hep-ph]].

[58] A. Khodjamirian, T. Mannel, N. Offen and Y. -M. Wang, "$B \to \pi\ell\nu_l$ Width and $|V_{ub}|$ from QCD Light-Cone Sum Rules," Phys. Rev. D **83**, 094031 (2011) [arXiv:1103.2655 [hep-ph]].

[59] A. F. Falk and M. Neubert, "Second order power corrections in the heavy quark effective theory. 1. Formalism and meson form-factors," Phys. Rev. D **47**, 2965 (1993) [hep-ph/9209268].;

[60] A. F. Falk and M. Neubert, "Second order power corrections in the heavy quark effective theory. 2. Baryon form-factors," Phys. Rev. D **47**, 2982 (1993) [hep-ph/9209269].

[61] I. Caprini, L. Lellouch and M. Neubert, "Dispersive bounds on the shape of $\bar{B} \to D^{(*)}l\bar{\nu}$ form-factors," Nucl. Phys. B **530**, 153 (1998) [hep-ph/9712417].

[62] Y. Sakaki and H. Tanaka, "Constraints of the Charged Scalar Effects Using the Forward-Backward Asymmetry on $B \to D^{(*)}\tau\bar{\nu_\tau}$," Phys. Rev. D **87**, 054002 (2013) [arXiv:1205.4908 [hep-ph]].

[63] J. G. Korner and G. A. Schuler, "Exclusive Semileptonic Heavy Meson Decays Including Lepton Mass Effects," Z. Phys. C **46**, 93 (1990).

[64] A. Kadeer, J. G. Korner and U. Moosbrugger, "Helicity analysis of semileptonic hyperon decays including lepton mass effects," Eur. Phys. J. C **59**, 27 (2009) [hep-ph/0511019].

[65] A. Khodjamirian, R. Ruckl, S. Weinzierl and O. I. Yakovlev, "Perturbative QCD correction to the $B \to \pi$ transition form-factor," Phys. Lett. B **410**, 275 (1997) [hep-ph/9706303].;

[66] E. Bagan, P. Ball and V. M. Braun, "Radiative corrections to the decay $B \to \pi e \nu$ and the heavy quark limit," Phys. Lett. B **417**, 154 (1998) [hep-ph/9709243].;

[67] P. Ball, "$B \to \pi$ and $B \to K$ transitions from QCD sum rules on the light cone," JHEP **9809**, 005 (1998) [hep-ph/9802394].;

[68] P. Ball and R. Zwicky, "New results on $B \to \pi$, K, η decay formfactors from light-cone sum rules," Phys. Rev. D **71**, 014015 (2005) [hep-ph/0406232].;

[69] G. Duplancic, A. Khodjamirian, T. .Mannel, B. Melic and N. Offen, "Light-cone sum rules for $B \to \pi$ form factors revisited," JHEP **0804**, 014 (2008) [arXiv:0801.1796 [hep-ph]].

[70] E. Dalgic, A. Gray, M. Wingate, C. T. H. Davies, G. P. Lepage and J. Shigemitsu, "B meson semileptonic form-factors from unquenched lattice QCD," Phys. Rev. D **73**, 074502 (2006) [Erratum-ibid. D **75**, 119906 (2007)] [hep-lat/0601021].;

[71] J. A. Bailey, C. Bernard, C. E. DeTar, M. Di Pierro, A. X. El-Khadra, R. T. Evans, E. D. Freeland and E. Gamiz *et al.*, "The $B \to \pi \ell \nu$ semileptonic form factor from three-flavor lattice QCD: A Model-independent determination of $|V_{ub}|$," Phys. Rev. D **79**, 054507 (2009) [arXiv:0811.3640 [hep-lat]].

[72] A. Al-Haydari *et al.* [QCDSF Collaboration], "Semileptonic form factors $D \to \pi$, K and $B \to \pi$, K from a fine lattice," Eur. Phys. J. A **43**, 107 (2010) [arXiv:0903.1664 [hep-lat]].

[73] G. Buchalla, A. J. Buras and M. E. Lautenbacher, "Weak decays beyond leading logarithms," Rev. Mod. Phys. **68**, 1125 (1996) [hep-ph/9512380].

[74] A. Bazavov *et al.* [Fermilab Lattice and MILC Collaborations], "B- and D-meson decay constants from three-flavor lattice QCD," Phys. Rev. D **85**, 114506 (2012) [arXiv:1112.3051 [hep-lat]].

[75] H. Na, C. J. Monahan, C. T. H. Davies, R. Horgan, G. P. Lepage and J. Shigemitsu, "The B and B_s Meson Decay Constants from Lattice QCD," Phys. Rev. D **86**, 034506 (2012) [arXiv:1202.4914 [hep-lat]].

[76] http://www.latticeaverages.org/

[77] D. Choudhury, D. K. Ghosh and A. Kundu, "B decay anomalies in an effective theory," Phys. Rev. D **86**, 114037 (2012) [arXiv:1210.5076 [hep-ph]].

[78] B. Aubert *et al.* [BaBar Collaboration], "Measurement of —V(cb)— and the Form-Factor Slope in $\bar{B} \to D l \bar{\nu}$ Decays in Events Tagged by a Fully Reconstructed B Meson," Phys. Rev. Lett. **104**, 011802 (2010) [arXiv:0904.4063 [hep-ex]].

[79] W. Dungel *et al.* [Belle Collaboration], "Measurement of the form factors of the decay $B^0 \to D^{*-}\ell^+\nu$ and determination of the CKM matrix element $|Vcb|$," Phys. Rev. D **82**, 112007 (2010) [arXiv:1010.5620 [hep-ex]].

[80] H. Albrecht *et al.* [ARGUS Collaboration], "Observation of the Charmless B Meson Decays," Phys. Lett. B **209**, 119 (1988).

[81] C. Bebek *et al.* [CLEO Collaboration], "Search for the Charmless Decays $B \to p\bar{p}\pi$ and $p\bar{p}\pi\pi$," Phys. Rev. Lett. **62**, 8 (1989).

[82] X. Fu *et al.* [CLEO Collaboration], "Observation of exclusive B decays to final states containing a charmed baryon," Phys. Rev. Lett. **79**, 3125 (1997).

[83] B. Aubert *et al.* [BaBar Collaboration], "The BaBar detector," Nucl. Instrum. Meth. A **479**, 1 (2002) [hep-ex/0105044].

[84] A. Abashian, K. Gotow, N. Morgan, L. Piilonen, S. Schrenk, K. Abe, I. Adachi and J. P. Alexander *et al.*, "The Belle Detector," Nucl. Instrum. Meth. A **479**, 117 (2002).

[85] M. Gronau and J. L. Rosner, "Charmless B Decays Involving Baryons," Phys. Rev. D **37**, 688 (1988).

[86] G. Eilam, M. Gronau and J. L. Rosner, "CP Asymmetries in Charmless Baryonic Decays of Charged B Mesons," Phys. Rev. D **39**, 819 (1989).

[87] S. M. Sheikholeslami and M. P. Khanna, "B meson weak decays into baryon anti-baryon pairs in $SU(3)$," Phys. Rev. D **44**, 770 (1991).

[88] S. M. Sheikholeslami, G. K. Sidana and M. P. Khanna, "$SU(3)$ predictions for B meson nonleptonic weak decays into (3/2)+ baryon (3/2)+ anti-baryon pairs," Int. J. Mod. Phys. A **7**, 1111 (1992).

[89] N. G. Deshpande, J. Trampetic and A. Soni, "Remarks on B Decays Into Baryonic Modes and Possible Implications for $V_(ub)$)," Mod. Phys. Lett. **3A**, 749 (1988).

[90] M. Jarfi, O. Lazrak, A. Le Yaouanc, L. Oliver, O. Pene and J. C. Raynal, "Decays of B mesons into baryon - anti-baryon," Phys. Rev. D **43**, 1599 (1991).

[91] P. Ball and H. G. Dosch, "Branching ratios of exclusive decays of bottom mesons into baryon - anti-baryon pairs," Z. Phys. C **51**, 445 (1991).

[92] V. L. Chernyak and I. R. Zhitnitsky, "B meson exclusive decays into baryons," Nucl. Phys. B **345**, 137 (1990).

[93] G. Kaur and M. P. Khanna, "B meson decays to baryon anti-baryon pairs," Phys. Rev. D **46**, 466 (1992).

[94] H. -Y. Cheng and K. -C. Yang, "Charmless exclusive baryonic B decays," Phys. Rev. D **66**, 014020 (2002) [hep-ph/0112245].

[95] M. Z. Wang *et al.* [Belle Collaboration], "Observation of $B^0 \to p\bar{\Lambda}\pi^-$," Phys. Rev. Lett. **90**, 201802 (2003) [hep-ex/0302024].

[96] M. Z. Wang *et al.* [Belle Collaboration], "Observation of $B^+ \to p\bar{p}\pi^+$, $B^0 \to p\bar{p}K^0$, and $B^+ \to p\bar{p}K^{*+}$," Phys. Rev. Lett. **92**, 131801 (2004) [hep-ex/0310018].

[97] M. -Z. Wang *et al.* [Belle Collaboration], "Study of the baryon-antibaryon low-mass enhancements in charmless three-body baryonic B decays," Phys. Lett. B **617**, 141 (2005) [hep-ex/0503047].

[98] Y. -J. Lee *et al.* [Belle Collaboration], "Observation of $B^+ \to p\bar{\Lambda}\gamma$," Phys. Rev. Lett. **95**, 061802 (2005) [hep-ex/0503046].

[99] Y. -J. Lee *et al.* [BELLE Collaboration], "Observation of $B^+ \to \Lambda\bar{\Lambda}K^+$," Phys. Rev. Lett. **93**, 211801 (2004) [hep-ex/0406068].

[100] B. Aubert *et al.* [BaBar Collaboration], "Measurement of the $B^+ \to p\bar{p}K^+$ branching fraction and study of the decay dynamics," Phys. Rev. D **72**, 051101 (2005) [hep-ex/0507012].

[101] M. -Z. Wang *et al.* [Belle Collaboration], "Study of $B^+ \to p\bar{\Lambda}\gamma$, $p\bar{\Lambda}\pi^0$ and $B^0 \to p\bar{\Lambda}\pi^-$," Phys. Rev. D **76**, 052004 (2007) [arXiv:0704.2672 [hep-ex]].

[102] J. T. Wei *et al.* [BELLE Collaboration], "Study of $B^+ \to p\bar{p}K^+$ and $B^+ \to p\bar{p}\pi^+$," Phys. Lett. B **659**, 80 (2008) [arXiv:0706.4167 [hep-ex]].

[103] N. Gabyshev *et al.* [Belle and BELLE Collaborations], "Study of decay mechanisms in $B^- \to \Lambda_c^+ \bar{p}\pi^-$ decays and observation of low-mass structure in the $\Lambda_c^+\bar{p}$ system," Phys. Rev. Lett. **97**, 242001 (2006) [hep-ex/0409005].

[104] B. Aubert *et al.* [BaBar Collaboration], "Evidence for the $B^0 \to p\bar{p}K^{*0}$ and $B^+ \to \eta_c K^{*+}$ decays and Study of the Decay Dynamics of B Meson Decays into $p\bar{p}$ final states," Phys. Rev. D **76**, 092004 (2007) [arXiv:0707.1648 [hep-ex]].

[105] J. H. Chen *et al.* [Belle Collaboration], "Observation of $B^0 \to p\bar{p}K^{*0}$ with a large K^{*0} polarization," Phys. Rev. Lett. **100**, 251801 (2008) [arXiv:0802.0336 [hep-ex]].

[106] K. Abe *et al.* [Belle Collaboration], "Observation of $\bar{B^0} \to D^{0(*)}p\bar{p}$," Phys. Rev. Lett. **89**, 151802 (2002) [hep-ex/0205083].

[107] B. Aubert *et al.* [BaBar Collaboration], "Measurements of the Decays $B^0 \to \bar{D}^0 p\bar{p}$, $B^0 \to \bar{D}^*$ 0 $p\bar{p}$, $B^0 \to D^- p\bar{p}\pi^+$, and $B^0 \to D^{*-} p\bar{p}\pi^+$," Phys. Rev. D **74**, 051101 (2006) [hep-ex/0607039].

[108] B. Aubert *et al.* [BaBar Collaboration], "Correlated leading baryon-antibaryon production in $e^+e^- - > c\bar{c} \to \Lambda_c^+ \Lambda_c^- X$," Phys. Rev. D **82**, 091102 (2010) [arXiv:1006.2216 [hep-ex]].

[109] B. Aubert *et al.* [BaBar Collaboration], "Observation and study of baryonic B decays: $B \to D^{(*)}p\bar{p}$, $D^{(*)}p\bar{p}\pi$, and $D^{(*)}p\bar{p}\pi\pi$," arXiv:0908.2202 [hep-ex].

[110] P. del Amo Sanchez *et al.* [BABAR Collaboration], "Observation and study of the baryonic B-meson decays $B \to D^{(*)}p\bar{p}\pi\pi$," Phys. Rev. D **85**, 092017 (2012) [arXiv:1111.4387 [hep-ex]].

[111] W. -S. Hou and A. Soni, "Pathways to rare baryonic B decays," Phys. Rev. Lett. **86**, 4247 (2001) [hep-ph/0008079].

[112] J. L. Rosner, "Low mass baryon anti-baryon enhancements in B decays," Phys. Rev. D **68**, 014004 (2003) [hep-ph/0303079].

[113] H. -Y. Cheng, "Exclusive baryonic B decays Circa 2005," Int. J. Mod. Phys. A **21**, 4209 (2006) [hep-ph/0603003].

[114] C. -K. Chua, W. -S. Hou and S. -Y. Tsai, "Possible hints and search for glueball production in charmless rare B decays," Phys. Lett. B **544**, 139 (2002) [hep-ph/0204186].

[115] H. -Y. Cheng and K. -C. Yang, "Three body charmful baryonic B decays $\bar{B} \to D(D^*)N\bar{N}$," Phys. Rev. D **66**, 094009 (2002) [hep-ph/0208185].

[116] H. -Y. Cheng and K. -C. Yang, "Charmful baryonic B decays $\bar{B}^0 \to \Lambda_c \bar{p}$ and $\bar{B} \to \Lambda_c \bar{p}\pi(\rho)$," Phys. Rev. D **65**, 054028 (2002) [Erratum-ibid. D **65**, 099901 (2002)] [hep-ph/0110263].

[117] B. Kerbikov, A. Stavinsky and V. Fedotov, "Model independent view on the low mass proton anti-proton enhancement," Phys. Rev. C **69**, 055205 (2004) [hep-ph/0402054].

[118] D. V. Bugg, "Reinterpreting several narrow 'resonances' as threshold cusps," Phys. Lett. B **598**, 8 (2004) [hep-ph/0406293].

[119] J. Haidenbauer, U. -G. Meissner and A. Sibirtsev, "Near threshold p anti-p enhancement in B and J/Ψ decay," Phys. Rev. D **74**, 017501 (2006) [hep-ph/0605127].

[120] V. Laporta, "Final stare interaction enhancement effect on the near threshold $p\bar{p}$ system in $B^{\pm} \to p\bar{p}\pi^{\pm}$ decay," Int. J. Mod. Phys. A **22**, 5401 (2007) [arXiv:0707.2751 [hep-ph]].

[121] C. -K. Chua, W. -S. Hou and S. -Y. Tsai, "Charmless three-body baryonic B decays," Phys. Rev. D **66**, 054004 (2002) [hep-ph/0204185].

[122] C. Q. Geng and Y. K. Hsiao, "Angular distributions in three-body baryonic B decays," Phys. Rev. D **74**, 094023 (2006) [hep-ph/0606141].

[123] C. -H. Chen, H. -Y. Cheng, C. Q. Geng and Y. K. Hsiao, "Charmful Three-body Baryonic B decays," Phys. Rev. D **78**, 054016 (2008) [arXiv:0806.1108 [hep-ph]].;

[124] C. Q. Geng and Y. K. Hsiao, "Study of $\bar{B} \to \Lambda\bar{p}\,\rho(\phi)$ and $\bar{B} \to \Lambda\bar{\Lambda}\bar{K}^*$," Phys. Rev. D **85**, 017501 (2012) [arXiv:1109.3032 [hep-ph]].

[125] M. Suzuki, "Partial waves of baryon-antibaryon in three-body B meson decay," J. Phys. G **34**, 283 (2007) [hep-ph/0609133].

[126] R. Aaij *et al.* [LHCb Collaboration], "Measurement of the $B_s^0 \to \mu^+\mu^-$ branching fraction and search for $B^0 \to \mu^+\mu^-$ decays at the LHCb experiment," Phys. Rev. Lett. **111**, 101805 (2013) [arXiv:1307.5024 [hep-ex]].

[127] S. Chatrchyan *et al.* [CMS Collaboration], "Measurement of the $B_s \to \mu^+\mu^-$ branching fraction and search for $B^0 \to \mu^+\mu^-$ with the CMS Experiment," Phys. Rev. Lett. **111**, 101804 (2013) [arXiv:1307.5025 [hep-ex]].

[128] A. J. Buras, J. Girrbach, D. Guadagnoli and G. Isidori, "On the Standard Model prediction for BR($B_{s,d} \to \mu^+\mu^-$)," Eur. Phys. J. C **72**, 2172 (2012) [arXiv:1208.0934 [hep-ph]].

[129] R. Aaij *et al.* [LHCb Collaboration], LHCb-CONF-2012-002

[130] K. De Bruyn, R. Fleischer, R. Knegjens, P. Koppenburg, M. Merk, A. Pellegrino and N. Tuning, "Probing New Physics via the $B_s^0 \to \mu^+\mu^-$ Effective Lifetime," Phys. Rev. Lett. **109**, 041801 (2012) [arXiv:1204.1737 [hep-ph]].

[131] R. Fleischer, "On Branching Ratios of B_s Decays and the Search for New Physics in $B_s^0 \to \mu^+\mu^-$," Nucl. Phys. Proc. Suppl. **241-242**, 135 (2013) [arXiv:1208.2843 [hep-ph]].

[132] D. Becirevic, N. Kosnik, F. Mescia and E. Schneider, "Complementarity of $B_s \to \mu^+\mu^-$ and $B \to Kl^+l^-$ in New Physics searches," Nucl. Phys. Proc. Suppl. **234**, 177 (2013) [arXiv:1209.0969 [hep-ph]].

[133] R. Fleischer, "Theory News on $B_{s(d)} \to \mu^+\mu^-$ Decays," arXiv:1212.4967 [hep-ph].

[134] A. J. Buras, R. Fleischer, J. Girrbach and R. Knegjens, "Probing New Physics with the $B_s \to \mu^+\mu^-$ Time-Dependent Rate," JHEP **1307**, 77 (2013) [arXiv:1303.3820 [hep-ph]].

[135] R. Knegjens, "Phenomenology with a non-zero B_s decay width difference," PoS Beauty **2013**, 053 (2013) [arXiv:1305.6834 [hep-ph]].

[136] W. Altmannshofer, "The $B_s \to \mu^+\mu$ and $B_d \to \mu^+\mu$ Decays: Standard Model and Beyond," PoS Beauty **2013**, 024 (2013) [arXiv:1306.0022 [hep-ph]].

[137] B. Misra and J. P. Saha, "A complete determination of New Physics parameters in leptonic decays of $\mathbf{B_s^0}$," arXiv:1308.2518 [hep-ph].

[138] RAaij *et al.* [LHCb Collaboration], "Measurement of form-factor independent observables in the decay $B^0 \to K^{*0}\mu^+\mu^-$," Phys. Rev. Lett. **111**, 191801 (2013) [arXiv:1308.1707 [hep-ex]].

[139] S. Descotes-Genon, J. Matias and J. Virto, "Understanding the $B \to K^*\mu^+\mu^-$ Anomaly," Phys. Rev. D **88**, 074002 (2013) [arXiv:1307.5683 [hep-ph]];

[140] W. Altmannshofer and D. M. Straub, "New physics in $B \to K^*\mu\mu$," Eur. Phys. J. C **73**, 2646 (2013) [arXiv:1308.1501 [hep-ph]];

[141] R. Gauld, F. Goertz and U. Haisch, "On minimal Z' explanations of the $B \to K^*\mu^+\mu^-$ anomaly," Phys. Rev. D **89**, 015005 (2014) [arXiv:1308.1959 [hep-ph]];

[142] A. J. Buras and J. Girrbach, "Left-handed Z' and Z-FCNC quark couplings facing new $b \to s\mu^+\mu^-$ data," JHEP **1312**, 009 (2013) [arXiv:1309.2466 [hep-ph]];

[143] R. Gauld, F. Goertz and U. Haisch, "An explicit Z'-boson explanation of the $B \to K^*\mu^+\mu^-$ anomaly," JHEP **1401**, 069 (2014) [arXiv:1310.1082 [hep-ph]].;

[144] F. Beaujean, C. Bobeth and D. van Dyk, "Comprehensive Bayesian Analysis of Rare (Semi)leptonic and Radiative B Decays," arXiv:1310.2478 [hep-ph];

[145] A. Datta, M. Duraisamy and D. Ghosh, "Explaining the $B \to K^*\mu^+\mu^-$ anomaly with scalar interactions," arXiv:1310.1937 [hep-ph];

[146] R. R. Horgan, Z. Liu, S. Meinel and M. Wingate, "Calculation of $B^0 \to K^{*0}\mu^+\mu^-$ and $B_s^0 \to \phi\mu^+\mu^-$ observables using form factors from lattice QCD," arXiv:1310.3887 [hep-ph];

[147] S. Descotes-Genon, J. Matias and J. Virto, "Optimizing the basis of $B \to K^* l^+ l^-$ observables and understanding its tensions," arXiv:1311.3876 [hep-ph].

[148] A. J. Buras, F. De Fazio, J. Girrbach and M. V. Carlucci, "The Anatomy of Quark Flavour Observables in 331 Models in the Flavour Precision Era," JHEP **1302**, 023 (2013) [arXiv:1211.1237 [hep-ph]];

[149] A. J. Buras, F. De Fazio and J. Girrbach, "The Anatomy of Z' and Z with Flavour Changing Neutral Currents in the Flavour Precision Era," JHEP **1302**, 116 (2013) [arXiv:1211.1896 [hep-ph]].

[150] C. Q. Geng and Y. K. Hsiao, "Semileptonic $B- \to p\bar{p}\ell - \bar{\nu}_\ell$ decays," Phys. Lett. B **704**, 495 (2011) [arXiv:1107.0801 [hep-ph]].

[151] K. J. Tien *et al.* [M. Z. Wang for the Belle Collaboration], "Evidence for Semileptonic $B^- \to p\bar{p}l\bar{\nu}$ Decays," arXiv:1306.3353 [hep-ex].

[152] C. Q. Geng and Y. K. Hsiao, "Rare $B^- \to \Lambda\bar{p}\nu\bar{\nu}$ decay," Phys. Rev. D **85**, 094019 (2012) [arXiv:1204.4771 [hep-ph]].

[153] A. J. Buras and M. Munz, "Effective Hamiltonian for $B \to X(s)e^+e^-$ beyond leading logarithms in the NDR and HV schemes," Phys. Rev. D **52**, 186 (1995) [hep-ph/9501281].;

[154] M. Misiak, "The $b \to se^+e^-$ and $b \to s\gamma$ decays with next-to-leading logarithmic QCD corrections," Nucl. Phys. B **393**, 23 (1993) [Erratum-ibid. B **439**, 461 (1995)].;

[155] B. Grinstein, M. J. Savage and M. B. Wise, "$B \to X(s)e^+e^-$ in the Six Quark Model," Nucl. Phys. B **319**, 271 (1989).;

[156] N. Sinha and R. Sinha, "CP violating anomalous trilinear gauge couplings from $B \to K^*\ell^+$ lepton-," hep-ph/9707416.

[157] A. Ali, P. Ball, L. T. Handoko and G. Hiller, "A Comparative study of the decays $B \to K$, $K^{(*)}\ell^+\ell^-$ in standard model and supersymmetric theories," Phys. Rev. D **61**, 074024 (2000) [hep-ph/9910221].

[158] W. Altmannshofer, P. Paradisi and D. M. Straub, "Model-Independent Constraints on New Physics in $b \to s$ Transitions," JHEP **1204**, 008 (2012) [arXiv:1111.1257 [hep-ph]].

[159] D. Becirevic, N. Kosnik, F. Mescia and E. Schneider, "Complementarity of the constraints on New Physics from $B_s \to \mu^+\mu^-$ and from $B \to Kl^+l^-$ decays," Phys. Rev. D **86**, 034034 (2012) [arXiv:1205.5811 [hep-ph]].

[160] R. Dutta, A. Bhol and A. K. Giri, "Effective theory approach to new physics in $b \to u$ and $b \to c$ leptonic and semileptonic decays," Phys. Rev. D **88**, 114023 (2013) [arXiv:1307.6653 [hep-ph]].

[161] Y. -Y. Fan, W. -F. Wang, S. Cheng and Z. -J. Xiao, "Semileptonic decays $B \to D^{(*)} l\nu$ in the perturbative QCD factorization approach," Chin. Sci. Bull. **59**, 125 (2014) [arXiv:1301.6246 [hep-ph]].

[162] S. -M. Zhao, X. Liu and S. -J. Li, "Study on $B_s \to D_{s,J}(2317, 2460) l\bar{\nu}_l$ Semileptonic Decays in the CQM Model," Eur. Phys. J. C **51**, 601 (2007) [hep-ph/0612008].

[163] K. Azizi and M. Bayar, "Semileptonic $B_q \to D_q^* \, l \, \nu_l$ ($q = s$, d, u) Decays in QCD Sum Rules," Phys. Rev. D **78**, 054011 (2008) [arXiv:0806.0578 [hep-ph]].

[164] M. Bayar and K. Azizi, "Semileptonic $B_q \to D_q^* l \nu_l$ ($q = s$, d, u) transitions in QCD," Nucl. Phys. Proc. Suppl. **186**, 395 (2009) [arXiv:0809.3866 [hep-ph]].

[165] R. -H. Li, C. -D. Lu and Y. -M. Wang, "Exclusive B_s decays to the charmed mesons $D_s + (1968, 2317)$ in the standard model," Phys. Rev. D **80**, 014005 (2009) [arXiv:0905.3259 [hep-ph]].

[166] G. Li, F. -l. Shao and W. Wang, "$B_s \to D_s(3040)$ form factors and B_s decays into $D_s(3040)$," Phys. Rev. D **82**, 094031 (2010) [arXiv:1008.3696 [hep-ph]].

[167] X. J. Chen, H. F. Fu, C. S. Kim and G. L. Wang, "Estimating Form Factors of $B_s \to D_s^{(*)}$ and their Applications to Semi-leptonic and Non-leptonic Decays," J. Phys. G **39**, 045002 (2012) [arXiv:1106.3003 [hep-ph]].

[168] M. Atoui, D. Becirevic, V. Morenas and F. Sanfilippo, "$'B_s \to D_s l\nu'$ near zero recoil in and beyond the Standard Model," arXiv:1310.5238 [hep-lat].

[169] Y. -Y. Fan, W. -F. Wang and Z. -J. Xiao, "Study of $\bar{B}_s^0 \to (D_s^+, D_s^{*+}) l^- \bar{\nu}_l$ decays in the pQCD factorization approach," Phys. Rev. D **89**, 014030 (2014) [arXiv:1311.4965 [hep-ph]].

[170] D. Becirevic and N. Kosnik, "Soft photons in semileptonic $B \to D$ decays," Acta Phys. Polon. Supp. **3**, 207 (2010) [arXiv:0910.5031 [hep-ph]].

[171] M. Beneke and T. Feldmann, "Symmetry breaking corrections to heavy to light B meson form-factors at large recoil," Nucl. Phys. B **592**, 3 (2001) [hep-ph/0008255].

[172] R. N. Faustov and V. O. Galkin, "Weak decays of B_s mesons to D_s mesons in the relativistic quark model," Phys. Rev. D **87**, 034033 (2013) [arXiv:1212.3167].

List of Publications

- Effective theory approach to NP in $b \to u$ and $b \to c$ leptonic and semileptonic decays.
  Rupak Dutta, Anupama Bhol, Anjan K. Giri
  Physical Reveiw D 88, 114023 (2013)
  arXiv:1307.6653 [hep-ph]

- Baryonic $b \to s\, l\, \bar{l}$ transition decays.
  Rupak Dutta, Anupama Bhol, Anjan K. Giri
  Journal of Physics G: Nuclear and Particle Phys. 41 (2014) 065002.

- Study of $B_s \to D_s^{(*)}\, l\, \nu_l$ semileptonic decays.
  Anupama Bhol
  Europhysics Letters 106 (2014) 31001.